Technische Universität München
TUM School of Medicine and Health

Acute calcium-dependent axon degeneration after spinal cord injury in mice

Bogdan-Nicolae Marincu

Vollständiger Abdruck der von der TUM School of Medicine and Health der Technischen Universität München zur Erlangung eines **Doktors der Medizin (Dr. med.)** genehmigten Dissertation.

Vorsitz: apl. Prof. Dr. Ute Reuning

Prüfende der Dissertation:

1. Prof. Dr. Thomas Misgeld
2. apl. Prof. Dr. Marc Hanschen

Die Dissertation wurde am 05.10.2023 bei der Technischen Universität München eingereicht und durch die TUM School of Medicine and Health am 07.05.2024 angenommen.

Table of Contents

Acknowledgements

First and foremost, I want to thank my family: my wife Adelina, my daughter Lara, and my son Tobias. Without their boundless support and understanding, I wouldn't have been able to finish this thesis. During the hardest times, they have always been my guiding light.

My full gratitude goes out to my supervisor, Prof. Dr. Thomas Misgeld, who was generous in his guidance and patience throughout the whole process, supporting me along this long and windy road. And to my colleague and co-author, Philip Williams, who graciously shared his knowledge and expertise with me.

A heartfelt thank you to three incredible teachers who have spurred my interest for science and have had a decisive impact on my life: Prof. Dr. Adrian Neagu, Prof. Dr. Danina Muntean, and the late Prof. Ioan Nedin.

Finally, I want to thank my parents. I wouldn't be here without you.

Abstract

Spinal cord injury has a severe and debilitating impact on any individual suffering from it. Moreover, it places a long-lasting burden on the patient, their family, and society as a whole. Despite medical and technological progress at large, the impact of this crippling injury has increased during the last decades. To date, there is still no clinical treatment that can offer full recovery of function and a return to pre-injury standards of living. This thesis provides an investigation of the hyperacute phase of injury (the first 4 hours after impact), inspired by the success of similar therapeutic interventions for acute ischaemic brain injuries, trying to find the decisive factors that could reduce axonal damage post impact injury.

This study describes a novel experimental approach to *in vivo* imaging of the lumbar spinal cord following an impact injury, using two-photon microscopy and transgenic mouse lines. It details a reproducible methodology with consistent inter-rater results, comprised of a self-developed, semiautomatic image processing algorithm and an injury grading scale based on morphologic criteria and intracellular calcium imaging. The results prove the existence of a post-impact therapeutic time window, during which injured axons have the potential to recover if certain conditions are met. This thesis shows that the pathological rise of intracellular calcium has a pivotal role in axon degeneration following an impact injury. Preventing this calcium rise leads to an improved recovery of injured axons. Several pharmaceutic interventions are described, targeting different voltage-gated ion channel blockers, all of which were unable to impact axonal degeneration.

These results, together with others from our laboratory, show that the formation of mechanically induced disruptions of the axonal membrane are the main cause for pathologically increased intracellular calcium levels. A therapeutic intervention during the hyperacute phase of injury must hence be aimed at resealing these mechanical defects, rather than focus on blocking the calcium influx through ion channels. There are several candidates that could potentially achieve this, but further work is needed to prove their effectiveness. Such acute interventions need to be combined with subacute and chronic therapies to improve the clinical outcome of spinal cord injuries.

Abbreviations

aCSF	artificial cerebrospinal fluid
AMPA	α-amino-3-hydroxy-5-methyl-4-isoxazolepropionic acid
ATP	adenosine triphosphate
CFP	cyan fluorescent protein
CNS	central nervous system
cpCitrine	circularly permuted Citrine
CSF	cerebrospinal fluid
FRET	fluorescence resonance energy transfer
GaAsP	gallium arsenide phosphide
LPA	lysophosphatidic acid
NMDA	N-methyl-D-aspartate
PMCA	plasma membrane Ca^{2+}-ATPase
PNS	peripheral nervous system
ROS	reactive oxygen species
SCI	spinal cord injury
SERCA	sarcoplasmic-endoplasmic reticulum Ca^{2+}-ATPase
VGCC	voltage-gated calcium channels
YFP	yellow fluorescent protein

1 Introduction

Spinal cord injury (SCI) is one of the most debilitating injuries a patient can suffer. It affects up to 500 000 people each year worldwide, altering their life quality and reducing their life expectancy (Biering-Sorensen, Bickenbach, El Masry, Officer, & von Groote, 2011; Eli, Lerner, & Ghogawala, 2021). In the United States of America alone there are estimated 17000 new cases of SCI each year, with a total of approximately 300 000 people living with the consequences of SCI ("Spinal cord injury facts and figures at a glance," 2012). A review of the scientific articles published on the topic showed that the prevalence of SCI ranges from 906/million in the United States of America to 250/million in France (Singh, Tetreault, Kalsi-Ryan, Nouri, & Fehlings, 2014). Furthermore, during the last 30 years, the worldwide prevalence of SCI has increased 5,5 times, from 236 to 1298 cases/million (Anjum et al., 2020). Patients stem from all classes of society and span across the whole age spectrum, but males between 15 and 35 years old are most often injured (Dobkin & Havton, 2004; van Den Hauwe, Sundgren, & Flanders, 2020). Such injuries have a devastating impact on the physical, psychological, social, and financial status of the patients and of those around them. The direct costs of patient care following SCI are $1.1-4.6 million for each patient during their lifetime. Spinal cord injuries have been linked to cardiovascular complications (prevalence of up to 65%) (Biering-Sorensen et al., 2017; Myers, Lee, & Kiratli, 2007; West, Alyahya, Laher, & Krassioukov, 2013), chronic pain (prevalence of 30% - 90%) (Boldt et al., 2014; Rekand, Hagen, & Gronning, 2012), and mild to severe depression (49% prevalence) (Biering-Sorensen et al., 2011; Khazaeipour, Taheri-Otaghsara, & Naghdi, 2015). The rate of re-hospitalization is about 30%, with diseases of the genitourinary system being the leading cause ("Spinal cord injury facts and figures at a glance," 2012). Patients with SCI also have lower rates of school enrolments and more than 60% of adults are unemployed (Biering-Sorensen et al., 2011), thus casting a heavy economic burden especially on the affected individuals and on their families, but also on society as a whole (Ding et al., 2022).

Etiologically, SCI can be divided into traumatic and non-traumatic injuries. The latter occur when an acute or chronic disease (e.g. degenerative pathologies, tumours, infectious diseases) causes the primary injury. Traumatic SCI occur when the damage is caused directly by an external agent. Common causes of traumatic SCI include penetrating bullet wounds and other forms of violence (26%), non-penetrating lesions from vehicular accidents (38%) and

sports accidents (7%), as well as falls (22%) (Dobkin & Havton, 2004; Eckert & Martin, 2017). More than 2/3 of all spinal cord injuries are thus caused by a form of trauma without direct severing of axonal tracts. The drastic consequences of spinal cord injury are due to the specific anatomy of the spinal cord, where a large number of long projecting axon tracts are densely packed. They control essentially all motor, sensor, and vegetative functions of the extremities and trunk of the organism (Y. Zhang et al., 2021).

1.1 Anatomy and physiology of the spinal cord

The spinal cord is a part of the central nervous system (CNS) that extends from the *medulla oblongata* to the lumbar region and ends with the *conus terminalis*. It consists of billions of tightly packed neurons and glia, containing the longest cell projections in the CNS. Like the brain, the spinal cord is covered by three layers of meninges, spanning its whole length. The outermost layer is the *dura mater*, followed by an intermediary tissue called *arachnoida mater*, and the innermost layer, the *pia mater*. The space between the *pia* and the *dura mater* is filled with cerebrospinal fluid (CSF) and the *dura mater* is covered with fibrous and adipose connective tissue, all of which contribute to the protection of the spinal cord. The most important protective layer, however, is the vertebral column, spanning from the *foramen magnum* to the *Os coccygis*.

The spinal cord is responsible for sensory, autonomic, and motor control throughout the body. While it does have its own intrinsic circuitry, which plays a major role in reflex motor activity, central pattern generation and proprioception, it also bundles the axonal projections that connect the brain to the rest of the body and vice versa. Sensory information is transmitted by afferent fibers, which project to the thalamus, cerebellum, and medial lemniscus. These ascending fibers form the spinothalamic tract, the spinocerebellar tract, and the dorsal column illustrated in Figure 1. Motor commands are transmitted through the pyramidal tracts, which consist of efferent fibers of neurons originating in the cerebral cortex. These terminate either in the brainstem (forming the corticobulbar tract), or at different segments of the spinal cord (forming the corticospinal tract). Additional descending projections outside the pyramidal tract form the extrapyramidal tract system (see Figure 1).

While the main characteristics of this neuronal architecture are similar across mammals, there are several differences in spinal cord anatomy between humans and mice, the model

organism used for this thesis: The human spinal cord has a diameter of about 12.5 mm, while in the mouse it has only 2 mm. Furthermore, humans have 31 pairs of spinal cord segments (eight cervical, twelve thoracic, five lumbar, five sacral, and one coccygeal spinal cord segments), while mice have 34 (eight cervical, thirteen thoracic, six lumbar, four sacral, and three coccygeal spinal cord segments). And while the human vertebral column is composed of seven cervical, twelve thoracic, five lumbar, five sacral, and one caudal/coccygeal vertebrae, the mouse vertebral column – which is relevant to this study – is typically composed of seven cervical, thirteen thoracic, six lumbar, four sacral, and twenty-eight caudal vertebrae (Harrison et al., 2013). Because the spinal column grows faster than the spinal cord, the latter ends at the L1 vertebra in humans and at the L3 vertebra in rodents (Silva, Sousa, Reis, & Salgado, 2014). Moreover, some details in fiber tract location vary between species, as do details in connectivity. A comparison of fiber tract location between humans and rodents is illustrated below.

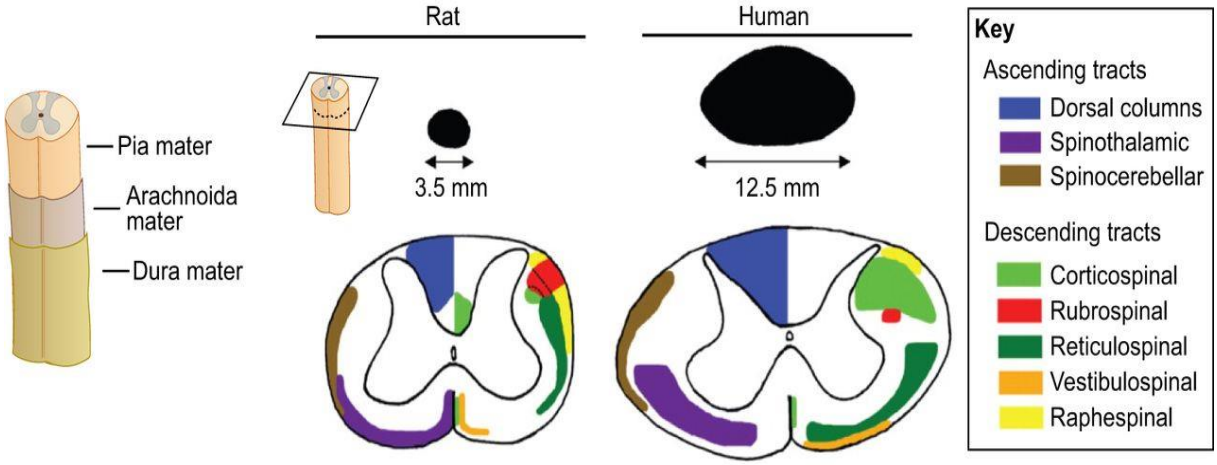

Figure 1: Differences between the anatomy of the rodent and the human spinal cord. Figure modified from (Kjell & Olson, 2016)

Still, there are also many similarities across species, making the rodent spinal cord a very suitable model of human spinal cord anatomy and physiology: The spinal cords of humans and rodents both contain fiber tracts, interneurons, and glial cells packed very densely and in similar radial distribution - grey matter in the centre and white matter surrounding it. The former is organised in a shape that resembles the letter “H” or a stylised butterfly. The white

matter surrounds this grey matter core and is thus more easily exposed to external injury. These myelinated white matter tracts will be the main subject of this thesis.

Due to the architecture described above, the spinal cord is exposed to two kinds of vulnerabilities: a geometric one (due to the length and density of the fibers) and a functional one (due to the indispensable interaction between axons and glia to fulfil the metabolic needs of the former). The spinal cord, therefore, has a high risk of suffering extensive and irreversible damage in the case of injury (Stys, 2005).

1.2 Pathology of spinal cord injury

Most spinal cord injuries occur due to blunt force trauma (e.g. motor vehicle accidents, falls, sport injuries) and only a minority of injuries are caused by penetrating trauma (van Den Hauwe et al., 2020). Such severe injuries, in which all the spinal axons may be transected, are associated with a higher mortality rate (Krause, Sternberg, Lottes, & Maides, 1997), especially in the case of paraplegic patients (Hagen, Lie, Rekand, Gilhus, & Gronning, 2010; Yeo et al., 1998). In such cases the functional recovery is minimal, with no robust and reproducible repair strategies currently available (Aminoff, 2014). After light or moderate injuries, however, some axons survive and there have been patients who have shown spontaneous recovery. But even in such fortunate cases the treatment requires years of therapy and the degree of recovery is often very limited (Fakhoury, 2015).

Although the characteristics of initial neuronal damage depend on the nature and dynamics of the injury, some common features of subsequent damage appear to exist (i.e. disruption of the cell membrane integrity, perturbation of ion homeostasis, etc. (Agrawal & Fehlings, 1996; Ahuja, Wilson, et al., 2017; Pettus, Christman, Giebel, & Povlishock, 1994; Pettus & Povlishock, 1996; Stys, 2005; Witiw & Fehlings, 2015)). These shared mechanisms appear of particular interest for further study and comparison across models.

The damage after injury is typically multi-phasic: a first, acute phase induced by the primary injury is followed by secondary damage, and a third chronic phase of scar formation and potentially remodelling. The primary mechanisms of acute injury comprise the immediate damage suffered by axons after laceration, contusion, or infarction due to a vascular insult. It may be caused (a) by direct trauma from a foreign body (e.g. bullet, knife) or dislocated bone fragments, (b) by compression from bone fragments, haematomas or disc fragments, or (c) by

ischaemia after compression or dissection/transection of the spinal arteries. This damage is currently considered beyond repair. On a macroscopic scale, the consequences include neurogenic shock (i.e. hypotension, bradycardia, and peripheral vasodilatation) and spinal shock (i.e. complete and transient loss of all neurologic functions below a certain segment, not caused by anatomic discontinuity) (Ditunno, Little, Tessler, & Burns, 2004). The treatments of primary injuries focus on the immediate stabilisation of the patient, decompression and eventual realignment of the spinal cord, and less on the limitation of tissue damage during the secondary phase. On the microscopic scale, it has been shown in rodent models that the axonal segments found in the immediate vicinity of the transection site undergo a process of rapid fragmentation called acute axonal degeneration (Kerschensteiner, Schwab, Lichtman, & Misgeld, 2005).

The secondary injury represents a more complex picture comprising various mechanisms and cascades triggered by the primary injury. The physical damage suffered by the cellular structures leads to oedema and to disturbances of cellular homeostasis. Any axonal energy failure, regardless of its primary cause (i.e. inflammatory, ischemic, physical or otherwise), will eventually lead to axonal degradation (Buki & Povlishock, 2006), a process that often begins focally (Lingor, Koch, Tönges, & Bähr, 2012). This leads to morphological changes, which occur over a period ranging from minutes to weeks after the primary injury and will lead to further degradation of axonal tracts (Silva et al., 2014). Such phenomena of delayed damage were first described in detail by Allen in 1911. He suggested that secondary mechanisms lead to further damaging of the spinal cord after the primary injury and found that the outcome can be improved after removing the inflammatory fluid in experimentally injured dogs (Allen, 1911). Sadly, more than a century after this realization, current therapies still rely on high doses of steroids (mainly methylprednisolone (Bracken, 2012; Karsy & Hawryluk, 2019)) as the main therapy for secondary axonal injuries. The use of corticosteroids as a neuroprotective treatment following SCI is controversial. In several clinical studies, this treatment failed to improve the primary endpoints, although it did lead to an improved functional outcome after 1 year. But it is not without downsides. The use of corticosteroids increases the risk of wound infection, gastrointestinal bleeding, and sepsis. Other studies have shown that steroids (i.e. methylprednisolone) have no significant benefits regarding motor recovery and patients who received them had a significantly higher rate of total complications (Evaniew et al., 2015).

Because of this, there are conflicting guidelines from the American Association of Neurological Surgeons and the AO Spine Foundation respectively, regarding their use in an acute setting (Karsy & Hawryluk, 2019). Their mechanism in this setting is still not fully understood and several studies are looking for better treatment alternatives for the secondary stage of SCI. That is why we decided to study the mechanisms of the secondary phase of axon degeneration.

The third and final phase following SCI is the chronic phase, which spans from days to years after the initial damage. It involves a complex interplay of white matter demyelination, grey matter disintegration, and the formation of glial scars. Other factors involved are axonal remodelling and cell plasticity (Jacobi & Bareyre, 2015; Onifer, Smith, & Fouad, 2011), as well as long-term reactions of the immune system (Orr & Gensel, 2018). Since the third stage of SCI is a complex topic that is not the subject of the current thesis, I will refrain from discussing it further. This three-stage process typically leads to lasting neurological impairments related to loss of afferent and efferent functions of the affected spinal cord segments (Silva et al., 2014).

The focus of my thesis is to identify mechanisms that could exacerbate axon degeneration during the immediate post-contusion stage and to discover potential therapeutic targets that could influence the fate of damaged axons.

1.3 Pathophysiology of axon injury after acute spinal cord injury

The three main molecular mechanisms behind the acute phase of axon degeneration are decreased metabolic support, increased energy demand, and toxicity. While these mechanisms are non-exclusive and can appear both in the acute and chronic stages of spinal cord injury (Simons, Misgeld, & Kerschensteiner, 2014), during the acute phase they typically follow the abovementioned order. In the following paragraphs, I will discuss how these mechanisms lead to axon degeneration and how they are linked to an increase of intracellular calcium ions, which marks the impeding axonal demise. The goal of this brief review is twofold: (i) to understand the current knowledge of the injury mechanisms during the acute phase of SCI and (ii) to tease out possible pharmacological interventions that could target one or more of these mechanisms with the aim of limiting axonal damage.

Secondary axon degeneration initiated by (relative) anoxia/ischemia

The mammalian CNS has a very high metabolic rate, thus being in constant need of oxygen and glucose for its normal function. Unfortunately, it has very limited reserves of energy, so that it heavily depends on a steady and continuous external supply of glucose, which is delivered from the circulation via glucose transporter proteins. The glucose is then transformed into adenosine triphosphate (ATP) via oxidative phosphorylation. One cause of energetic imbalance is thus an interruption of the steady supply of ATP anywhere along the length of axonal projections. This will render them non-functional via rapid depolarization, ionic imbalance, and conduction failure. Possible mechanisms for this supply interruption include haemorrhage, vasospasm, thrombosis, and inflammation (Silva et al., 2014). Another cause of energetic imbalance is increased energetic demand, which is likely to appear due to traumatic damage suffered by the myelin sheath after impact (Simons et al., 2014), or decreased energy production due to mitochondrial damage (G. Cheng, Kong, Zhang, & Zhang, 2012; Yang et al., 2015). This is why I refer to this energetic imbalance as relative ischemia. Regardless of its underlying mechanism, relative anoxia/ischemia and the consecutive ionic imbalance dramatically increase the magnitude of traumatic neuronal injury by facilitating several proteolytic processes (Bartus, 1997; Buki & Povlishock, 2006), which I will discuss in later paragraphs.

The first consequence of energetic imbalance is the failure of the Na/K-ATPase. This causes the accumulation of intracellular Na^+ (approximately four- to fivefold compared to physiologic levels) and the loss of axoplasmic K^+ (Stys, 1998). The influx of sodium ions in axons occurs mainly through voltage-gated Na^+ channels (Stys & Lopachin, 1998) and α-amino-3-hydroxy-5-methyl-4-isoxazolepropionic acid (AMPA) receptors (Ouardouz, Malek, Coderre, & Stys, 2006; Tsutsui & Stys, 2013). The extracellular accumulation of K^+ further contributes to the depolarization of axons. These events lead to the reverse operation of several ionic exchangers, most importantly Na^+/Ca^{2+} and Na^+/H^+ (Agrawal & Fehlings, 1996; Stys, Waxman, & Ransom, 1992). The malfunction of these transporters will lead to further increase in intracellular calcium levels and to pH dysregulation. The resulting extracellular acidosis activates acid-sensing ion channels, further contributing to the accumulation of intracellular Na^+ and Ca^{2+} (Vergo et al., 2011). Self-promoting mechanisms of ionic imbalance form a type of positive feedback loop, which amplifies over time and activates/promotes other pathologic signalling cascades. Of these, the accumulation of intracellular calcium is pivotal.

Secondary axon degeneration mediated by increased intracellular calcium

Most of the intracellular calcium is bound to proteins (e.g. calmodulin, calbindin, and parvalbumin) and sequestered in the endoplasmic reticulum and mitochondria (Kostyuk & Verkhratsky, 1994). The total concentration of calcium in myelinated axons is approaching 1 mM (Stys, Lehning, Saubermann, & LoPachin, 1997), but the concentration of free Ca ions is maintained at ~100 nM under physiological conditions (Stys, 2005). The most important ion transporters working to maintain calcium homeostasis are the plasma membrane Ca^{2+}-ATPase (PMCA) and the sarcoplasmic-endoplasmic reticulum Ca^{2+}-ATPase (SERCA). Relative energy depletion of the axon will cause the malfunction of these and several other ionic transporters, leading to intracellular calcium overload (see Figure 2).

Under ischemic conditions, free intracellular calcium increases from a baseline concentration of ~100 nM to tens of micromolar (Nikolaeva, Mukherjee, & Stys, 2005). Notably, ischemic CNS axons show an increase of free intracellular calcium even in Ca-free perfusate (Ouardouz et al., 2003). This is due to the intracellular calcium stores, which are an established source of free Ca^{2+} during ischemia.

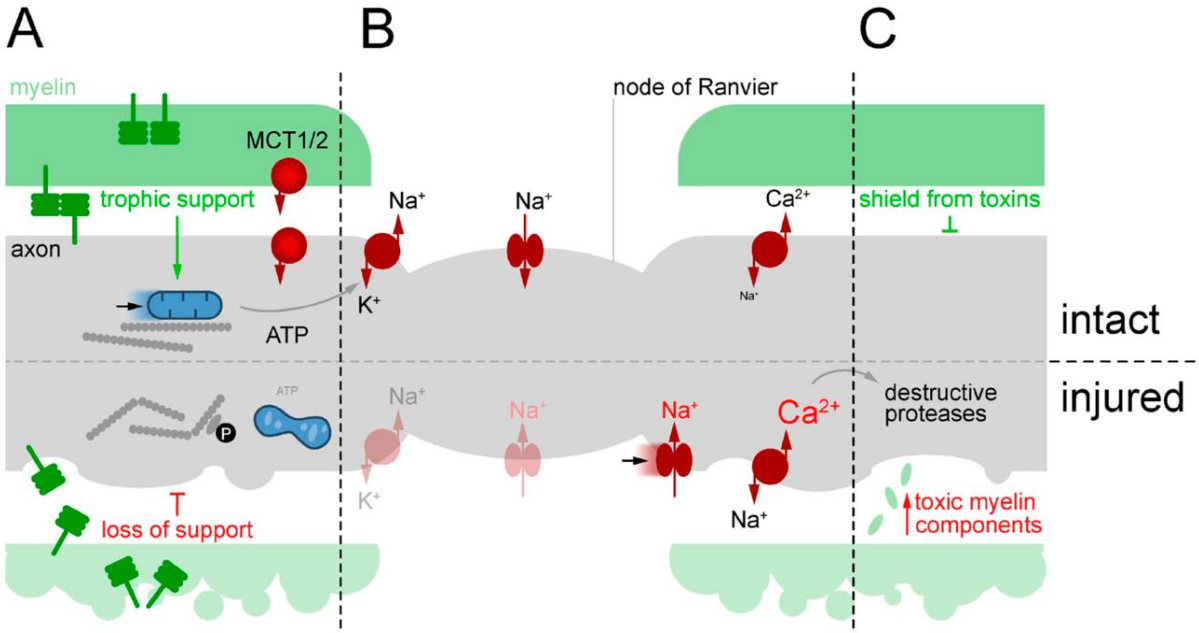

Figure 2: Schematic representation of three non-exclusive axonal injury mechanisms: (A) loss of metabolic support, (B) increased energy demand, and (C) toxicity. Figure from (Simons et al., 2014).

In some cases, the release from internal calcium stores is sufficient to damage the neurons without any additional influx of extracellular calcium (Ouardouz et al., 2003). This release can be reduced by administering ryanodine or the L-type calcium channel blocker nimodipine, since the L-type calcium channels and the ryanodine receptors on the endoplasmic reticulum have been shown to act interdependently in contributing to the release of calcium from intracellular stores (Nikolaeva et al., 2005; Ben C. Orem, Rajaee, & Stirling, 2021; Ouardouz et al., 2003; Ouardouz, Zamponi, Barr, Kiedrowski, & Stys, 2005). Also, nimodipine is known to interfere with the activation of the ryanodine receptors through the L-type calcium channels (Nehrt, Rodgers, Shapiro, Borgens, & Shi, 2007; Ouardouz et al., 2003)

The strong depolarization suffered by axons after injury will lead to the further rise of intracellular calcium levels by opening the voltage-gated calcium channels (VGCC) found in the axonal membrane (Fern, Ransom, & Waxman, 1995; Leppanen & Stys, 1997; Ouardouz et al., 2003). *In vitro* experiments have shown that selectively blocking L-type and N-type calcium channels using pharmacological agents (i.e. verapamil, diltiazem, nifedipine, and ω-conotoxin) had a protective effect on spinal cord axons after 60 minutes of anoxia (Imaizumi, Kocsis, & Waxman, 1999).

Mitochondria also contain substantial quantities of calcium. Under physiological conditions, the mitochondrial influx of this ion is regulated primarily by the mitochondrial calcium uniporter (Kirichok, Krapivinsky, & Clapham, 2004) and the Na^{+}/Ca^{2+} exchanger (Castaldo et al., 2009; Stirling & Stys, 2010). Mitochondrial demise has severe consequences for the affected axonal segment, aggravating the underlying energetic depletion and leading to devastating disturbances in homeostasis. Traumatic axonal injury leads to morphological alterations of axonal mitochondria, including swelling and rupture of the cristae and membranes (Hill, Coleman, & Menon, 2016). It is assumed that these alterations are mediated by the excessive sequestration of calcium. This sequestration disrupts the mitochondrial transmembrane potential and causes the opening of the membrane permeability transition pore, which allows calcium to leave the mitochondria and also increases the permeability of the mitochondrial membrane to molecules larger than 1.5 kDaltons. This mechanism is responsible for neuronal apoptosis (Buki & Povlishock, 2006). Several experiments using selective blockers of calcium release have been tried, but the most effective strategies of inhibiting calcium release from intracellular stores during *in vitro* ischemia were combinatorial treatments, which targeted both the endoplasmatic reticulum Ins(1, 4, 5)P_3 receptors and the

mitochondrial Na^+/Ca^{2+} exchanger. These results suggest that post-traumatic intracellular calcium release is mediated by multiple pathways. Such interventions were also followed by improved electrophysiological recovery of the axons, further underlining the direct relationship between intracellular calcium accumulation and axonal injury (Nikolaeva et al., 2005; Stirling & Stys, 2010).

Another source of calcium influx in the setting of traumatic axonal injury is through mechanical disruptions in the axolemma caused by shear and tensile forces. The seminal work on this topic in the context of traumatic brain injury was done in the Povlishock laboratory, where experiments have shown that traumatically induced mechanoporation of the axolemma leads to influx of normally excluded molecules, such as calcium (Pettus et al., 1994; Pettus & Povlishock, 1996). The authors proposed that mechanoporation leads to upstream axoplasmic swelling and eventual axonal fragmentation. The presence of such mechanopores was confirmed by later work, including experiments done in our laboratory (Williams et al., 2014). Mechanoporation following traumatic injury leads to focal disturbance of calcium homeostasis, which in turn activates various cysteine protease pathways capable of degrading the cytoskeleton (Buki, Siman, Trojanowski, & Povlishock, 1999). The focal disruption of microtubules and neurofilaments leads to accumulation of organelles and vesicles, which in turn causes axonal swelling and eventual fragmentation. The retraction of severed axon stumps is often preceded by the formation of a blob-like structure called retraction bulb or ball (Buki & Povlishock, 2006). In our present work, we used the formation of such a retraction ball as a definitive criterion for axonal discontinuity.

Lastly, focal axonal calcium overload activates various signalling cascades, which can lead to the demise of the affected axon segment. One of the most important of these cascades of axonal degeneration causes the activation of two cysteine protease families: calpains and caspases.

Calcium-activated proteases execute secondary axon degeneration

Calpains are a family of cysteine proteases, which have been linked to cytoskeletal remodelling, cell differentiation, vesicular trafficking, apoptosis, and necrosis (Zatz & Starling, 2005). Calpain proteolysis plays a common and important role in a variety of acute neurodegenerative conditions, including focal ischemia (stroke), global ischemia, traumatic

brain injury, and spinal cord injury (Bartus, 1997). Calpains also play an important role in Wallerian degeneration, particularly in neurofilament proteolysis, and experiments done by Kerschensteiner et al. have shown that applying calpain inhibitors prevents acute axonal degeneration after transection (Kerschensteiner et al., 2005). Accordingly, these proteases have increased activity within minutes after traumatic axonal injury, leading to retrograde transport impairment (Buki et al., 1999; Saatman et al., 2003). The mechanoporation and the influx of calcium following mechanical injury also result in increased calpain activity, which is an early predictor of axonal beading (Kilinc, Gallo, & Barbee, 2009). Beside their location in the cytoplasm, calpains have also been found in mitochondria, where they can open the mitochondrial permeability transition pore directly (Buki & Povlishock, 2006). Furthermore, calpain activation has been linked to apoptosis (Norberg et al., 2008). Lastly, there is evidence relating calpain proteolysis to Alzheimer's disease, Parkinson's disease, Huntington's disease and amyotrophic lateral sclerosis (Bartus, 1997), all diseases with a pronounced axonal pathology. Not surprisingly, this powerful and destructive protease system is under stringent endogenous control, including by calpastatin, a peptide that inhibits calpain activity (Ma, 2013). The significance of calpain activation as a seminal step in the post-traumatic axon degeneration cascade is underscored by the fact that exogenously applied calpain inhibitors improve axonal survival and neurological function after experimental SCI *in vivo* (Schumacher, Siman, & Fehlings, 2000).

Caspases play important roles in shaping the nervous system: they are central regulators of apoptotic cell death, including of neurons, but also in autophagy and neurite pruning (Sokolowski et al., 2014; Wu et al., 2014). Work done in the Povlishock laboratory also shows that caspase cleavage of the beta-amyloid precursor protein occurs in traumatic axonal injury and is associated with the formation of Abeta peptide, thus supporting the link between such injury and the later development of dementia (Stone et al., 2002). Furthermore, Büki and Povlishock consider the activation of the "caspase death cascade" in traumatically injured axonal segments to be the point of no return, which inevitably leads to axonal disconnection (Buki & Povlishock, 2006).

Neurodegeneration caused by toxicity via glutamate

Glutamate is the main excitatory neurotransmitter in the mammalian CNS (Y. Zhou & Danbolt, 2014). But if it accumulates to pathologically high levels, glutamate has an excitotoxic effect, being involved in both chronic neurological disorders (e.g. Alzheimer's disease, amyotrophic lateral sclerosis, Parkinson's disease) and acute pathologies (e.g. ischemia, mechanical injury) (Hernández et al., 2018; D. Liu, Xu, Pan, & McAdoo, 1999). Neurons and oligodendrocytes are especially susceptible to excitotoxic damage via glutamate due to the high affinity of their glutamate receptors (Oyinbo, 2011).

In the case of an ischemic injury of the white matter, axons and glial cells release glutamate through vesicular fusion or reverse glutamate transport (Back et al., 2007; Ziskin, Nishiyama, Rubio, Fukaya, & Bergles, 2007). In the case of traumatic spinal cord injury, glutamate is released excessively both in and around the site of injury mainly through the reversed functioning of Na^+-glutamate transporters following the post-traumatic reversal of the ionic gradient (McAdoo, Xu, Robak, & Hughes, 1999; Park, Velumian, & Fehlings, 2004). Under physiological circumstances, Na^+-dependent glutamate transporters are maintaining transmembrane glutamate concentrations by transporting glutamate or aspartate, three sodium ions, and one proton in exchange for one potassium ion (Zerangue & Kavanaugh, 1996). But after SCI, the depolarization of the damaged axons and the dysregulation of ionic gradients leads to a release of glutamate, which will further aggravate the disturbance in the ionic gradients, causing a rise in intracellular sodium and calcium ions, as described in the previous paragraphs. The excess glutamate also causes indirect damage by binding to the N-methyl-D-aspartate (NMDA) and AMPA-kainate receptors, leading to ischemia and the generation of reactive oxygen and nitrogen species (Dawson & Dawson, 1996; Dumont et al., 2001). The consequences of the latter will be briefly discussed further in later paragraphs of this section.

The importance of glutamate in white matter degeneration has been extensively described by the work done in the Stys laboratory (Ouardouz, Coderre, Basak, et al., 2009; Ouardouz, Coderre, Zamponi, et al., 2009; Stirling & Stys, 2010; Stys, 2005), which inspired us to test its potential roles as a therapeutic target after mild contusion. Stys and colleagues have also shown that exposure to glutamate causes myelin degradation *in vitro* (S. Li & Stys, 2000). Liu et al. have further demonstrated the importance of glutamate in the setting of acute spinal cord injury (D. Liu et al., 1999). The literature reports that the myelinated axons of the spinal cord and several glial cells express a variety of NMDA, glutamate, and AMPA-type

glutamate receptors (Ouardouz, Coderre, Basak, et al., 2009; Ouardouz, Coderre, Zamponi, et al., 2009).

Previous experiments have shown that application of AMPA receptor agonists or the increase of extracellular glutamate concentration promotes axonal injury (Domercq, Etxebarria, Perez-Samartin, & Matute, 2005; S. Li & Stys, 2000; Pitt, Gonzales, Cross, & Goldberg, 2010). Furthermore, antagonists of AMPA or NMDA have shown to have a protective effect on white matter lesions (Bakiri, Hamilton, Karadottir, & Attwell, 2008; Wrathall, Choiniere, & Teng, 1994). These and several other papers have led us to include glutamate receptor antagonists as a pharmacological tool in our search for factors that might promote axon survival after mild contusion injury. In the context of experimental autoimmune encephalitis, a more recent paper, published after my experiments were finished, showed that the direct application of glutamate and related agonists has no significant effect (Witte et al., 2019).

Neurodegeneration caused by toxicity via oxidative stress

Reactive oxygen species (ROS) play a substantial role in secondary axonal degeneration following traumatic injury (Fatima, Sharma, Das, & Mahdi, 2015). Three sources are mainly responsible for ROS release: mitochondria, membrane lipids, and immune cells. Under physiological conditions, there is a balance between the formation of ROS and its scavenging by antioxidants. In an injury setting, the disruption of axonal homeostasis will result in an imbalance between the two processes. The neurodegenerative implications of ROS in both an acute trauma setting and in a chronic inflammatory setting are of themselves big and separate areas of research. In the following paragraphs I will give but a brief illustration of possible ways in which ROS could be implicated in post-traumatic neurodegeneration.

ROS attack the free fatty acids released from the cell membranes following spinal cord trauma, resulting in lipid peroxidation and the formation of free radicals, all of which further contribute to axonal damage (Toborek et al., 1999). Previous work has shown that impaired mitochondrial function and lipid peroxidation occur within one hour after SCI, but the compensatory activation of scavenger molecules is observed only after 24 hours (Azbill, Mu, Bruce-Keller, Mattson, & Springer, 1997). Lipid peroxidation also leads to the formation of aldehyde products, which in turn affect the Na/K-ATPase and further aggravate the energetic

imbalance of the cell (Jamme et al., 1995; Silva et al., 2014). There is also evidence that activation of glutamate receptors and calcium influx, both of which take place after SCI as presented above, lead to ROS formation (Coyle & Puttfarcken, 1993). For example, the high levels of intracellular calcium can disrupt the mitochondrial electron transport system, resulting in the formation of ROS, which in turn attack various axonal components (e.g. phospholipids, proteins, nucleic acids) (Azbill et al., 1997; Hall & Braughler, 1989).

ROS can exacerbate blood flow impediments, adding to ischemia, oedema, and subsequent inflammation (Sandler & Tator, 1976). The complex inflammatory reaction that follows SCI will activate resident microglia and leukocytes, which leads to the release of cytokines and ROS. Nitric oxide is another reactive molecular species that is elevated during axonal inflammation and causes neuronal damage even at low micromolar concentrations (Smith, Kapoor, Hall, & Davies, 2001). It also seems to be an important mediator between glutamate receptor activation and calcium release from intra-axonal stores (Stirling & Stys, 2010).

Besides their role in acute axonal injury, ROS have also been implicated in several chronic neurodegenerative disorders, including Alzheimer's disease, Parkinson's disease, and amyotrophic lateral sclerosis (Lin & Beal, 2006). In the case of multiple sclerosis and experimental autoimmune encephalomyelitis, *in vivo* experiments performed in our laboratory have shown that focal intra-axonal mitochondrial pathology is an early sign of axonal damage, preceding morphological axonal changes. ROS can cause such mitochondrial pathology and trigger focal axonal degeneration, which begins with beading and progresses towards the fragmentation of the axons. In converse, neutralization of ROS can rescue axons that have entered this degenerative process (Nikic et al., 2011). Further *in vivo* experiments done in our laboratory have shown that axonal mitochondria undergo spontaneous contractions accompanied by redox changes and that such contractions are amplified in a setting of acute or chronic neuronal injury (Breckwoldt et al., 2014).

Both *in vivo* and *in vitro* experiments have shown that scavenging ROS and reducing oxidative stress after SCI improves functional recovery, reduces locomotor impairment, and also decreases inflammation (Bros, Millward, Paul, Niesner, & Infante-Duarte, 2014; Khayrullina, Bermudez, & Byrnes, 2015; D. Liu, Shan, Valluru, & Bao, 2013; F. T. Liu et al., 2014). Clinical studies have also confirmed the presence of oxygen-derived free radicals in SCI

patients, further supporting oxide scavengers and even antioxidants as possible therapies during the acute phase of injury (Fatima et al., 2015).

Pharmaceutical targets of neurodegeneration in the current study

Based on the literature knowledge described above, we decided for a neuroprotective strategy that is based on pharmacological intervention performed during the first four hours after impact. Preventing the rise of intracellular calcium and blocking the glutamate receptors seemed the most promising points of intervention. My hope was to prevent or at least delay the axonal degeneration I observed after impact injury. This is why, for the experimental part, I decided to target the following three influx pathways:

1. The Na^{+}/Ca^{2+} exchanger that operates in reverse order as a consequence of the post injury ionic imbalance (Stys & Lopachin, 1998; Stys et al., 1992). To this end I used Bepridil hydrochloride (Sigma-Aldrich).
2. Voltage-gated calcium channels likely to be present in axons (Ouardouz et al., 2003; Stys, 2005). To target these, I used A combination of blockers consisting of Nimodipine (Sigma-Aldrich) and ω-Conotoxin GVIA (Tocris).
3. The glutamate receptors that were reported to contribute to axon degeneration in other settings (Ahuja & Fehlings, 2016; Bakiri et al., 2008; D. Liu et al., 1999; Ouardouz, Coderre, Basak, et al., 2009; Ouardouz, Coderre, Zamponi, et al., 2009; Ouardouz et al., 2006). For this I applied MK 801 maleate (Tocris) and 6-Cyano-7-nitroquinoxaline-2,3-dione disodium salt (Tocris).

These experiments and their results are described in further chapters.

1.4 Therapeutic approaches to spinal cord injury

Currently, there are no efficient therapies for SCI patients. To date, no clinical evidence exists to definitively recommend the use of any neuroprotective pharmacologic agent, including steroids, for the treatment of acute spinal cord injury in order to improve functional recovery (Consortium for Spinal Cord Medicine, 2008). Furthermore, current clinical guidelines advise not to administer medications aimed at providing neuroprotection and

prevention of secondary deterioration in the acute stage after acute traumatic SCI, including methylprednisolone, nimodipine, and naloxone (National Clinical Guideline, 2016). Recommended therapeutic interventions refer to stabilization, decompression, and realignment of the spinal cord, with the consecutive treatment of potentially involved fractures.

On a macroscopic level, despite the existing inconsistencies in the literature, there have been reported cases in which therapeutic hypothermia might have conferred neuroprotection after spinal cord trauma by diminishing the destructive secondary cascade (Alkabie & Boileau, 2016; J. Wang & Pearse, 2015). Still, such an approach would be difficult to reproduce on a large scale and in the various settings in which SCI occurs. Furthermore, as SCI patients often exhibit associated symptoms (ranging from hypotension to shock), a systemic treatment would probably affect the survival of the patient. Hence, no pharmacological intervention after SCI has yet crossed the translational barrier. Still, numerous experimental therapeutic approaches are being pursued (Ahuja, Nori, et al., 2017; Vismara, Papa, Rossi, Forloni, & Veglianese, 2017; Witiw & Fehlings, 2015). In the following paragraphs I will give a brief literature review of the main therapeutic approaches that are being pursued.

Neuroprotective strategies

Neuroprotective therapeutic approaches aim to minimize the damage suffered by axons during the secondary degeneration phase through inhibition of various degenerative cascades and/or activation of protective cellular mechanisms. The paths currently being followed include selective blockade of neurodegenerative pathways, as well as inhibition of inflammatory or apoptotic response to injury. To date, several pharmacologic agents have shown significant effects in animal models, but have failed to cross the chasm of translational medicine, being unable to show adequate improvements in human patients.

Inspired by the successful use of the antiepileptic riluzole in the treatment of amyotrophic lateral sclerosis (Bhatt & Gordon, 2007), several randomized clinical trials have tried to replicate its neuroprotective effects in the context of traumatic and non-traumatic SCI (Fehlings et al., 2021; Fehlings et al., 2012; Nagoshi, Nakashima, & Fehlings, 2015). Riluzole selectively blocks tetrodotoxin-sensitive sodium channels and inhibits presynaptic glutamate release (Ahuja & Fehlings, 2016). Minocycline is an antibiotic that inhibits microglial activation and reduces inflammatory responses. After encouraging results from a phase II

placebo-controlled randomized trial (Casha et al., 2012), a phase III trial was conducted using this drug (NCT01828203). However, both riluzole and minocycline have failed to cross the barrier of translational medicine and the initial neuroprotective effects were not reproduced in later clinical trials (Fan, Wei, & Feng, 2022). Granulocyte colony-stimulating factor is another promising avenue that is currently being pursued. It has been shown to protect against glutamate-induced apoptosis and to reduce tumor necrosis factor-α *in vivo* (Nishio et al., 2007) and a double-blind randomized clinical trial has shown it can improve the clinical outcome in patients with incomplete chronic SCI (Derakhshanrad, Saberi, Yekaninejad, Joghataei, & Sheikhrezaei, 2018).

Neuroregenerative strategies

In contrast to the above-mentioned therapies, the neuroregenerative approaches focus mainly on the processes taking place during the tertiary phase of degeneration. The primary aim is to remove any physical barriers of neuronal growth at the site of injury, creating proper conditions for the regeneration of axons and promoting the latter.

The glial scar that forms during the third stage of SCI is traditionally thought to represent a physical barrier for the regeneration of axons. Degradation of extracellular matrix chondroitin sulphate proteoglycans using Chondroitinase ABC has been shown to reverse chronic atrophy of rubrospinal neurons and to promote sprouting of intact and injured spinal projections after SCI in Wistar rats (Barritt et al., 2006; Carter, McMahon, & Bradbury, 2011). Neurite outgrowth inhibitor A (Nogo-A) is a myelin-associated protein that promotes the collapse of the axonal growth cone and thus inhibits axonal regeneration. Blocking Nogo-A or inhibition of its downstream pathway promotes axonal regeneration and compensatory plasticity following lesions of the central nervous system (Chen et al., 2000; Schwab, 2010). Several clinical trials have investigated the benefits of a monoclonal Nogo-A antibody in the treatment of amyotrophic lateral sclerosis and SCI (Fehlings et al., 2011; Meininger et al., 2014), including a first-in-man intrathecal application, which yielded promising results in patients with tetraplegia (Kucher et al., 2018), making this one of the more promising therapeutic approaches.

In contrast to the traditional belief that the glial scar is a physical barrier for axonal regeneration, other experiments have shown that glial tissue can represent a roadmap for the

regrowth of transected axons and that the overexpression of connective tissue growth factor actually promotes axonal regrowth in zebrafish (Mokalled et al., 2016). There is also evidence showing that astrocyte scar formation rather aids than prevents axon regeneration in the mouse CNS (M. A. Anderson et al., 2016). And a more recent study has suggested that the processing of myelin debris after SCI through the autophagy pathway may promote angiogenesis (T. Zhou et al., 2019). Such findings suggest that reactive astrocytes may be permissive for axon outgrowth, while fibroblasts and macrophages are likely inhibitory (Katoh, Yokota, & Fehlings, 2019; Williams & He, 2016).

Several approaches to neuroregeneration have been tried, using endogenous growth strategies (e.g. infusion of growth factors), exogenous transplantation of stem cells and pluripotent cells, or implantation of biomaterial scaffolds. This is a vast field of study, which would necessitate a large amount of space to properly summarize it. Hence, I only mention that to date none of these have managed to elicit relevant effects in human patients (Katoh et al., 2019). Further investigation and a combination of the above mentioned approached are likely necessary for these strategies to elicit significant effects in a clinical setting.

1.5 Experimental approaches to model spinal cord injury

For over a century, numerous different animal models have been used to study SCI. The first such model in mammals was described by Allen, who in 1911 developed a weight drop contusion model in dogs (Allen, 1911). Over the years, a variety of animal models have been used, including cats, dogs, rats, and mice (Blight, 1983; Blight, Toombs, Bauer, & Widmer, 1991; Joshi & Fehlings, 2002). Such animal models have played a pivotal role in at least two aspects: improving our understanding regarding the molecular pathways involved in SCI and enabling us to study the efficacy of different therapeutic interventions (Cheriyan et al., 2014). Various methods have been used to study the pathophysiology of neural degeneration and regeneration, including some more artificial ones (e.g. photochemically induced spinal cord injury (Bunge, Holets, Bates, Clarke, & Watson, 1994) and lesions induced through the administration of chemical reagents directly into the spinal cord (D. Liu et al., 1999)). A recent review concluded that out of all the available models for simulating SCI, the ones relying on contusion and compression injury best simulate the biomechanics and pathology of human SCI

(Sharif-Alhoseini et al., 2017). In the following brief mechanistic classification, I will focus on the well-established *in vivo* approaches to traumatic SCI described in the literature, as I believe these have more resemblance to the clinical setting of SCI.

Transection models

In transection models of SCI, the continuity between the caudal and rostral segments of the spinal cord is severed after opening of the *dura mater*. A full transection refers to a complete severing of the spinal cord. A partial transection refers to a hemisection of the spinal cord (i.e. lateral or dorsal hemisection), in which some axonal segments are preserved. The lateral hemisection is usually sufficient to maintain bladder and bowel function, making post-operative animal care easier (Silva et al., 2014). Transection models are relatively easy to perform and have been used in a variety of animals including rats, mice, cats, dogs, and primates (Cheriyan et al., 2014). Although they have offered us significant insights into axonal degeneration and have been used to study axon regeneration (Alilain, Horn, Hu, Dick, & Silver, 2011), they are significantly different from the spinal cord injuries usually seen in humans. Moreover, partial transection models can be hampered by spared fiber tracts that can be mistaken as regenerated fibers (Steward, Zheng, & Tessier-Lavigne, 2003).

Distraction models

This technique involves the controlled stretching of the spinal cord. In such settings two clamps distract the spinal cord to simulate a remote or non-contiguous SCI, which is an infrequent manifestation of acute spinal trauma caused by a stretching mechanism (Silberstein & McLean, 1994). Several distractor devices have been used to study this particular type of SCI in cats, dogs, monkeys, and pigs. It is a comparatively minimal-invasive technique, as a laminectomy is not necessary. Some devices use a computer software to control and record the delivered force and to minimize the impact variability (Seifert, Bell, Elmer, Sucato, & Romero, 2011), while others can inflict contusion, distraction, and dislocation lesions using the same device (Choo et al., 2009). Still most of these devices have been used in only a limited number of studies and thus require further validation, since the majority are not commercially available (Cheriyan et al., 2014).

Compression models

The first type of such a model was first described in 1978 and used a modified aneurysm clip to compress the spinal cord (Rivlin & Tator, 1978). The clip is closed with a specific force around the spinal cord, producing an acute injury, and is then left to compress the cord for a select amount of time (Cheriyan et al., 2014). The resulting injury mimics the neuropathology observed in human SCI: it begins with haemorrhage and oedema, progresses to a phase or reorganization, and ends in a chronic phase, forming glial scars and a cystic cavity (Silva et al., 2014). It is a relatively inexpensive model, but the actually delivered impact force cannot be controlled. The clip compression model has been used extensively by the Fehlings laboratory (Joshi & Fehlings, 2002) and has provided valuable insights into the injury and repair mechanisms that are initiated after cord compression. An alternative compression model uses calibrated forceps to inflict the SCI and was first described in 1991 (Blight, 1991). Both models have been used in guinea pigs, rats, and mice. Although the forceps technique is comparatively simple and inexpensive, it also lacks the acute impact component that other models possess. Hence it does not simulate an important aspect of the most common human SCI mechanisms, making it much less common than other injury models (Cheriyan et al., 2014).

Contusion models

In comparison to the previously described techniques, the contusion model best mimics the lesions seen in humans after traumatic SCI (T. E. Anderson & Stokes, 1992). Contusion devices are designed to inflict a transient, acute injury to the spinal cord, using weight-drop apparatuses, electromagnetic mechanisms or even compressed air (Cheriyan et al., 2014). The Infinite Horizon Impactor (seen in Figure 3) is the most widely used, commercially available contusion device (Silva et al., 2014), which was one of the reasons we chose it for the present work. It was first described in a model of thoracic SCI in rats (S. W. Scheff, Rabchevsky, Fugaccia, Main, & Lumpp, 2003). The device uses a stepping motor controlled by a computer to inflict consistent and reproducible contusion injuries to the exposed spinal cord. A metal impactor tip causes the injury, and an attached sensor directly measures the force between the impactor and the spinal cord tissue. This minimises errors introduced by specimen movement. When the predetermined force threshold is reached, the tip is automatically and immediately withdrawn, and the exact force transmitted is displayed on the attached computer. Thus no

weight bounce phenomenon occurs (Cheriyan et al., 2014). This mechanism enables the device to deliver reproducible injuries of varying magnitudes, while all the data related to the mechanical parameters of the injury are recorded by the computer software (S. Scheff & Roberts, 2009). Although it is an invasive technique, which requires a laminectomy that preserves the *dura mater* and hence the acquisition of the necessary surgical skills, as well as a relatively pricey piece of equipment, we considered this model to be best suited for our present work as it is well-established to deliver a scalable and reproducible level of SCI.

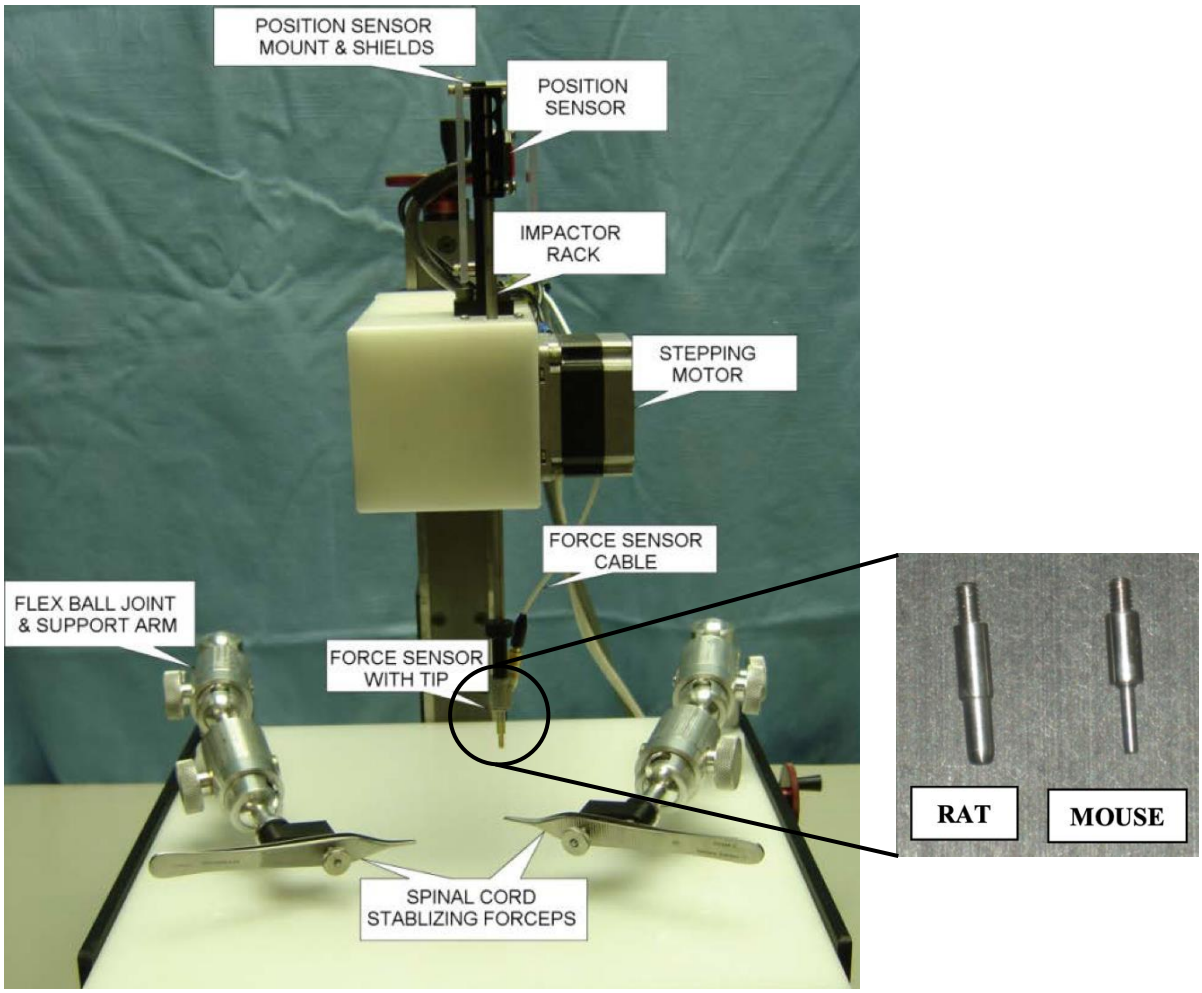

Figure 3: The Infinite Horizon Impactor (left) and a close-up view of the impactor tip (right) produced by Precision Systems and Instrumentation. The stepping motor propels the force sensor with tip. Figures taken from the device's user manual (Instrumentation, 2012).

1.6 *In vivo* imaging of spinal cord injury

To study the mechanisms that determine the divergent fate of contused axons, our laboratory has established a technique to image axons *in vivo* after spinal contusion in mice (Kerschensteiner et al., 2005; Williams et al., 2014). This model uses the Infinite Horizon Impactor previously described. By following sensory axons in the dorsal column over time using *in vivo* fluorescent techniques, my colleagues have found that contusion injury is characterised by a phase of reversible axon damage. During a critical time period of several hours after lesion, axons that have developed swellings in response to injury can either degenerate or recover (Williams et al., 2014).

Understanding the mechanisms of acute axonal degeneration after an impact injury poses major challenges if classic microscopy and static imaging tools are used. This is why we decided to use two-photon microscopy and genetically encoded calcium indicators to study the acute degeneration of spinal cord axons *in vivo*. Two-photon fluorescence light microscopy was invented by Denk and his collaborators (Denk, Strickler, & Webb, 1990) and has since revolutionised the way we image biological processes. Briefly, the technique uses the combined energy of two photons to excite a fluorophore. If the combined energy of the two photons is greater than the energetic gap between the ground state and the excited state, the fluorophore absorbing it will transition from the former to the latter. The fluorophore then emits fluorescent light while transitioning back to its initial ground state. The relaxation process is identical in one- and two-photon fluorescence. A schematic depiction of this process can be found in Figure 4.

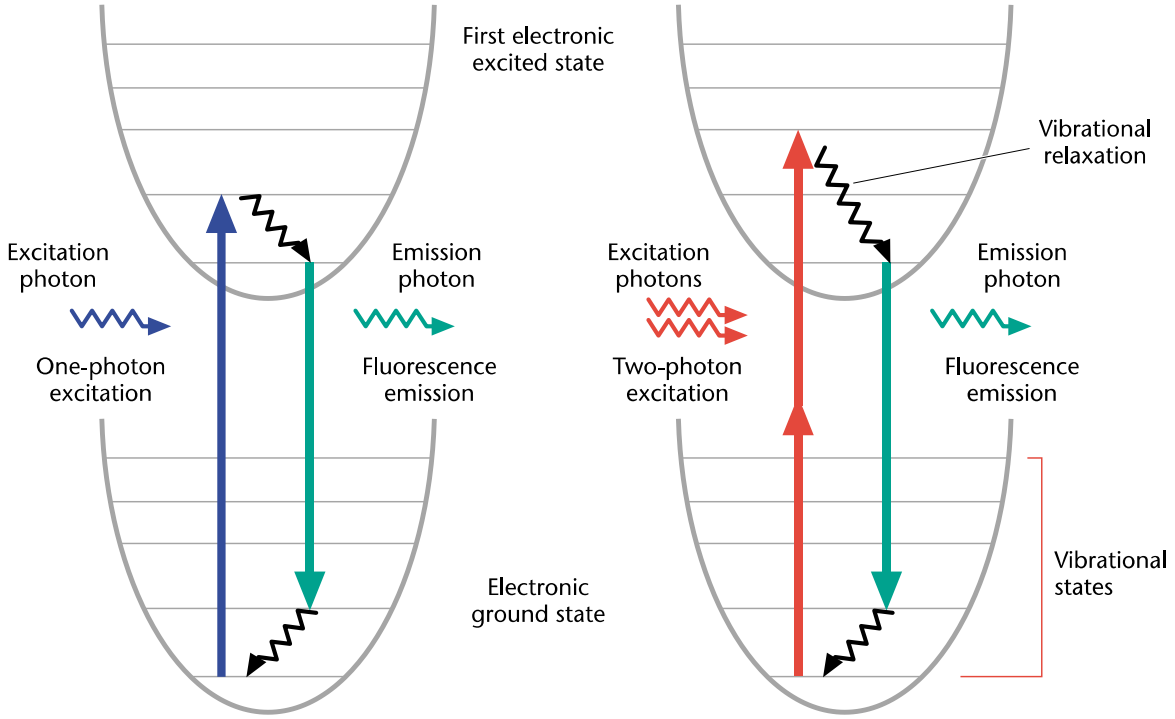

Figure 4: Jablonski diagram comparing the excitation of one-photon and two-photon fluorophores (So, 2001).

Two-photon microscopy offers a series of advantages compared to confocal microscopy. The first is the low phototoxicity of this technique, which is intrinsic to the way two-photon excitation is achieved. For a fluorophore to reach the excited state, it typically needs to interact with photons in the high energy (i.e. ultraviolet or blue/green) spectral range when using the single photon technique. The same effect can be achieved using much less energetic photons (i.e. in the red or infrared spectral range) when employing two-photon microscopy. But because the probability of a simultaneous absorption of two photons is extremely low, a high flux of photons is needed to elicit fluorescence. This flux is generated by a pulsed laser source, such as a titanium-sapphire laser. The direct result of using pulsed illumination is an extremely high instantaneous light intensity at the focal point, but a relatively low average energy absorption by the sample, making this technique exquisitely suitable for *in vivo* imaging (Rubart, 2004). Photodamage and phototoxicity, both of which are of concern when doing *in vivo* imaging over several hours, are thus significantly reduced using the low-energy photons generated by this light source.

Briefly, the laser emits ultrashort pulses of light (in the range of femtoseconds) at microsecond intervals (80-100 MHz). The light pulses pass through a dichroic mirror and are directed using mirrors to raster scan the specimen. After fluorescence is achieved at the focal point, the emission light travels back through the dichroic mirror, allowing us to separate multiple emission wavelengths and only the desired wavelength to reach the detector.

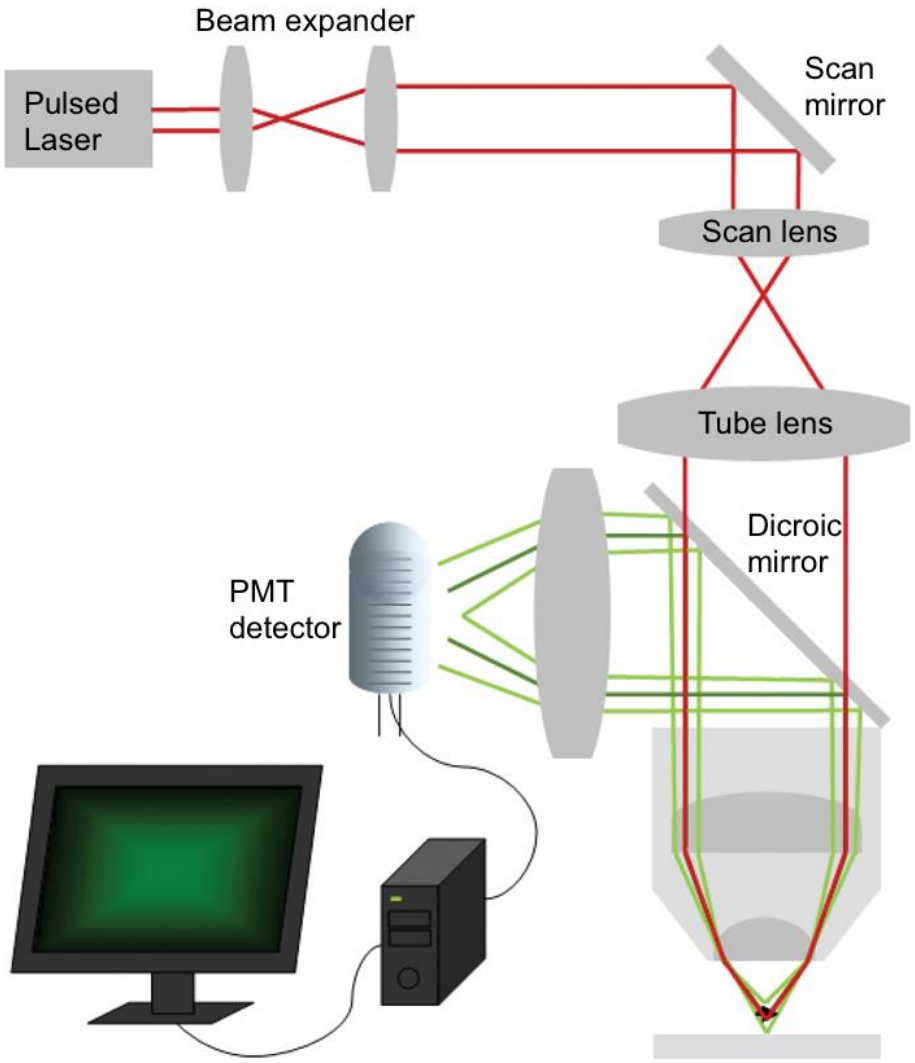

Figure 5: Schematic representation of a two-photon microscope setup. Figure modified from (Franke & Rhode, 2012).

The other advantages of the two-photon approach are the minimization of light scattering, the reduction of excitation outside of the focal point (leading to a suppression of background signal), and increased imaging depth, making it possible to image cells up to 1000

μm beneath the sample surface. First, near-infrared light is less scattered in biological tissues compared to shorter wavelength visible light. Furthermore, CNS tissue is more transparent to photons in the near infrared spectrum, like the ones typically employed by two-photon systems. Second, fluorescence is only emitted at the focal point, where excitation photon density is high enough, offering a high sensitivity. The probability of two excitation photons arriving almost simultaneously at the same point in space is directly proportional to the square of the intensity (Rubart, 2004). The intensity of the beam also decreases with the square of the distance above and below the focal plane (Franke & Rhode, 2012). Thus, any sample point minimally distanced from the focal point will not achieve the necessary photon energy to emit fluorescence. Moreover, any scattered excitation light also does not elicit fluorescence and hence does not contribute to out-of-focus emission. In comparison, systems employing one-photon microscopy have two sources of out-of-focus light: excitation above and below the focal plane, as well as fluorescence elicited by scattered photons. Another advantage is depth discrimination. One-photon microscopy generates uniform fluorescence from each section above and below the focal plane. In contrast, two-photon microscopy allows us to concentrate about 80% of the total fluorescence signal in a region of approximately 1μm around the focal point (So, 2001).

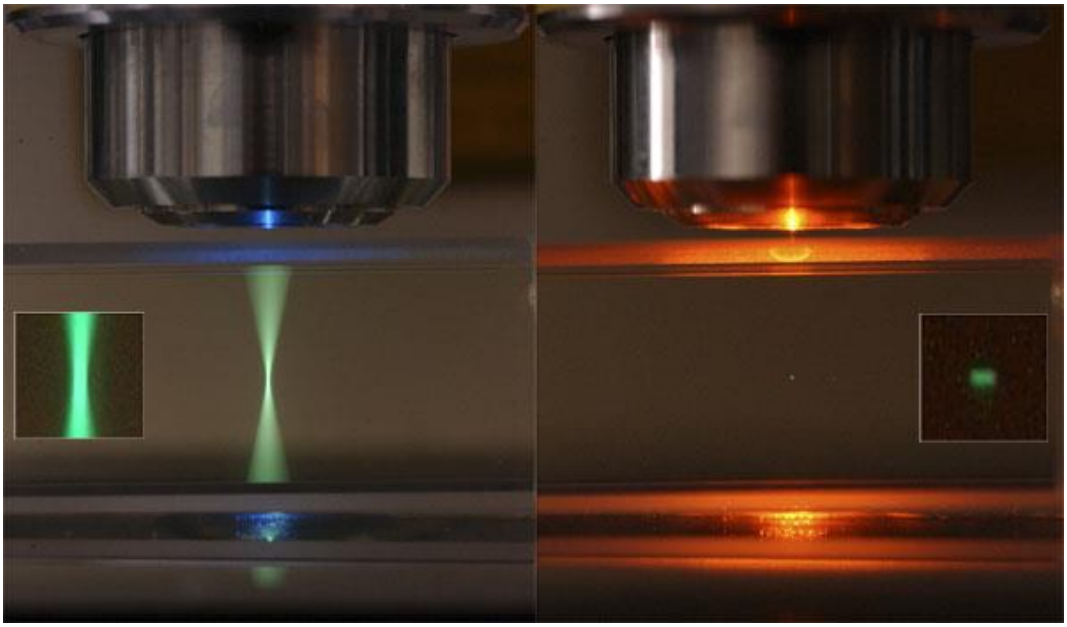

Figure 6: Comparison between the excitation area using one-photon microscopy (left) and two-photon microscopy (right). Image by (Ruzin & Aaron) from http://microscopy.berkeley.edu/courses/TLM/2P/index.html

The major disadvantages of this technique are the technical know-how needed to operate and the costs required to acquire a two-photon microscope, as well as the lower resolution of the technique due to the longer excitation wavelength and the larger spectral overlap of many fluorophores in 2-photon excitation compared to one-photon confocal imaging. Moreover, compared to other imaging modalities, such as widefield or light-sheet imaging, conventional scanning 2-photon imaging is relatively slow. Extremely expensive lasers are needed (see below) and excitation cross sections tend to be broad, making multi-wavelength imaging challenging. Still, as our experimental design largely allowed us to use a single excitation wavelength, the two-photon technique was best suited for our experimental model.

To study the acute degeneration of axonal tracts after impact injury and to continuously monitor the same structures over 4 hours post impact, it is essential to choose an approach that permits single cell differentiation. Transgenic mice, which have been genetically modified to express fluorescent sensors, are an established model in the field of *in vivo* imaging of axonal degeneration and fulfil the criteria required for such an experiment. These sensors are specifically tailored to permit the study of intracellular calcium concentration, which plays a pivotal role in axon degeneration. The class of genetically encoded fluorescent calcium indicators we used was extensively described by our collaborators in previous works (Direnberger et al., 2012; Garaschuk, Griesbeck, & Konnerth, 2007; Geiger et al., 2012).

For most of our experiments, we used a ratiometric troponin C-based calcium indicator (TN-XXL), in which a troponin molecule is sandwiched between a cyan fluorescent protein (CFP) and a circularly permuted Citrine (cpCitrine) fluorescent protein, as shown in Figure 7. The troponin molecule causes the sensor to react to increases in the intracellular calcium concentration, causing a conformational change of the molecule. In this contracted state, the CFP acts as a donor and the cpCitrine as an acceptor fluorophore. Briefly, light of ~430 nm wavelength (one-photon) / ~840 nm (two-photon) is used to excite the CFP fluorophore. If the intracellular calcium concentration is low, the sensor will predominantly emit light around 480 nm wavelength. If the intracellular calcium levels are high, the troponin will cause the molecule to contract, allowing the absorbed energy to be passed to the cpCitrine fluorophore. The latter will then emit light centered on ~530nm wavelength and hence the fluorescence emission spectrum of the probe will shift towards the red side of the spectrum. This energy transfer is called fluorescence resonance energy transfer or Förster Resonance Energy Transfer (FRET).

It enables us to use the TN-XXL fluorophore as a ratiometric sensor, permitting the study of intracellular calcium levels after the impact injury. While single fluorophore calcium sensors also exist, they are less suited for the purpose of the current thesis, being prone to bleaching, increased pH-sensitivity, and higher movement artifacts. The main advantages of a FRET based ratiometric sensor like the one depicted in Figure 7 during *in vivo* imaging are insensitivity to movement artefacts, a consistent expression level, and resistance to bleaching (Garaschuk et al., 2007).

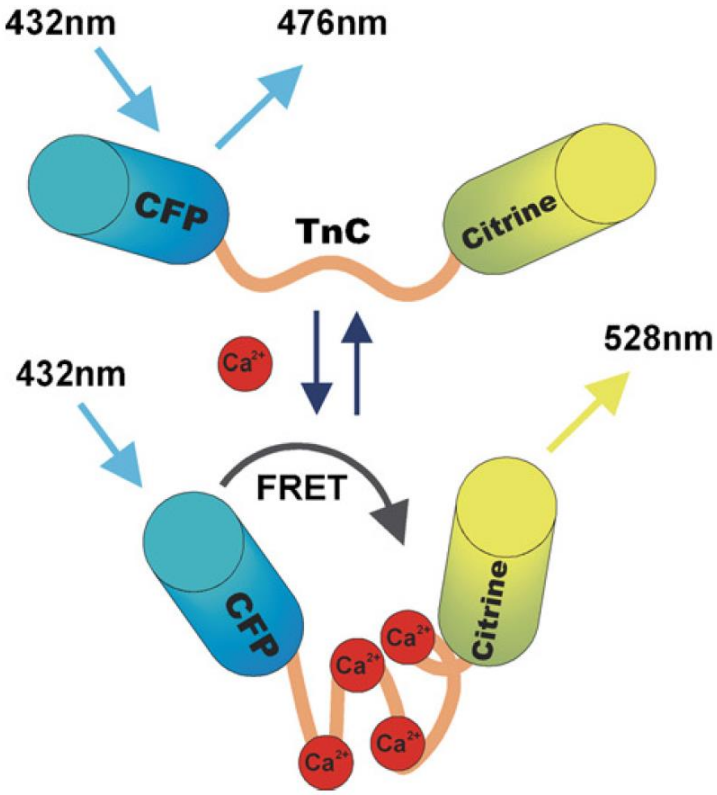

Figure 7: Schematic drawing of the TN-XXL calcium sensor protein and its conformational change after fluorescence resonance energy transfer (Garaschuk et al., 2007).

The above-described approach allowed us to continuously image large populations of axons before and after the impact injury, and to perform a retrospective analysis of fate predictors (e.g. high calcium levels, axonal swelling). We then performed follow-up experiments to pharmacologically manipulate the underlying degeneration pathways, combined with a direct optical assessment of alterations in axonal fate - an approach that is much more direct than analyses based on histological post-mortem examination (Misgeld & Kerschensteiner, 2006).

1.7 Aim of the thesis

The aim of the current project was to (i) to establish a reproducible methodology around this impact injury model, (ii) to identify factors that could influence or bias the results during continuous *in vivo* imaging of injured axons, and (iii) to find pharmacological mediators that could be employed to change the fate of contused axons in favour of recovery.

After careful study of the existing literature, I could gain some insights about the distinctions between the three stages of post traumatic neurodegeneration, as well as the therapeutic and experimental approaches currently in use. Given the extensive experience our laboratory has in using single cell *in vivo* imaging of the spinal cord to study axonal fate after primary transection or under immune attack (Misgeld & Kerschensteiner, 2006; Misgeld, Nikic, & Kerschensteiner, 2007; Sorbara, Misgeld, & Kerschensteiner, 2012), we aimed the project to which this thesis contributed, to the study of secondary axon degeneration after mild spinal cord contusion. Inspired by the critical time window for revascularization in stroke patients, we hypothesised the existence of a similar treatment period for spinal cord impact injuries, during which an intervention would lead to less axonal degeneration.

To achieve the aforementioned aims I analysed the mechanical, surgical, and pharmaceutical factors involved in creating such a model. To implement a reproducible methodology, it is paramount that the operation of all the equipment is done in a systematised fashion. Hence, I outline every step in detail. I also underline possible caveats that can appear during the impact, the fixation, or the imaging process. The surgical techniques used in this project require an exact operation of the mechanical equipment involved and a high amount of surgical dexterity and consistency to not bias the outcome of the experiment, especially when combined with the local application of pharmaceutical mediators. I therefore describe a set of reproducible steps based on anatomical landmarks, which can be applied to several models that use transgenic mice. I also studied the interaction between intact or acutely injured axons and different pharmaceutical agents. Finally, I describe an automated image processing method and a data analysis approach, which allowed our results to be reproduced by two researchers with varying degrees of expertise. I believe that our specific approach for studying acute spinal cord injury *in vivo* can make a unique contribution to this field.

2 Materials and Methods

2.1 Animals

I used male and female transgenic mice aged between 10 and 20 weeks. I chose the Thy1-TNXXL strain to study axon morphology, calcium dynamics, and pharmacological response (Mank et al., 2008). For the experiments regarding photostability and pH sensitivity, I used the Thy1-YFP16 x Thy1-CFP5 mouse line (Griesbeck, Baird, Campbell, Zacharias, & Tsien, 2001). The mouse lines were obtained from collaborating laboratories or Jackson Laboratories, then bred and raised in our facility. The breeding facility is tested quarterly to monitor the health status of the animals. All experiments were conducted in accordance with local regulations and approved by the Bavarian government (Regierung von Oberbayern).

2.2 Surgical procedure

I performed all surgical procedures and acquired the resulting images based on the methods described by Misgeld et al. (Misgeld et al., 2007) and Romanelli et al. (Romanelli et al., 2013). I did all the procedures following an adapted protocol established in our laboratory.

Preparation

I anaesthetised the mice with ~0.25 ml anaesthetic (Ketamine 87 mg/kg, Xylazine 13 mg/kg) injected intraperitoneally, using a 0.5 ml insulin syringe (U-100 BD Micro-Fine). Afterwards, I placed them on a heated surface to ease the maintenance of their physiologic body temperature. I also placed them in a receptacle that protected them from ambient light, to prevent any unnecessary stress during the initial stages of anaesthesia. After ten minutes I checked for pain response to toe pinching. In the case of a positive response (e.g. twitching), I put the mouse back in the receptacle for another ten minutes, after which I repeated the check. When no pain response was obtained, I continued with the hair removal. This was done using a conventional hair trimmer while holding it under the nozzle of a vacuum cleaner. Afterwards, I wiped the trimmed area with a tissue soaked in ethanol, to ensure sterile operating conditions and to remove any leftover hair fragments. For the surgical procedure, I placed the mouse on a heating pad, restrained its limbs using rubber bands, and covered its eyes with eye-cream (Bepanthen Eye and Nasal Ointment 5%) to prevent them from drying.

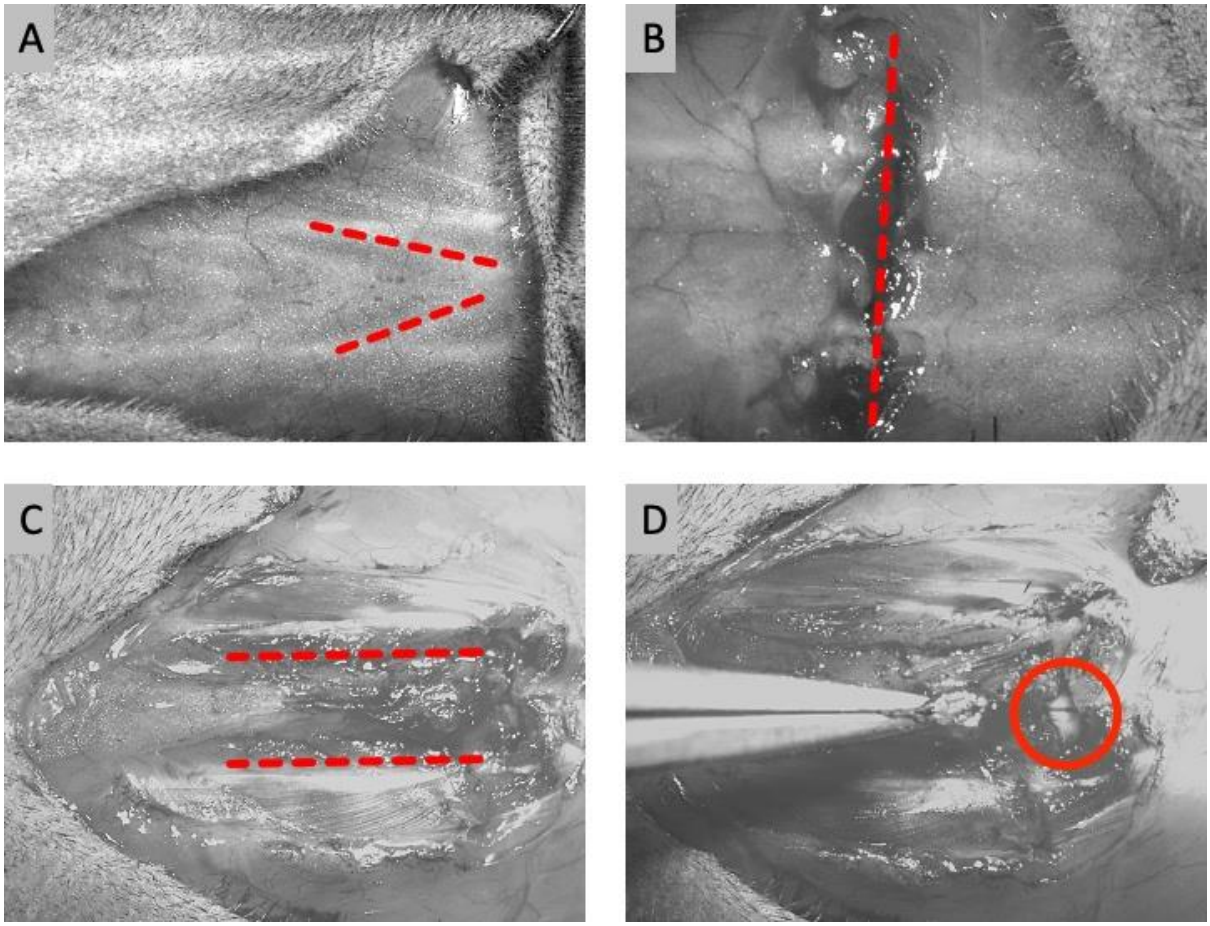

Figure 8: To access the lumbar spinal cord of the anesthetised mouse, I used several anatomical landmarks for orientation (e.g. the ligaments outlined in panel A). I performed the first muscular incision transversally (panel B), followed by two longitudinal incisions caudo-rostrally (panel C). Afterwards, I lifted the resulting U-shaped muscle patch to expose the spinal cord (encircled in panel D). In all panels the rostrum is on the left.

Muscular incisions

From this point on I performed all the steps using a surgical microscope (Olympus SZ61). For precise handling, I used two types of forceps (Fine Science Tools, Dumont #2 Laminectomy Forceps – 12 cm and Dumont #3 Forceps – 12 cm). I first made a small longitudinal skin incision along the most elevated point of the vertebral column (i.e. mid thoracic region) using the muscle scissors (Fine Science Tools, Noyes Spring Scissors with 14 mm blades). Then I placed a medical gauze cylinder under the mouse, to lift the surgical site. This offered me better access to the spinal cord by bending the dorsal side of the vertebral column in a convex way, thus increasing the gaps between the vertebrae. I applied retracting hooks to spread the skin and get better visibility of the surgical site. To ensure comparable

results, a consistent reproduction of the surgical procedure is essential. Therefore, I used the following anatomical orientation landmarks (ordered by importance): (i) the larger lumbar vertebrae with their prominent dorsal processes, (ii) the v-shaped ligaments along the vertebral column, and (iii) the superficial blood vessels running perpendicularly to the vertebral column. These anatomical landmarks can be seen in panels A and B of Figure 8.

To determine the optimal location for the initial, transverse muscular incision, it was important never to cut caudal of the V-shaped ligaments shown in Figure 8A. Hence, I aimed for the region located 1-2 vertebrae caudal of the first lumbar vertebra and of the above-mentioned vascular landmarks. To find the intervertebral gap, I gently glided the forceps along the vertebral column, searching for the rostral side of the spinal process. After finding the proper intervertebral space, I performed the initial muscular incision in the transverse direction, by holding the muscle scissors perpendicularly to the vertebral column and cutting across between two vertebrae. The cut was made in the axial plane, close to the rostral end of the spinal process of the caudal vertebra, and spanned across the whole intervertebral space, cutting the intervertebral ligament as well as the paravertebral ligaments found on both sides of the vertebral column at that level (see Figure 8 panel B). It is paramount not to damage the spinal cord while performing the sagittal intervertebral cut.

Starting from the sagittal incision, I performed two more cuts longitudinally and rostrally along the next two vertebrae, running tangentially to the bone, as shown in Figure 8 panel C. The paravertebral ligaments were kept intact, because they offer stability to the spinal column, thus minimising the movement artefacts during image acquisition. At this point, the resulting three muscular incisions resembled a U-shape (as shown in Figure 8 panel C), with the opening in the rostral direction and a strip of muscle located between the lateral cuts. I intentionally preserved this tissue to use it as a handle during the laminectomy (see Figure 8 panel D).

Next, I used the bone scissors (Fine Science Tools, Vannas Spring Scissors with 4 mm blades) to cut the *ligamentum flavum* and/or any muscular tissue left between the vertebrae after the initial cut. It was important to always hold the scissors with the tip pointing laterally, never towards the spinal cord, and to cut through the whole width of the vertebral column. After all the muscle was trimmed away, the spinal cord and a prominent dorsal vein were exposed (as seen encircled in Figure 8 panel D).

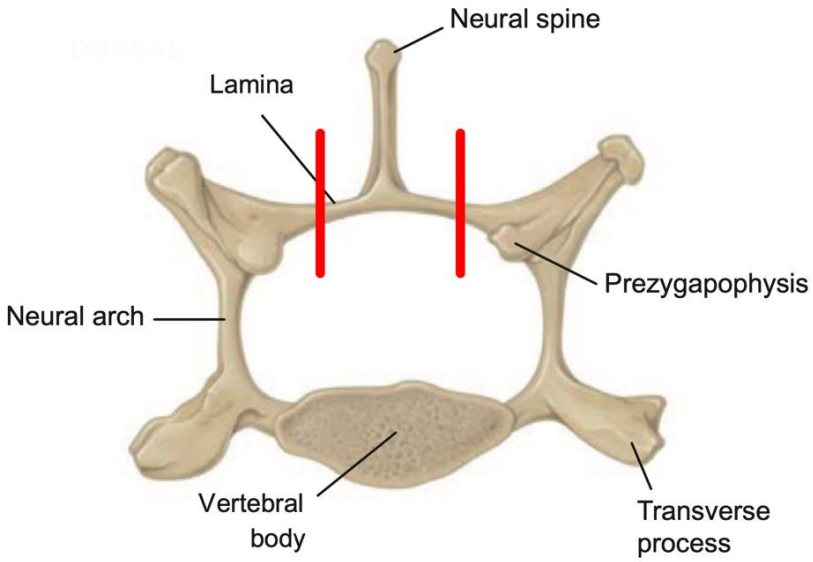

Figure 9: Mouse vertebra with the laminectomy lines marked in red. Figure modified from Comparative Anatomy and Histology: A Mouse, Rat, and Human Atlas (Jerome, Hoch, & Carlson, 2018).

Laminectomy

This is the most delicate part of the whole surgical procedure. It is of the utmost importance to perform the following steps without causing any damage to the spinal cord or the *dura mater*. To ensure optimal visibility, I cleaned any traces of blood using Sugi absorbent swabs (Kettenbach). I started the laminectomy by cutting the first rostral vertebra adjacent to the exposed spinal cord. During this step I lifted the vertebra by pulling on the muscle strip found on top of the spinal process, thus widening the intervertebral gap (as shown in Figure 8 panel D). Then I inserted the bone scissors between the spinal cord and the vertebra, on the lateral edge of the spinal process. To avoid damaging the spinal cord or the *dura mater*, I cut by always holding the blade of the scissors parallel to the spinal cord, while constantly keeping the scissor blade close to the lamina and avoiding any pressure on the spinal cord. First, I severed the lamina on one side of the spinal process, then on the opposite side (as indicated by the red lines in Figure 9). For cutting the laminae I used the Fine Science Tools bone scissors (Vannas Spring Scissors) with 4 mm blades.

If both lateral cuts span the whole length of the vertebra, the dorsal surface of the entire vertebra was at this point free and could be lifted from the spinal cord. This marked the first half of the laminectomy. For the second half, I repeated the steps listed in the previous

paragraph on the next rostral vertebra: lifting the vertebra by pulling on the free bone fragment, inserting the scissors parallel to the spinal cord and cutting the bone along its whole length, on each side of the spinal process.

At this point the spinal cord was exposed over the length of two vertebrae and the resulting two bone fragments were connected only on the rostral end by muscular tissue. I then cut this connecting tissue and disposed of the two bone fragments. Next, I removed the gauze cylinder placed underneath the mouse, cleaned the surgical site with artificial cerebrospinal fluid (aCSF) and covered the exposed spinal cord with an absorbable haemostatic gelatin sponge (Spongostan) to reduce bleeding and prevent the tissue from drying out.

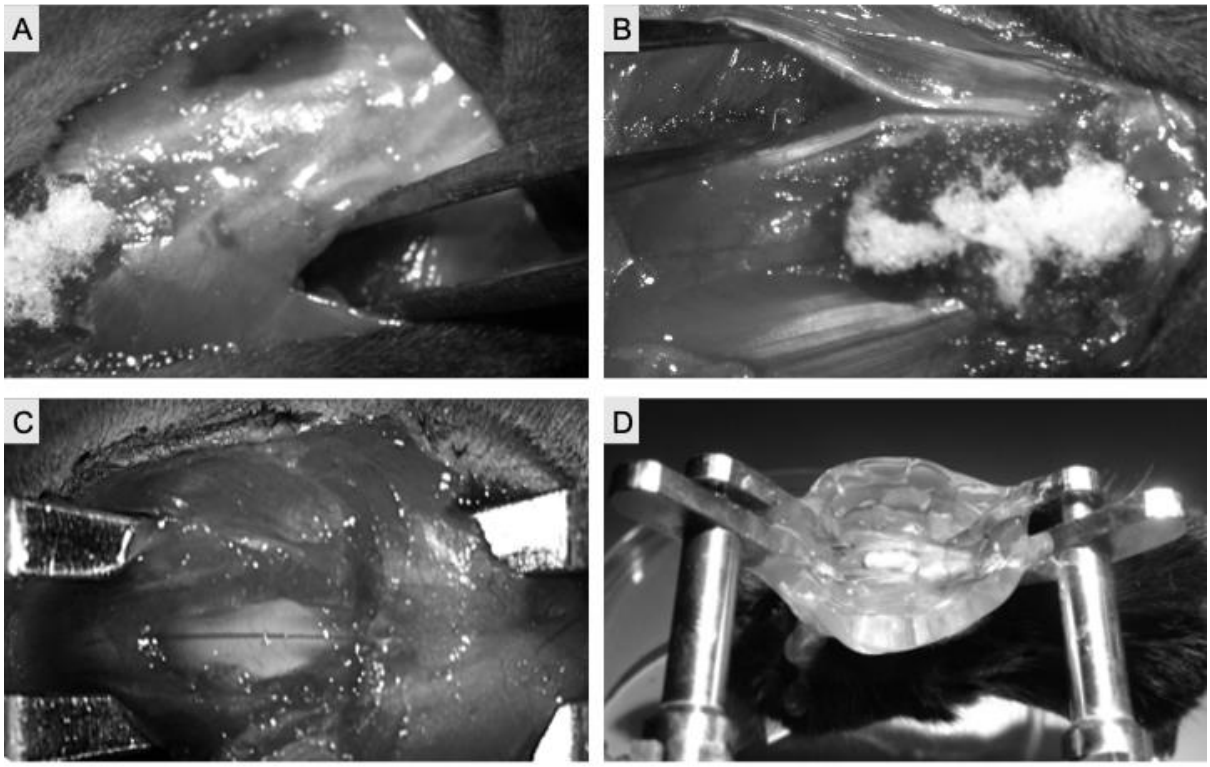

Figure 10: After performing the laminectomy, the mouse must be stabilized for the subsequent impact injury and imaging. For this I used the Narishige Compact Spinal Cord Clamps. The rightmost arm was used to clamp the tail, the middle one was inserted in the two caudal incisions in the lumbar region (panel A), and the leftmost arms was inserted in the two rostral incisions between tendons of the upper thoracic region (panel B). During the fixation the exposed spinal cord was covered with a gelatin sponge, which was briefly removed before final fixation to check for proper blood flow in the central vein, as well as positioning of the clamps and sample (panel C). Any debris were also removed during this step using aCSF. Afterwards I used a heated solution of 2% agarose dissolved in aCSF to build a watertight reservoir around the laminectomy site (panel D). Finally, the reservoir was filled with aCSF and different pharmacological compounds, depending on the experiment.

Clamping

To improve sample stability during imaging I used the Compact Spinal Cord Clamps (Narishige), which have three arms (Davalos et al., 2008). Each arm of the device has a clamp at its end, further referred to as the rostral (left), caudal (middle) and tail clamp (right).

To fixate the spinal column, I first used the spinous processes of the vertebrae for orientation, to find the second vertebra caudal to the laminectomy. I then made two symmetric cuts, one on each side of this vertebra, using the muscle scissors. The cuts had to be deep enough to reach under the vertebra and ran tangentially to the bone, to avoid muscle fibres getting stuck between the clamps and the bone (see Figure 10 panel A). An important caveat to consider during clamping is the position of the clamps along the dorsal column. Clamping between the bodies of two vertebrae can cause ischaemia and/or crushing of the spinal cord. To avoid this, the cuts were done along the length of the vertebra and not between the two vertebrae. Furthermore, by cutting in an oblique, caudo-rostral direction, similar to the insertion angle of the caudal clamps, I eased the clamping of the vertebral body.

Next, I used the vertebral processes to find the first vertebra rostral of the laminectomy. I cut any connective tissue covering the paravertebral ligaments at this level to expose these fibres. Once I could see the ligaments clearly, I looked for a ligament that connected to the first vertebra rostral to the laminectomy. Using the forceps to spread the gap between this ligament and the one next to it, I made a superficial cut between them, using the muscle scissors. This cut had to run along the ligaments without damaging them. This is another important aspect, since intact ligaments add stability to the sample during the imaging process. Using the forceps to spread the gap further, I severed the muscle fibres between the two ligaments using a scraping motion, rather than cutting, to avoid any damage to the rib cage. The depth of the cut has to end at the rib cage and its length must run up to the vertebra rostral to the laminectomy, but not beyond it. Next, I used the same technique to make a symmetric cut on the contralateral side of the vertebral column (see Figure 10 panel B).

Replication of the clamping procedure across different users is both important and difficult. For the present work, both users followed a fixed set of instructions at all times. The middle arm had always to be kept in a fixed position: raised ~1.5 cm and placed approximately in the middle of the clamping device, with the lower side of the clamps parallel to the table. The alignment of the clamping tips was checked through the microscope and adjusted if

necessary. The clamping of the sample was always done in the following order: (i) caudal, (ii) tail and (iii) rostral.

Next, I started clamping the sample by sliding the clamps in the cuts while pushing the mouse upwards and towards the clamps. Once the clamps were well positioned inside the cuts, I tightened the clamps. While tightening the clamps on the sides of the vertebra I observed the central vein (shown in Figure 10 panel C): if the blood flow is reduced while tightening, the clamps are either too tight, or they were placed between two vertebrae. In the latter case, the clamps have to be repositioned. Only after the mouse was clamped, I proceeded to adjust the orientation and angles of the rostral clamps, to get a straight and flat position of the spinal cord along the laminectomy site.

Sample preparation

First, I cleaned the surgical site by repeatedly washing it with aCSF. To remove persistent debris, I gently wiped the surface of the spinal cord with a small piece of a wet gelatin sponge, which can be seen in panels A and B of Figure 10.

To enable the use of a water-dipping-cone microscope objective, I constructed a reservoir around the imaging site. As building material, I used 2% agarose dissolved in aCSF. First, I heated the agarose in a microwave oven until a small portion of it melted (approximately 1-1.5 minutes at 700W). I kept the spinal cord covered with gelatin sponge to avoid the agarose running on the imaging site. As the fluidity of the agarose solution is directly proportional to its temperature, I applied it in layers using a pipette, each time waiting for the previous layer to cool down and become solid enough to support a new layer. Special attention was given to building a watertight structure, as this was essential for the subsequent imaging steps. Sealing the spaces between and around the rostral and caudal clamps is paramount.

I then removed the patch of gelatin sponge and filled the reservoir with aCSF, checking for potential leaks. If permeable spots are found, these must be filled with agarose before proceeding to the imaging phase. After this check, the sample is ready for image acquisition using a water-immersion dipping-cone objective.

2.3 Image acquisition

I acquired the images using a commercially available Olympus FV1000 MPE microscope equipped with a femto-second pulsed Titanium-Sapphire Laser (Mai Tai HP, Newport/Spectra-Physics). For excitation of the YFP I used light with a wavelength of 920 nm, while for studying calcium dynamics I tuned the laser to 840 nm and 4-6% power to excite the CFP. To detect the signal, I used gallium arsenide phosphide (GaAsP) and conventional multi-alkali photomultiplier tubes set at 500-600 mV voltage. All light was filtered through a 690 nm short pass dichroic mirror. For YFP imaging I used a 540/40 nm barrier filter in front of the detectors. To detect the FRET signals in Thy1-TNXXL mice, I used a CFP/YFP cube consisting of a 505 nm dichroic mirror to separate the signals from CFP and cpCitrine, as well as a 480/40 nm and 540/40 nm filter set in front of the detectors. For imaging FRET signals, emission light was first passed through a 565 nm short pass dichroic mirror and a CFP/YFP cube was positioned in front of GaAsP detectors. The objective used was a water-dipping-cone objective (Olympus 25x / 1.05).

Before acquiring images, I used the built-in confocal system at 405 nm and 0.1% power to find the site where the impact injury will be performed, using vascular landmarks. I looked for a sufficiently flat portion of the spinal cord, which would permit the acquisition of uniform stacks and minimise artefacts caused by breathing motion. These stacks would contain about 40-60 images recorded at a z-step size of 0.8 µm. Image stacks were acquired as pairs with roughly 10-20 µm of overlap along the rostro-caudal axis, resulting in an imaged volume of roughly 500 x 250 x 50 µm. Each image was recorded at a resolution of 640 x 640 pixels and 2x zoom, resulting in a pixel size of 397 nm. Every image was averaged twice using a Kalman software filter. The stacks were acquired at intervals of 10 minutes, with the first images recorded 3-10 minutes after impact injury.

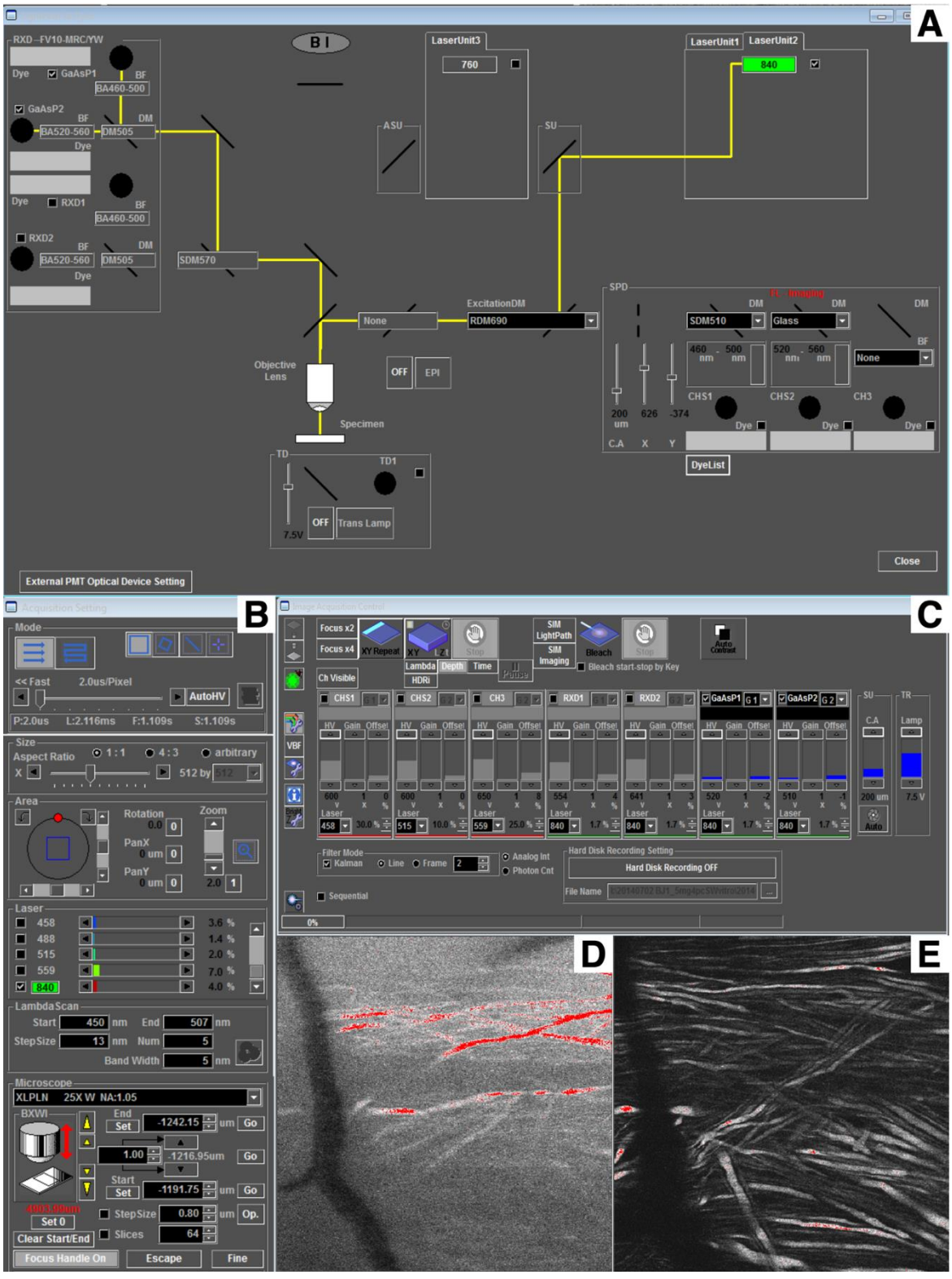

Figure 11: Screenshots from the software setup of the Olympus FV1000 MPE microscope used during *in vitro* recording showing the light path configuration (panel A), the raster scan and laser parameters (panel B), and the configuration of the GaAsP detectors (panel C). Panel D shows an orientation image obtained the built-in confocal system at 405 nm, while panel E shows an image of the same anatomical site acquired using the 2P system at 840 nm.

After selecting the imaging area, I recorded a set of pre-injury images. I then placed the clamping device under the Infinite Horizon Impactor (Precision Systems and Instrumentation). To properly target the impact region, I used the vascular landmarks to find the same site where the pre-injury images were recorded. Then I introduced the desired strength in the software controlling the impactor device (35-50 kDynes) and lowered the metal tip perpendicularly to the *dura mater* until it barely touched it. Immediately after the impact injury I remounted the clamping device under the microscope and recorded images from the same site as before.

I experimented with varying degrees of force and found that using a high impact force (i.e. 50 kDynes or more) caused severe damage to the vasculature, thus making it very difficult to find the same imaging site after the injury. Applying a low impact force resulted in a reduced number of fragmented and swollen axons. The ratio of intact/affected axons also varied with individual surgical skills and there were small differences between the programmed and the delivered impact force. I found that a force of approximately 40 kDynes rendered the best results.

After each stack acquisition, I replaced the aCSF in the agarose reservoir with clean aCSF heated at 37°C. I also checked for pain response to toe pinch every 60 minutes. If the response was positive, I injected a supplementary dose of anaesthetic intraperitoneally. Using the initially acquired images, I made sure all subsequent images were recorded from the same site, compensating for sample drift if necessary. The imaging was carried out for 4 hours after injury.

2.4 Image processing

I processed the raw data using FIJI (Fiji Is Just ImageJ), an open source, Java based image processing software (Schindelin et al., 2012). Given the large volume of data and the repetitive operations done for each image stack (about 50 stacks for each 4-hour study), I programmed a macro that significantly reduced the image processing time. The user could thus communicate with the macro through a graphical user interface. This lowered the risk of errors during this processing step and enabled any other person to use it, even without having previous programming experience. Briefly, the macro first prompts the user to manually enter the minimum and maximum intensity values for the two pseudo colours (i.e. red and green) used

for the CFP and cpCitrine signals. It then adjusts the lookup table for each of the two channels, creates a composite image, and performs a z-projection of all the slices. Lastly, it saves the resulting image under two formats (TIFF and PNG) and automatically moves on to the next raw data file. The whole process is repeated until all the files in the raw data folder are processed. During the whole operation, the macro offered real-time feedback to the user, informing him about the current step and offering an overview of the whole process. Upon successful completion, a confirmation dialog is displayed.

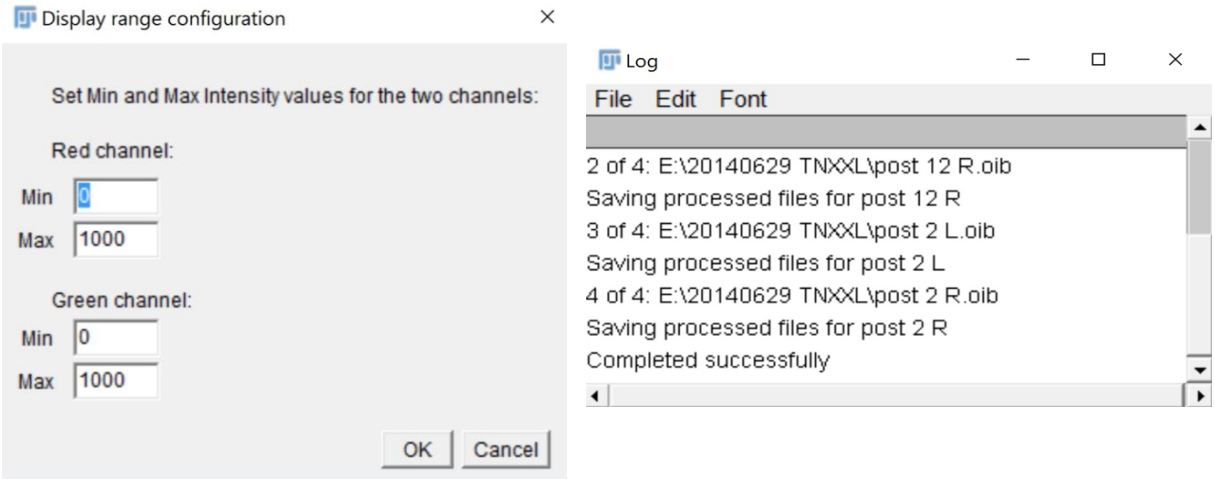

Figure 12: Partial screenshot of the FIJI macro I wrote to automate one of the image processing steps, showing the inputted intensity values for the two pseudo-colours on the left and a progress log on the right.

I then post-processed the resulting z-projected images using the image-processing software Adobe Photoshop. For each recorded time point I now had two z-projections, which overlapped by about 10-20 µm (for details see the Image acquisition section). By using this overlap as a guide, I manually stitched the two images into one overview image. Next, I imported all the resulting files in FIJI, thus obtaining a chronologic succession on the recorded data, which could easily be stitched and then viewed as a short video clip. Lastly, I applied the Scale Invariant Feature Transform registration plugin constrained to XY-translation and saved the resulting clip as a video file.

2.5 Data analysis

In the analysis we included only axons that could be followed over a distance of at least 50 μm during the whole duration of the experiment (i.e. 4 hours after impact injury). We observed the morphology of the axons and their calcium levels, using the Thy1-TNXXL line. As the selection of axons was done manually, we note the possibility of subjective bias towards axons with greater diameter and higher signal. Collateral neurites were excluded from the analysis, because in most cases they degenerated immediately after impact. We believe that this did not bias the result of our analysis, as these neurites were not encountered in all recordings and represented only a small population of the imaged axons (1-2 per sample).

For each axon included in the analysis we recorded the morphology and the calcium level at each time point, the first being immediately before the impact injury and the last being 4 hours after the lesion. For the morphologic analysis, we used a ternary grading system, in which all axons were in one of three possible states: intact, swollen, or fragmented. To improve grading accuracy, we studied the whole time-lapse recording, thus enabling a better estimation of the exact time point when an axon was swollen or fragmented. We verified each observed transition by manually adapting the contrast settings for the axon in question in the unprocessed image stacks. To confirm fragmentation, we looked for a sudden, clearly identifiable signal drop, which was consistent over the following time points. A characteristic "pulling-apart" motion of the axon on either side of the fragmentation point was also used as an indicator of fragmentation. The rare instances where ambiguities remained were excluded from the analysis.

For the FRET measurements indicating the rise in calcium levels we used a binary grading system: normal or elevated. We measured the calcium levels in the initial state (i.e. pre-injury) for all axons included in the analysis. Then we measured the signal at each transition point observed during the time lapse, as well as at the last recorded time point. For each measurement, we recorded the highest cpCitrine/CFP ratio along an axon and subtracted the background signal around this region. We then used the result as the calcium signal for that particular time point. If the resulting calcium signal was at least 50% higher than the initial measurement, we rated it as elevated. To verify that the FRET ratios were not influenced by pH changes after injury, we performed a set of injuries on Thy1-YFP16 x Thy1-CFP5 mice, in which YFP acted as a pH sensor.

2.6 Pharmacological experiments

Rise of intra-axonal calcium can lead to the activation of proteolytic cascades, which in turn lead to axon degeneration (Ma, 2013). To identify the possible sources of such calcium influx, I pharmacologically blocked several classes of calcium-transporting ion pumps, calcium-permeant ion channels, and ligand-gated receptors. Based on a literature review of potential sources of calcium influx in axons, I added the following blockers to the aCSF solution used in the contusion experiments, thus targeting three influx pathways: (i) Bepridil hydrochloride (Sigma-Aldrich, 200 µM in aCSF) to block the sodium-calcium exchanger that might operate in reverse direction after injury (Stys & Lopachin, 1998; Stys et al., 1992), (ii) Nimodipine (Sigma-Aldrich, 10 µM in aCSF) and ω-Conotoxin GVIA (Tocris, 1 µM in aCSF) as a combination of blockers for voltage-gated calcium channels likely to be present in axons (Ouardouz et al., 2003; Stys, 2005), and (iii) CNQX disodium salt (Tocris, 50 µM 6-Cyano-7-nitroquinoxaline-2,3-dione in aCSF) and MK 801 maleate (Tocris, 300 µM in aCSF) as a blocker of glutamate receptors that were reported to contribute to axon degeneration in other settings (Ahuja & Fehlings, 2016; Bakiri et al., 2008; D. Liu et al., 1999; Ouardouz, Coderre, Basak, et al., 2009; Ouardouz, Coderre, Zamponi, et al., 2009; Ouardouz et al., 2006). For the control group, I used dimethyl sulfoxide (Sigma-Aldrich DMSO, 0.5% in aCSF), as this was the solvent for some of the listed blockers. To facilitate the access of the calcium blockers to the respective channels, I made small holes in the *dura mater* using a dural hook crafted from the needle of an insulin syringe. The holes were always located laterally, on one side of the spinal cord, at the rostral and/or caudal end of the laminectomy. I then imaged the contralateral side of the spinal cord. In the case of the above-mentioned solutions, I pre-incubated the samples for 30 minutes. Then I performed the impact injury and kept applying the solution for 60 minutes after injury. All the solutions in the agarose well were replenished every 10 minutes and kept at body temperature during the whole experiment (as described previously).

3 Results

The results detailed in the following sections have been published in part in the paper authored by Williams et al. (Williams et al., 2014). As such, it is important to keep in mind that they were performed during the review process of this paper (at the request of one or more reviewers). Other results, not included in the paper above, offer a more rounded view of the project, going beyond the experimental hypothesis, including aspects like knowledge transfer and inter-experimenter reproducibility, which are essential for any research project.

3.1 Force calibration

To set up a protocol that would repeatedly produce the desired level of spinal cord injury, I first had to determine the adequate impact force. My objective was to have over 50% of the axons affected by the impact, while still obtaining a high enough number of analysable axons. I used the Thy1-TNXXL mouse line and started at a desired force of 35 kDynes (kDy), progressively increasing it in increments of 5 kDy. This resulted in four groups, classified by the desired impact force, as shown in the table below.

Table 1: Results obtained using four levels of desired impact force. All numbers are expressed as averages.

Desired Impact Force (kDy)	35	40	45	50
Number of Samples	5	4	3	3
Number of Analysable Axons	35	35.5	30.7	23
Unaffected Axons	53.1%	42.3%	18.5%	20.3%
Recovered Axons	5.1%	4.9%	3.3%	8.7%
Swollen Axons	35.4%	34.5%	65.2%	37.7%
Broken Axons	6.3%	18%	13%	33.3%

As the data in Table 1 show, an impact force of 35 kDy was insufficient to generate the desired effect, causing lesions in less than 50% of the analysable axons. Hence, I considered this level of impact force as insufficient and decided against it. A typical result from such an experiment is shown below.

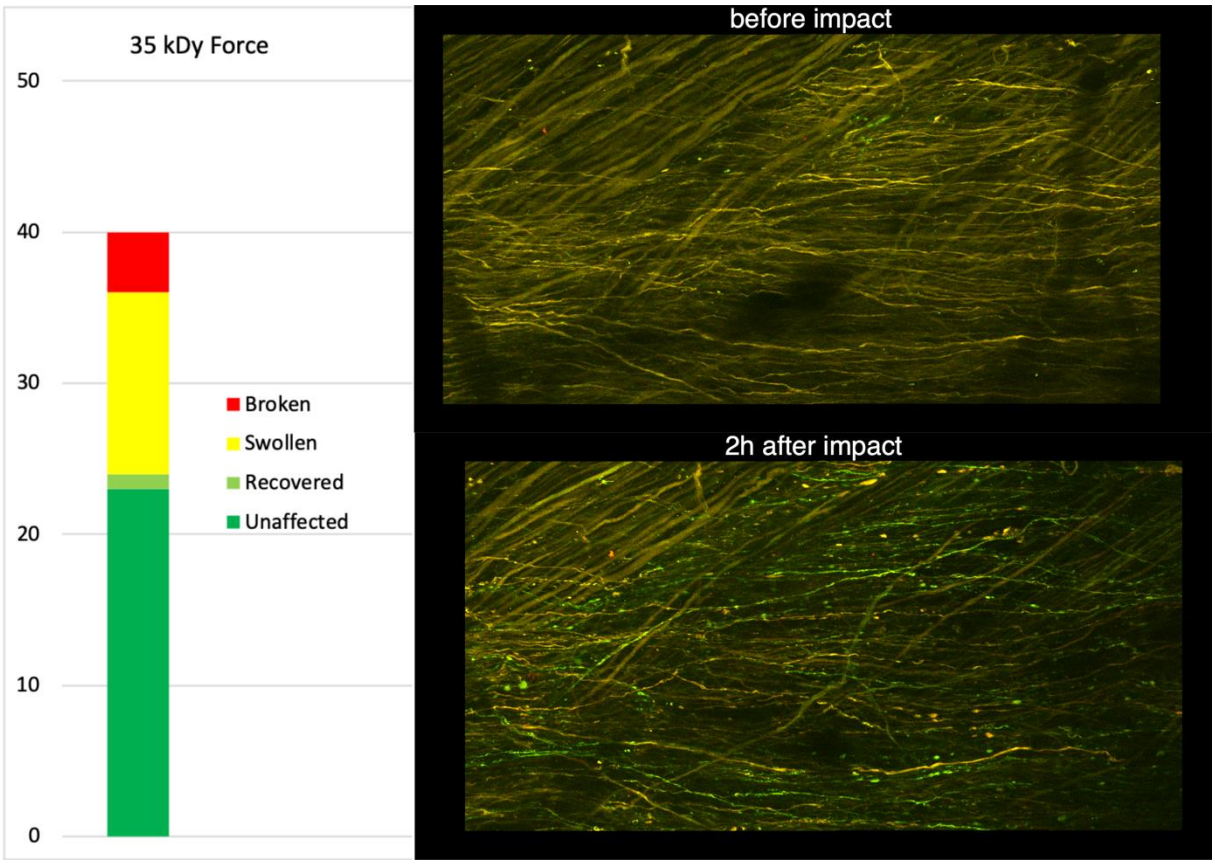

Figure 13: Results from one of the experiments performed with a desired impact force of 35 kDy. The bar graph on the left shows the number of analysed axons and their level of injury. Out of 40 analysable axons, 23 were unaffected (57.5%) by the impact. The two panels on the right contain *in vivo* images of the sample before the injury (upper panel) and two hours after it (lower panel). The images were obtained using two-photon microscopy.

At the other extreme, an impact force of 50 kDy was excluded because it drastically decreased the number of analysable axons compared to all the other levels of desired force. The average yield of analysable axons was 35% lower compared to the 40 kDy group and 25% lower than the 45 kDy group. Using a high impact force of 50 kDy also increased the difficulty of the experiment. The mice were less stable during the anaesthesia, often causing a premature interruption of the experiments. The success rate of the procedure dropped from >90% to 50%.

This was partly due to severe superficial haemorrhaging, which made image acquisition impossible, and partly due to a higher rate of death post injury. These complications were not encountered while using any of the other levels of impact. I thus decided against using a desired impact force of 50 kDy for the rest of the experiments and refrained from doing experiments with an even greater impact force.

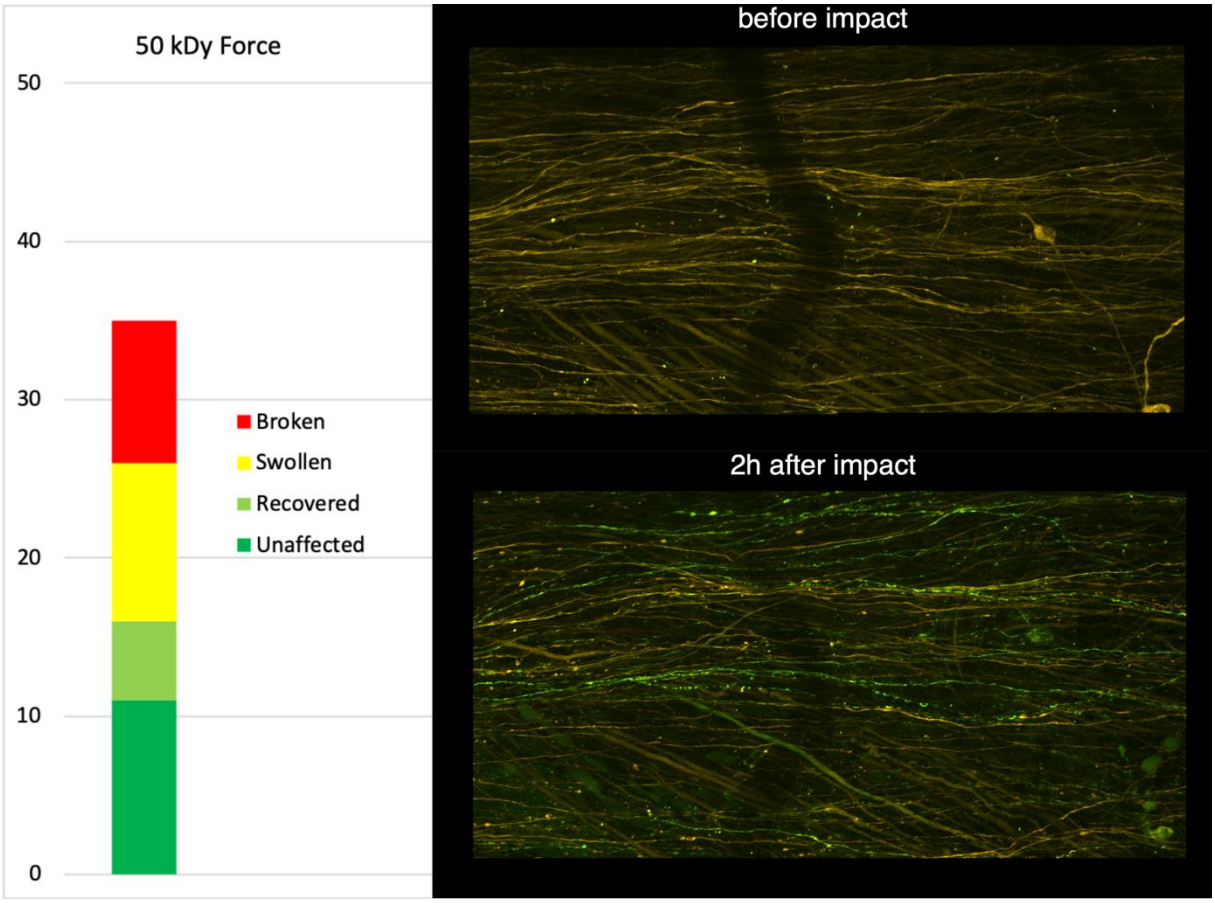

Figure 14: Results from one of the experiments performed with a desired impact force of 50 kDy. This particular sample had the highest number of analysable axons at this force level. The bar graph on the left shows the number of analysed axons and their level of injury. The panels on the right contain *in vivo* images of the sample before the injury (upper panel) and two hours after it (lower panel). The images were obtained using two-photon microscopy.

Thus, only desired impact forces of 40 and 45 kDy produced an adequate injury response (with over 50% of axons being affected by the impact) and proved practical from an imaging point of view (i.e. success rate of over 90%, stable samples, and no superficial bleeding). Although the samples impacted with 40 kDy consistently had a higher number of analysable axons (35.5 vs. 30.7 axons/sample on average; see data in Table 1), the difference

was not statistically significant (p=0.6). But the distribution of the injured axons in the 45 kDy group was heavily skewed towards the swollen axons, while the 40 kDy group had a more uniform distribution of injured axons (see Table 1 and Figure 17). Lastly, the percentage of recovered axons was also higher in the 40 kDy group.

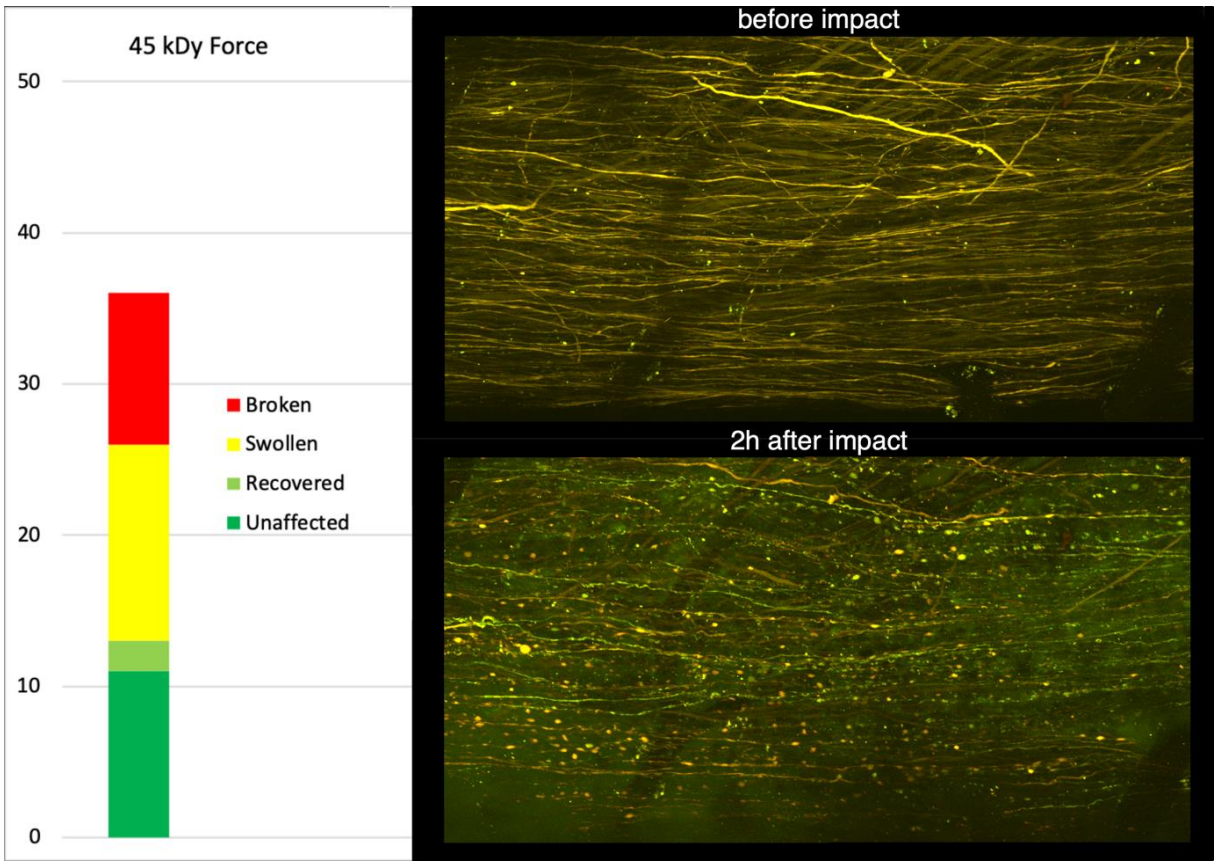

Figure 15: Results from one of the experiments performed with a desired impact force of 45 kDy. The bar graph on the left shows the number of analysed axons and their level of injury. The panels on the right contain *in vivo* images of the sample before the injury (upper panel) and two hours after it (lower panel). The images were obtained using two-photon microscopy.

Independent of the desired impact force, I could always observe spontaneous recoveries. After careful consideration and weighing of the above-mentioned arguments, I decided to perform all subsequent experiments using a desired impact force of 40 kDy. An example from a typical experiment using this impact force is shown in Figure 16.

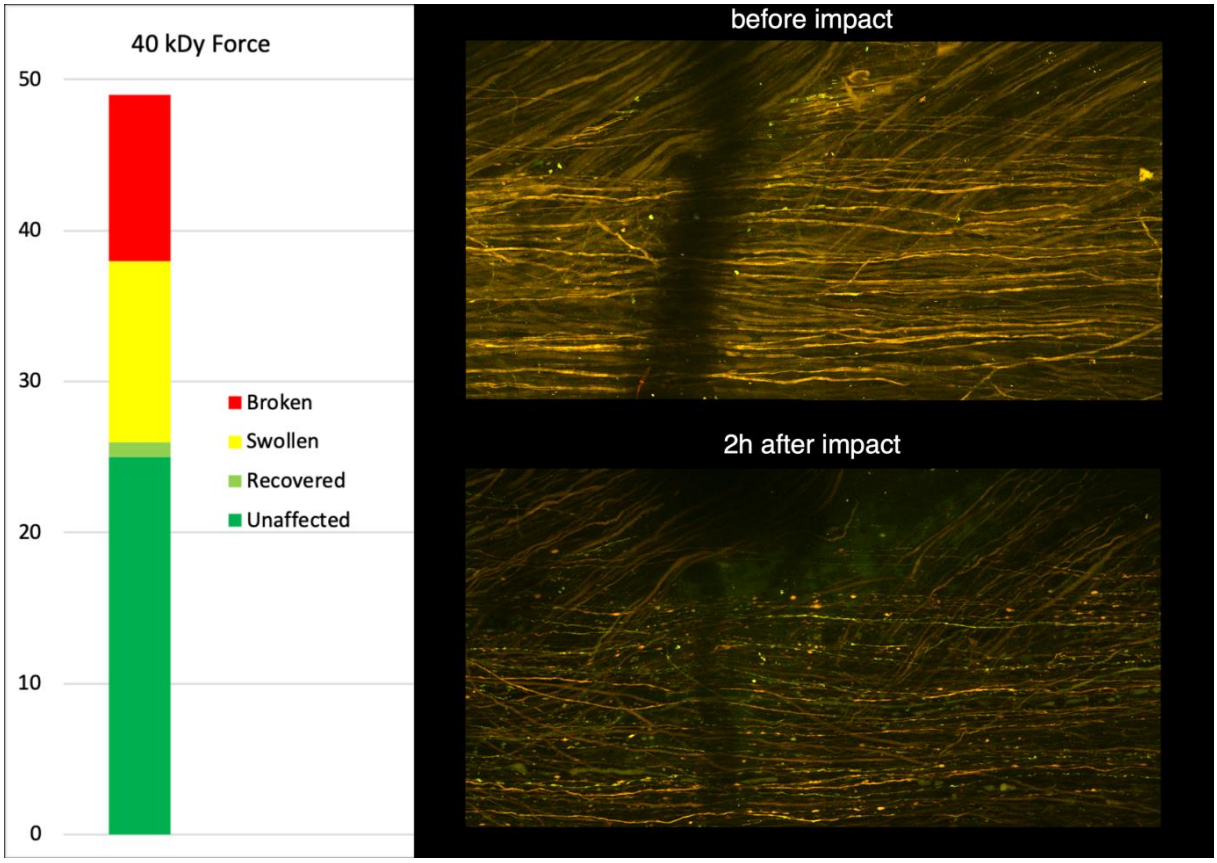

Figure 16: Results from one of the experiments performed with a desired impact force of 40 kDy. The bar graph on the left shows the number of analysed axons and their level of injury. The panels on the right contain *in vivo* images of the sample before the injury (upper panel) and two hours after it (lower panel). Images obtained using two-photon microscopy.

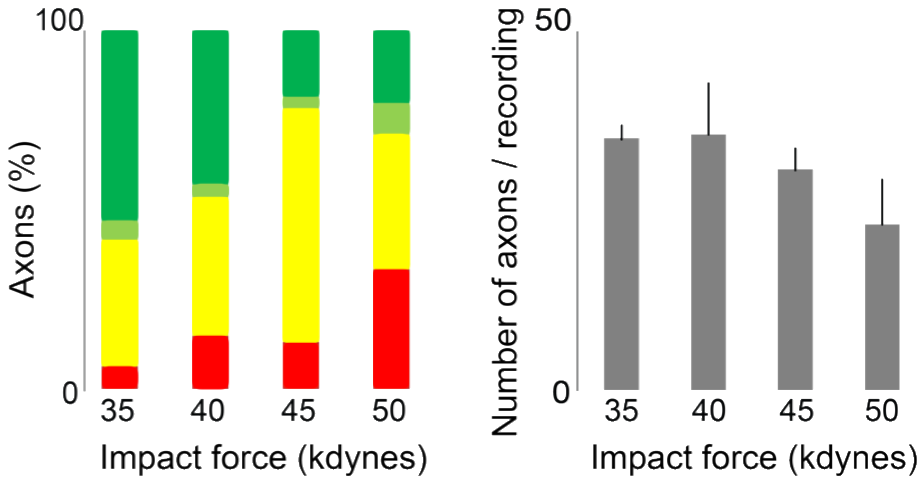

Figure 17: Morphologic distribution of analysable axons versus the desired impact force (left) and the number of analysable axons/sample (mean + s.e.m.) versus the desired

impact force (right). There is no significant difference between the number of analysable axons at 40 and 45 kDy (p=0.6), but the former yielded a more balanced morphological distribution.

Previous work done in our laboratory showed that most calcium recoveries occur during the first 100 minutes after the impact injury (Williams et al., 2014). To see if this metabolic recovery correlates with a recovery in axonal shape, I studied the number of morphologic recoveries during the same time span and concluded that all four levels of impact force produced axons that could recover (see Figure 18). There was no significant correlation between the level of injury force and the number of axons undergoing morphologic recovery during the first 100 minutes. The average number of recovered axons during the first 100 minutes after injury is depicted in the graph below.

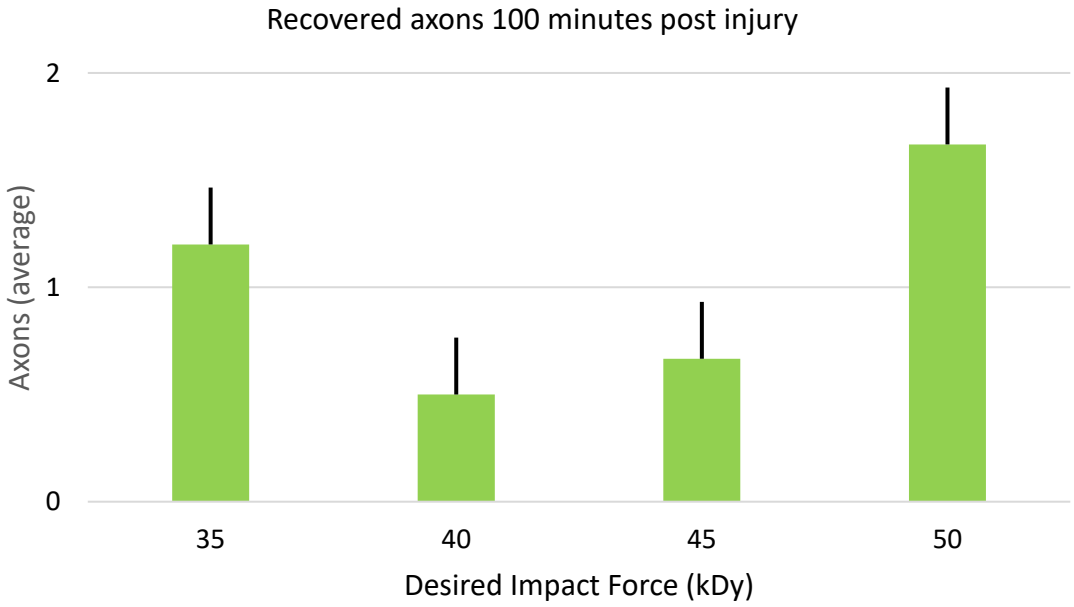

Figure 18: Average number of recovered axons per imaged area of the spinal cord, 100 minutes after the impact injury (with standard error bars) versus the desired impact force. There was no correlation between the desired injury force and the number of recovered axons.

3.2 Reproducibility

To evaluate the reproducibility of the grading method applied for the analysis of the imaged axons, we had two investigators analyse the same set of axons. The two evaluators were P.R. Williams, at the time a postdoctoral fellow with vast experience in laboratory work in general and image analysis in particular, and B.-N. Marincu, a beginner PhD student. Both independently analysed a dataset of 177 axons, containing the results from experiments done on five Thy1-TNXXL mice. The results are shown in Table 2. The numbers represent percentages of all the axons in the respective grading category. Sample sizes were chosen based on previous work done in our laboratory using similar methods.

Table 2: Disparity rates (expressed as a percentage of all axons in the respective category) between the evaluation results two evaluators with vastly different experience levels. The results are expressed as mean ± s.e.m. and show no relevant difference between the two evaluators (Williams et al., 2014).

Swelling	Elevation	Recovery	Breakdown	Return
2.8 ± 2%	5.1 ± 1.6%	4 ± 1.9%	6.2 ± 2.7%	2.1 ± 1.5%

After comparing the results obtained by both scorers, I concluded that, regardless of the different experience levels, this evaluation method can be reliably applied and reproduced by different evaluators without significant differences in the final result.

The analysed axons were classified based on their morphology and their FRET signal at specific time points. The morphologic classification was based mainly on visual analysis of the time-lapse images obtained with 2P microscopy (for the processing steps please refer to the Methods chapter). Important morphologic features were swelling and/or beeding, the formation of a blob-like structure termed retraction ball, and the discontinuation of the axon. The FRET signals were measured using the FIJI image analysis software (see Methods for details). Based on these criteria, the two evaluators classified the morphology of each axon as either unaffected, recovered, swollen, or broken. The signal was either elevated or returned to normal.

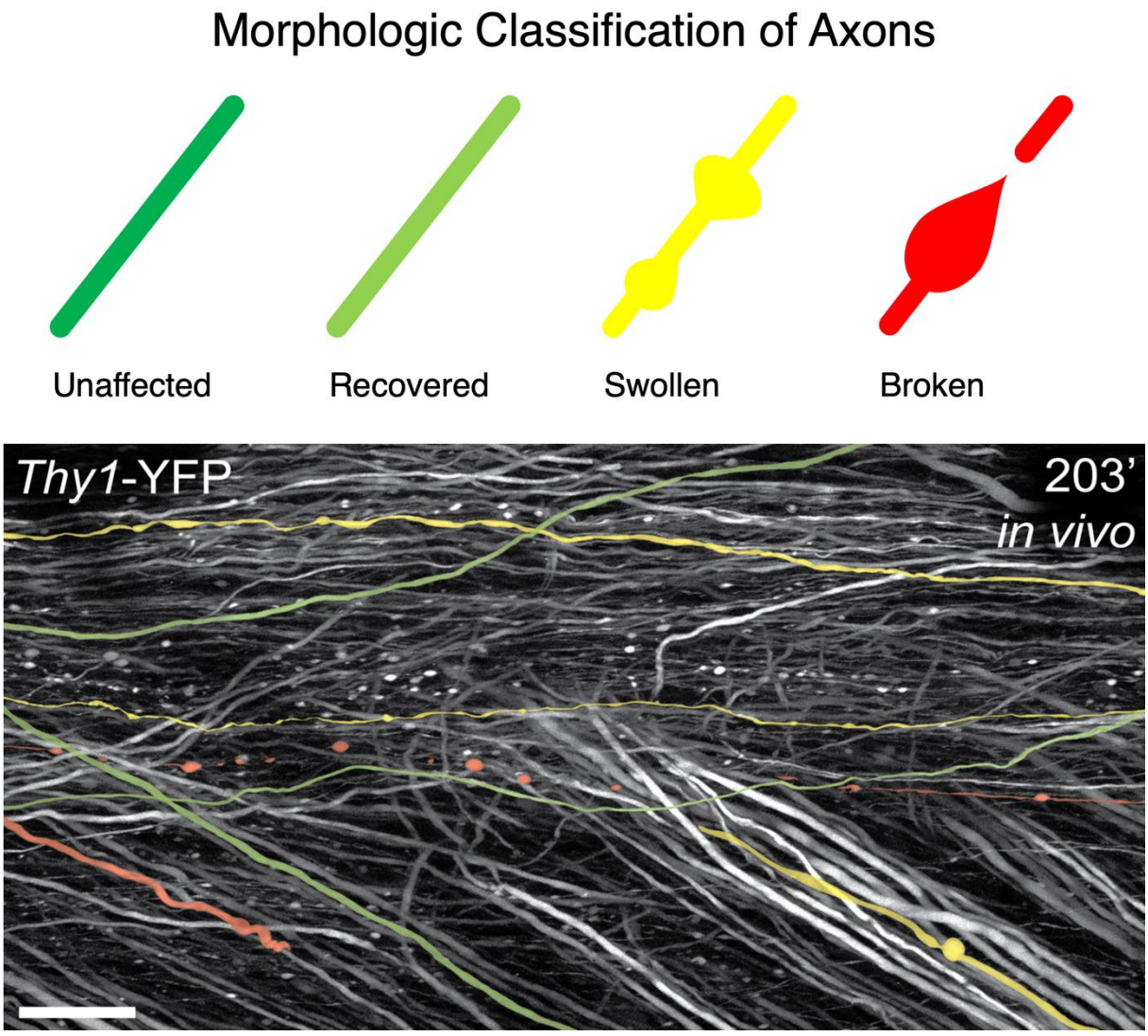

Figure 19: Schematic drawing (upper panel) representing the four morphologic states of the analysed axons and pseudo-coloured *in vivo* images (lower panel) obtained 203 minutes after injury (Williams et al., 2014). Recovered axons will often have similar morphology as the unaffected ones, although they present swelling and increased calcium signals during the time lapse. Swollen axons have characteristic modifications to their tubular structure and an altered signal. Broken axons will sometimes present a retraction ball before the discontinuation is clearly visible, or they will be broken immediately after impact.

3.3 Photostability and pH sensitivity

Although the TNXXL sensor has been thoroughly characterized in previous studies (Direnberger et al., 2012), the work done in our laboratory is a first regarding its usage in an impact injury setting. We thus needed to check for the stability of the genetically encoded

calcium indicators during an *in vivo* injury scenario and to ensure that the signals recorded were not impaired in any way by the changes induced in cellular medium or by the continuous imaging for 4 hours post injury. We thus tested our probes for pH sensitivity and photostability.

To ensure pH sensitivity was not an issue, we used genetically encoded sensors that are relatively insensitive to pH changes in the range of 6.8 to 9. Furthermore, they are less susceptible to this confounder than most single-wavelength indicators and we would expect an apparent drop in the FRET ratio only at pH values below 6.8 (Griesbeck et al., 2001). Still, to exclude any possible influence of pH we performed control experiments using the Thy1-YFP16 x Thy1-CFP5 mouse line. These sensors are not linked to each other and have different pH sensitivities, enabling them to act as an axonal pH sensor (Kuner & Augustine, 2000; Z. Zhang, Nguyen, Barrett, & David, 2010). We measured the ratio of the YFP/CFP signal in 99 axons from 3 mice, using two timepoints: the beginning of the experiment and two hours post injury (Figure 20). The results showed a total decrease in the YFP/CFP ratio of 0.33% after two hours (0.899 vs. 0.896, p = 0.31), which showed that pH modifications did not impact our measurements (Williams et al., 2014).

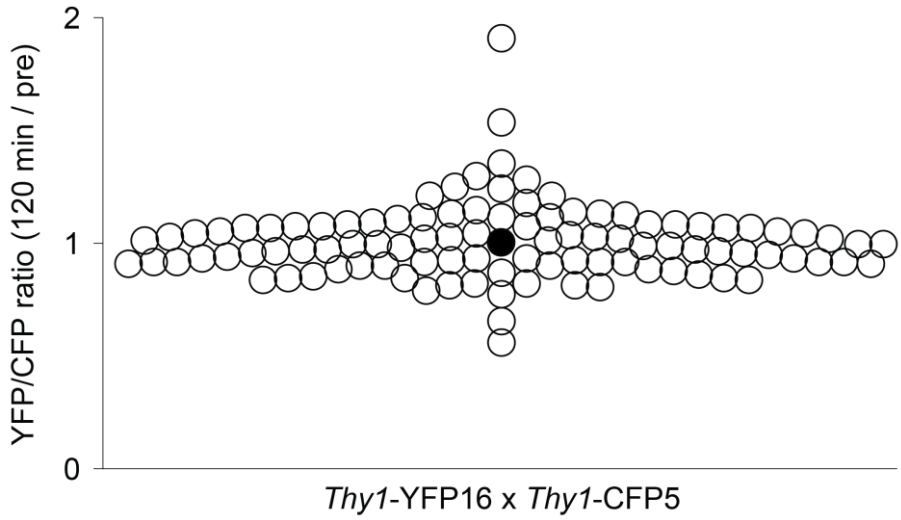

Figure 20: The YFP/CFP ratios were stable following spinal injury and repetitive imaging for 2 hours. This suggests that pH modifications had no significant influence on our measurements. Empty circles represent single axons, the filled circle represents the average.

When imaging with two-photon microscopes over an extended period of time, bleaching should always be regarded as a possible confounding factor. Although we are well aware that Citrine and CFP have different levels of photostability, axons have large reservoirs

of diffusible cytoplasmic fluorescent protein (Turney & Lichtman, 2012; Williams et al., 2014), which turn bleaching into less of a concern in the case of thicker axons, as is the case in our experiments. Still, to test if potential phototoxicity could influence our results, we used the same Thy1-TNXXL mouse line as a control. We imaged them under the same conditions (every 10 minutes, for 4 hours), but without performing the impact injury. Afterwards we measured the signals during the first and last minutes of the experiment (i.e. at 0, 10, 230, and 240 minutes). Then we analysed the bleach rates for CFP and Citrine, as well as the resulting drift in the FRET ratio. The results (Figure 21 panel a) showed a minimal drop in the Citrine/CFP ratio of 0.7 ± 0.3% per hour (results obtained by analysing 127 axons from 4 mice) (Williams et al., 2014).

To further back our argument against this potentially important confounding factor, we analysed some of the "unaffected" axons from our previous datasets (Figure 21 panel b), thus controlling for a possible influence of the lesion background. These axons showed an effective increase in the Citrine/CFP ratio of only 0.5 ± 0.4% per hour (results obtained by analysing 74 axons from 11 Thy1-TNXXL mice). Taken together, these data show that bleaching has no relevant effect on the calcium dynamics we describe (Williams et al., 2014).

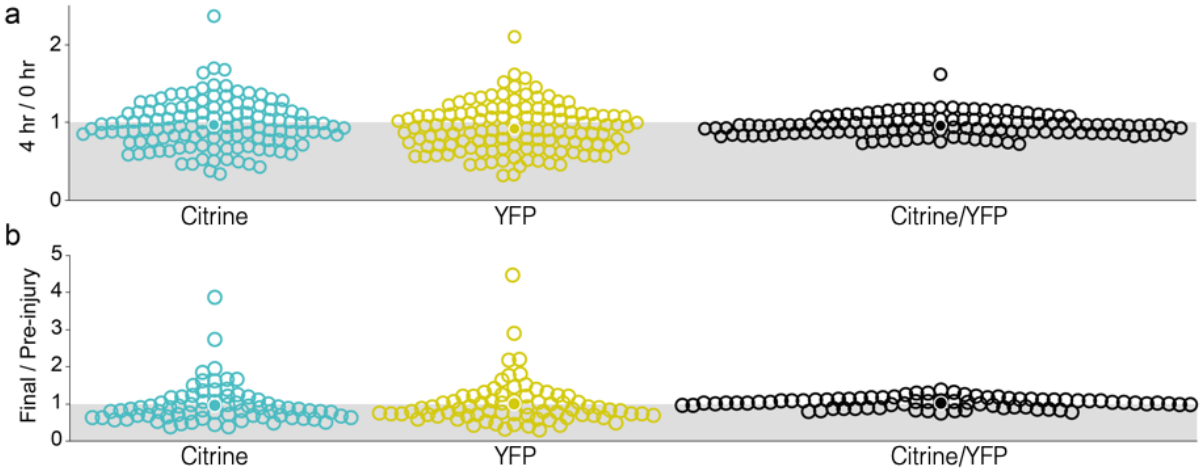

Figure 21: Analysis of uninjured axons showed that Citrine, YFP, and the ratio Citrine/YFP remained stable over the time lapse (panel a). In injured samples (panel b), axons with no calcium elevation during the entire time lapse showed no significant modification in Citrine signal, YFP signal, or the Citrine/YFP ratio. Empty circles represent single axons, filled circles represent the group average.

3.4 Pharmacology

For all the experiments performed using pharmacological agents we used a random number generator implemented in the Python™ programming language to blind the observer during the data analysis.

Previous experiments done in our laboratory have shown that the chelation of extracellular calcium by EGTA reduces the rate of axon fragmentation (Williams et al., 2014). Hence, we wanted to verify if the rise of extracellular calcium levels alone could increase the rate of axon fragmentation, or possibly reduce the recovery rate after impact injury. Therefore, we raised the calcium concentration in the applied aCSF up to the saturation point of 5.5 mM. This resulted in extensive swelling and beeding of the axons after 30 minutes, even without mechanical damage to the axons. The result led us to abandon this line of enquiry, because there was no method to differentiate the swellings caused by the high calcium levels from the ones resulting from the impact injury. A representative image of the axonal swellings caused by the rise in the extracellular calcium levels alone, with no mechanical damage induced to the tissue, can be seen below.

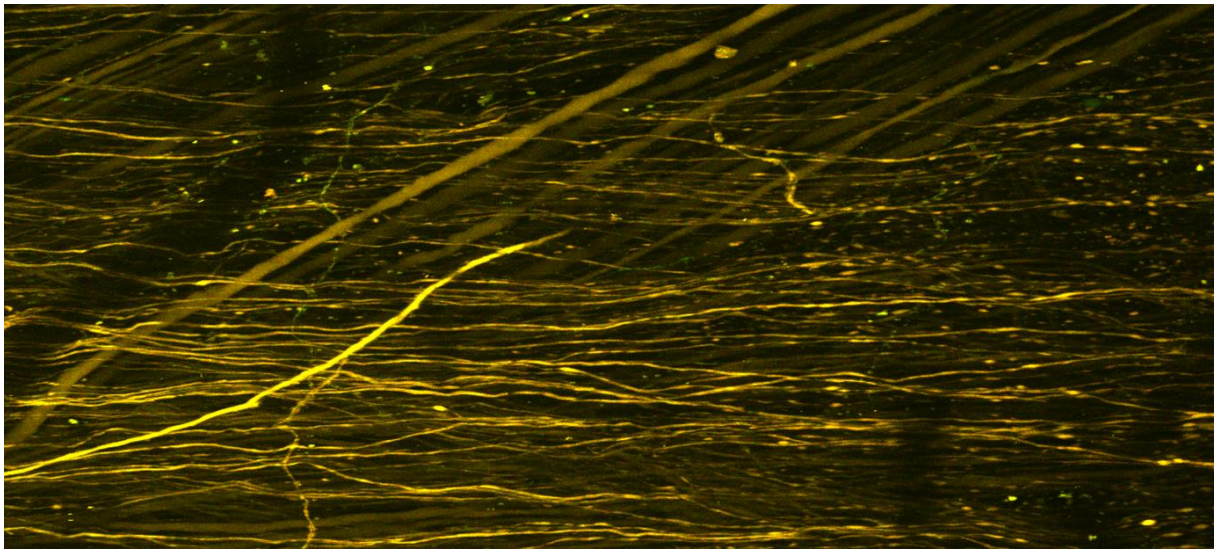

Figure 22: Axon swelling induced by high extracellular calcium, without any mechanical damage. Figure modified from (Williams et al., 2014).

Knowing that intracellular calcium influx activates calpain cascades, which can in turn lead to axonal fragmentation (Ma, 2013; Williams et al., 2014), I tried selectively blocking the

voltage gated calcium channels and the glutamate receptors. To this end I used three pharmacological cocktails: (i) Bepridil (n=3; 116 axons) to block the reverse action of the Na-Ca exchanger (and non-specifically block the calcium channels) (Stys & Lopachin, 1998; Stys et al., 1992), (ii) Nimodipine and ω-Conotoxin GVIA (n=3; 140 axons) to block the most likely voltage-gated calcium channels (Ouardouz et al., 2003; Stys, 2005), and (iii) CNQX disodium salt with MK 801 maleate (n=3; 111 axons) to block NMDA receptors (Ahuja & Fehlings, 2016; D. Liu et al., 1999; Ouardouz et al., 2006). A control group (n=3; 110 axons) received the solvent Dimethyl sulfoxide (DMSO). I chose these rather crude pharmacological approaches to obtain a first 'screen' of possibly involved pathways – in case of a notable effect, I intended to follow up with more detailed and tailored pharmacological treatments. As shown in Figure 23, the three above-mentioned pharmacological intervention groups had on average fewer recovered axons than the control group: 4 after applying Bepridil, 5 after Nimodipine and ω-Conotoxin GVIA, and 7 in response to CNQX disodium salt and MK 801, whereas the control group (DMSO) had on average 8 recovered axons. Similarly, the relative distribution depicted in Figure 24 shows no difference in axon recovery.

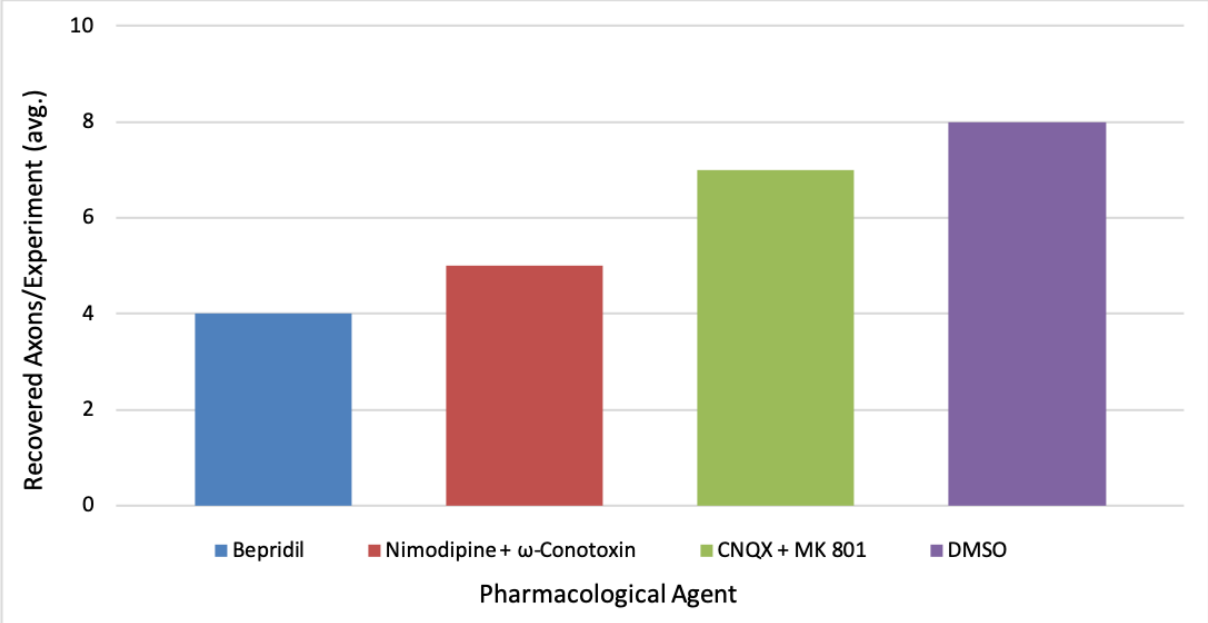

Figure 23: The three pharmacological intervention groups show no increase in the average number recovered axons when compared to the control group (DMSO).

There was also no relevant difference between the four groups, neither in the relative morphologic distribution of the affected axons (Figure 24), nor in the average number of analysable axons per experiment (Fig. 25). I thus refrained from pursuing this line of thought.

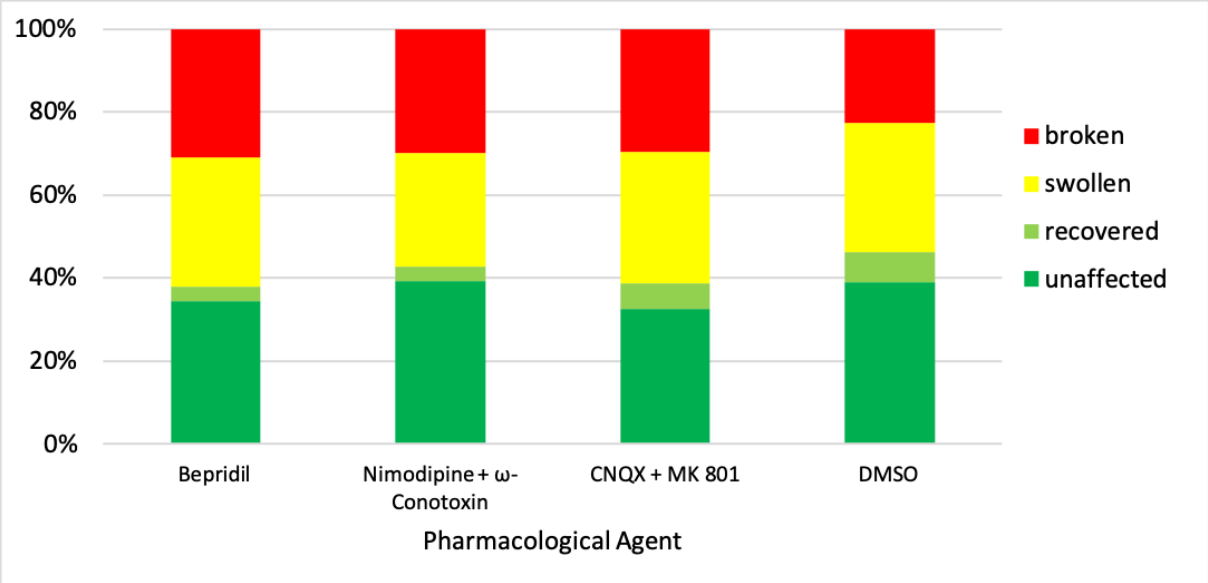

Figure 24: The relative morphologic distribution of the axons from samples treated with the three pharmacological cocktails was similar to that of the control group (DMSO).

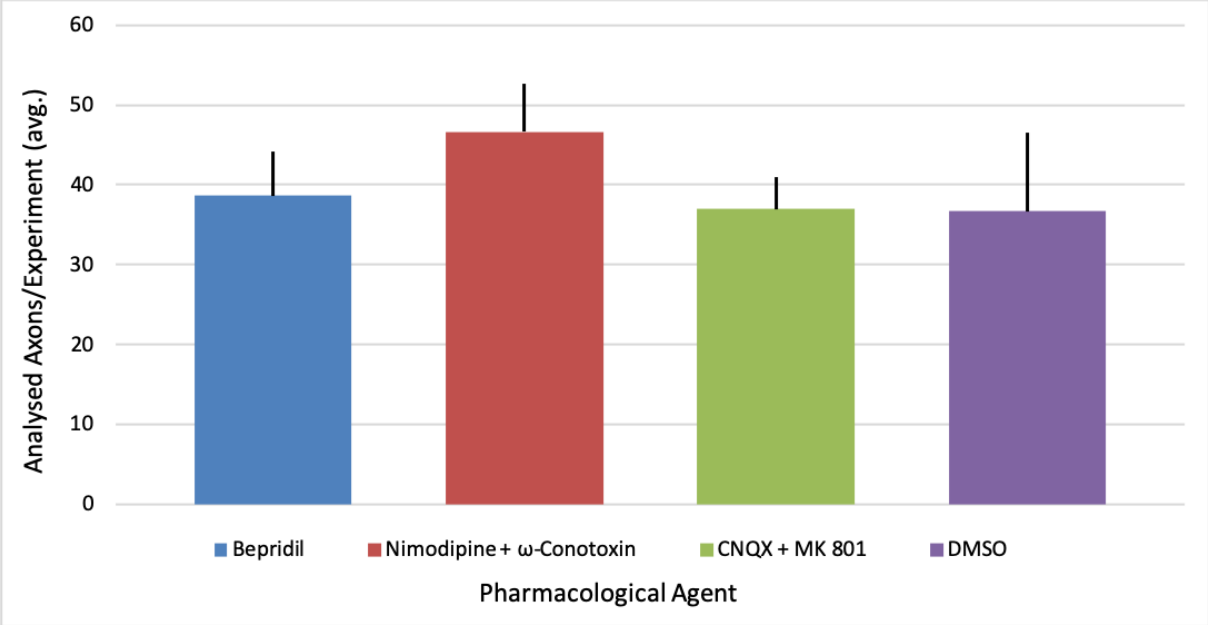

Figure 25: No statistically significant difference between the average number of analysable axons in the four groups. Each group had n=3 mice. Error bars indicate s.e.m.

4 Discussion and Conclusions

4.1 Summary

The aim of this thesis was to study the acute phase of axonal degeneration following an impact injury of the murine spinal cord *in vivo*. To accomplish this aim, I went through the following steps:

- Adopt a reproducible methodology around this spinal cord impact injury model, which can deliver similar results, independent of the person or laboratory involved.
- Identify factors that could influence or bias the results during continuous *in vivo* imaging of injured axons.
- Define a method for evaluating, grading, and analysing the data that would offer insights regarding the mechanism of axonal degeneration after contusion and yield similar results, irrespective of the experience and skill level of the evaluator.
- Experiment with different pharmacological interventions that could be applied in an acute setting to promote the recovery of contused axons.
- Prove the existence of a critical time window for such interventions after SCI, analogous to the one currently employed for stroke patients.

The defining methodological feature of my work is a unique approach for *in vivo* imaging of the acute phase of axonal degeneration after impact injury of the mouse lumbar spinal cord, which was developed in our lab and refined in this thesis. Briefly, the method includes:

- a standardised injury model capable of repeatedly inducing impact lesions of similar severity to the lumbar spinal cord with the aim of delivering a minimal contusion lesion
- a set of clear anatomical landmarks and detailed step-by-step instructions that are intended to increase the reproducibility of this method across a wide spectrum of scientists with varying degrees of practical skills and experience
- an *in vivo* imaging protocol that allows studying the acute phase of axonal degeneration after impact with single axon resolution.

This method was established as part of a study published by our laboratory (Williams et al., 2014), on which I was a co-author. In the following paragraphs, I will first discuss the

contribution of my work to the mentioned publication, then present the adopted technique and my results in the context of the existing literature on spinal pathology, and address the limitations of my study. Finally, I will outline potential future perspectives and knowledge gaps that may be filled through further studies.

4.2 Contribution of this thesis to the *in vivo* study of spinal contusion injury

The work outlined in this thesis was part of a bigger project done in our laboratory (Williams et al., 2014). In it, the authors used *in vivo* imaging to show that, during the acute phase of contusion SCI, injured axons persist in a state of sub-lethal damage, which lasts for several hours. Importantly, this is not a pre-terminal state, in which the ultimate fate of the axon has already been decided. During this time, the affected axons can either spontaneously recover or irreversibly degenerate. Concomitant *in vivo* imaging of the morphology and of the axonal calcium levels revealed that calcium elevation is a strong indicator for subsequent axonal fragmentation. This challenges the previously held view of calcium elevation as a "point of no return" (Buki & Povlishock, 2006). This finding offers a potential window for therapeutic intervention, which could tip the balance in favour of recovery for the axons found in this sub-lethal state. As the main source of intraaxonal calcium, experiments done by my collaborators identified the extracellular space. My thesis was hence tasked with exploring entry paths of calcium that could contribute to the calcium overload seen in many axons early after injury. Moreover, I contributed a detailed evaluation of reproducibility of the adopted injury technique and the image analysis approach. Beyond the work detailed in this thesis, further experiments done by my co-authors proved the post impact formation of so-called mechanopores (i.e. mechanically induced disruptions in the cell membrane), which are a dominant source of calcium influx (at least during the first hours after contusion SCI). This is in line with the results of my thesis, which failed to identify a pharmacological target that mediates post-injury calcium influx.

Some features of my work are explained by the specific context as part of a larger study, where results obtained by me were embedded in the context of my collaborators' work. Indeed, the experiments were in part inspired by specific suggestions and requests from reviewers of the first submitted version of the Williams et al. study. This explains the somewhat unconventional approach to the pharmacological experiments, such as the combinatorial use

of drugs or the speculative dose-finding strategy. In accordance with the work previously published by our laboratory (Williams et al., 2014), my results confirm not only that the rise of intracellular calcium levels is a reliable predictor of impeding axonal degeneration, but also that elevating extracellular calcium alone is enough to cause beading in uninjured axons of the lumbar spinal cord (this experiment has limited physiological relevance, but was specially requested by an expert reviewer). My work also shows that the local application of several ion channel blockers is incapable of tilting the balance of swollen axons towards recovery, reinforcing the notion of an unusual path across the axonal membrane (like the mechanopores mentioned above). While the specific agents I used were based on previously published literature, they were chosen to address specific aspects pointed out by the reviewers. The intention was to get a first impression of the efficacy of these pharmacological cocktails as therapeutic interventions. If proven successful, they would have been followed by further, more rigorous experiments on individual drugs and a detailed set of experiments to determine the most effective dosing, delivery path, and timing.

The control experiments on bleaching, phototoxicity, and pH that I performed were also part of the review process. From these I conclude that the genetically encoded biological sensors (Thy1-TNXXL) and the mouse lines used in this work are neither influenced by local pH modifications induced by an impact injury of the lumbar spinal cord, nor are they subject to significant bleaching or laser-induced damage after continuous *in vivo* imaging during the first four hours after impact. However, I cannot exclude the possibility of such biasing factors occurring under different imaging conditions or on a longer time scale, using different solutions or biological sensors. Future technical developments will likely lead to more sensitive sensors, as well as faster and more accurate imaging methods.

4.3 My work in the context of existing literature

The methodology described here, and the results obtained using it, filled a gap in the scientific literature regarding the potential of axon protective intervention after contusion injuries. Traditionally, spinal cord injury models have used one of the following four mechanisms for inducing the desired lesion: transection, distraction, compression, or contusion. While each of these methods has its advantages, the contusion injury best mimics

the kind of lesion most commonly seen in humans. In a real-life setting, distraction and compression injuries of the spinal cord rarely occur. And although transection lesions are relatively similar to injuries caused by sharp projectiles or stabbing, in such scenarios the main focus is — rightly so — on life support measures and not on direct treatment of the SCI. Moreover, transections do not offer a direct target for axon protective intervention (in contrast to invertebrates, mammalian axons cannot reconnect after being cut (Aminoff, 2014)) and current research correspondingly focusses on regenerative approaches (Ahuja, Wilson, et al., 2017; Bradke, Fawcett, & Spira, 2012; de Freria, Van Niekerk, Blesch, & Lu, 2021; Vismara et al., 2017; Walker & Echeverri, 2022). Hence, contusion injuries represent the most common form of injury in humans, as well as the most suitable target for axon protective intervention since the mechanism of injury does not sever the axons in an irredeemable fashion, as a transection would ("Spinal cord injury facts and figures at a glance," 2012).

My work relies heavily on previously done research in the field of CNS injury and aims to complement it. The seminal work that continues to inspire researchers to this day was published by Povlishock et al. (Povlishock, Becker, Cheng, & Vaughan, 1983). In it, the authors propose the existence of traumatically induced poration of the axonal membrane (what we have termed “mechanopores”). While their work is focussed mainly on traumatic brain injury, this paper inspired a whole set of similar observations (Farkas, Lifshitz, & Povlishock, 2006; Kilinc, Gallo, & Barbee, 2008; Kilinc et al., 2009), all of which served as the starting point for my investigations and for several of the pharmacological experiments described in this thesis. Povlishock and his collaborators emphasized the role of axonal calcium influx after traumatic brain injury, describing the consequent activation of the “caspase death cascade” as a point of no return (Buki & Povlishock, 2006). While such a point does probably exist, the experiments done by my colleagues and I show that for many axons it is preceded by a time window of 2-4 hours during which the progression toward the point of no return may be reversed, allowing the axons to return to their normal state. This led me to conclude that axons which are able to clear calcium will avoid the point of no return, while those axons that cannot, will likely degenerate. This was confirmed in a different setting by work later performed in our laboratory (Witte et al., 2019).

Keeping the focus on toxic intracellular calcium signalling, I also looked for inspiration in the context of chronic diseases such as Alzheimer’s and multiple sclerosis (Chu, Cummins, & Stys, 2020; Tsutsui & Stys, 2013). Work done by Stys and colleagues described how calcium

overload is caused by a release from intracellular stores, especially from the axoplasmic reticulum, thus precipitating axonal degeneration (B. C. Orem, Pelisch, Williams, Nally, & Stirling, 2017; Stirling & Stys, 2010; Stys, 2004). The morphologic changes they described as a consequence of this are similar to the ones I observed after adding calcium to the extracellular bathing solution. But in my experiments, these changes were also caused in healthy axons that weren't subjected to any mechanical or metabolic injury and hence didn't have any cause for calcium release from intracellular stores. This led me to explore other causes.

The work done by Stys and Stirling underlined the important link between voltage-gated sodium channels, AMPA receptors, and intracellular calcium signalling during the acute phases of axonal degeneration (Nikolaeva et al., 2005; Stirling, Cummins, Wayne Chen, & Stys, 2014; Stirling & Stys, 2010). Their findings suggested that blocking multiple routes of intracellular calcium accumulation may be necessary for preventing cellular degeneration. This was a big reason for using similar pharmacological compounds during my experiments. In the end, none of the blocking agents I explored managed to increase the average number of axons that recover after impact injury.

In contrast, experiments done by my colleagues and I have shown that applying a calcium chelator like EGTA in the bathing solution was sufficient to inhibit the degeneration of axons in the setting of acute SCI (Williams et al., 2014). This was later confirmed by work more recently published by our laboratory (Witte et al., 2019) and stands somewhat in opposition to the classically held belief that calcium from intracellular stores is the main cause for axon degeneration.

All these findings point to the initially suspected cause: the mechanopores. These defects in the axonal membrane are an integral part of the impact injury. Considering the high calcium concentration in the extracellular space compared to that inside the axons and the size such membrane defects can have (Williams et al., 2014), they must be regarded as the main factor that precipitates calcium-dependent axonal degeneration, independent of the calcium channels and pumps (as suggested by the classical dogma of axon degeneration). These nanoscale membrane disruptions are also responsible for the axon degeneration observed in the chronic setting of multiple sclerosis (Witte et al., 2019), making them a worthwhile subject of exploration for cellular repair therapies and interventions.

4.4 Methodological aspects and limitations

In a review paper published by Ahuja et al., the authors state that the ideal animal model used for the study of traumatic spinal cord injury "should anatomically and pathophysiologically resemble human SCI, require minimal training, be inexpensive and produce consistent results" (Ahuja, Wilson, et al., 2017). While our methodology largely fulfils these criteria and offers some practical advantages for the study of SCI, it still has some shortcomings. In the following paragraphs I will address these aspects.

Although the first research paper describing a model for SCI used a canine (Allen, 1911) and large animal models were commonly used in the 1950s - 1970s, during the last three decades rodent models have become the standard (Kwon et al., 2015; Sharif-Alhoseini et al., 2017). Rat and mouse models are most commonly used for basic SCI research, primarily because they are inexpensive compared to larger animal models, but also because their injury response is similar enough to that observed in humans (Ahuja, Wilson, et al., 2017). Large animal models have higher monetary costs, the maintenance and breeding work is often more complex, they require more elaborate institutional infrastructure, and are still unable to accurately mimic human response to SCI (N. Zhang, Fang, Chen, Gou, & Ding, 2014). However, rodent models of SCI have several inherent limitations and pose non-trivial hurdles when trying to translate the findings into clinical practice.

The rodent model used in our laboratory, like most models currently used in basic research, is based on animals bred and raised under tightly controlled conditions. The mouse lines I used in this study were genetically modified and inbred. They are genotypically and phenotypically very similar, since they all belong to the same mouse line, in stark contrast to wild mice. They are raised in an artificial environment, protected from outside pathogens, and fed processed chow throughout their lives. What drawbacks these conditions have, if any, regarding the pathophysiological response to injury and later translational endeavours is still unknown and not the topic of the current thesis. A panel discussion among academics, industry researchers, and granting agencies could reach no real consensus on this topic (Kwon et al., 2015). Considering the novelty of our methodological approach and given the extensive experience of our laboratory, using a mouse model was appropriate.

One clear limitation of this study is the mild and unrealistic nature of the contusion injury as well as the standardized conditions under which it was performed. To obtain adequate

image quality, I minimized the stress response of every mouse throughout the experiment and performed the contusion injury under conditions of anaesthesia, all of which are unphysiological conditions. In a real-life setting, the subject would be under severe stress (maybe even shock) and the SCI would most likely be a mix of severe contusion, partial or complete transection through bone fragments or foreign bodies, with the potential addition of a distraction component, depending on the trauma mechanism. Such severe SCI is nearly impossible to consistently replicate in an animal model. Although I did experiment with more severe levels of contusion injuries (as detailed in the Results section), they consistently resulted in significantly higher death rates during the first 1-3 hours after impact. These heavier injuries also caused heavy bleeding, making *in vivo* imaging of the axons impossible. Hence, I decided to study only mild contusion injuries, even though they reflect just one aspect of SCI.

The present study is limited to the highly acute phase (first four hours) of SCI. Chronic changes after SCI can potentially be observed using a spinal cord window model (Figley et al., 2013). This would offer further information about axonal degeneration and would allow the study of long-term outcomes after various therapeutic intervention, including combinations of pharmacological and behavioural therapies. Such techniques could also be combined with axonal regeneration therapies (Bradke et al., 2012). It would also entail acquiring the required surgical technique, post-interventional nursing, and adaptation of the animal living conditions. Observing the long-term effects of SCI was beyond the scope of the current thesis, but could represent an interesting target for future studies.

The cost of implementing our method has two main components: time spent training the researcher and money spent acquiring or producing the necessary equipment.

Regarding the latter, the Infinite Horizon Impactor has the major advantage of being commercially available. While the monetary cost of acquisition is relatively high compared to other existing models, this device can be used directly out of the box, with no need for additional modification or customization. Alternative models have been described, using calibrated weight drop models (Koozekanani, Vise, Hashemi, & McGhee, 1976), compression models using modified forceps (Blight, 1991), or in-house designed devices using a mini-invasive expandable balloon (Zheng et al., 2012). Still, the advantages of the Infinite Horizon Impactor have significantly contributed to its wide-spread use. This impactor has been successfully used to induce SCI at the thoracic level (S. Scheff & Roberts, 2009), the lumbar level (Williams et al., 2014), and could easily be adapted for injuries at the cervical level. It

also offers the advantage of an incrementally modifiable impact force – and subsequently injury severity – using only its software component. This enabled me to study lesions of various degrees of magnitude using the same equipment. This adds a pillar of strength when aiming for reproducibility among multiple users and across laboratories.

The second major hardware component involved in this study is the two-photon microscope setup. It has a very high acquisition cost, but it is not essential for replicating the methodology described in this thesis. One could alternatively employ more accessible imaging techniques or use behavioural assessments to evaluate the effectiveness of therapeutic interventions, while still employing the other parts of the technique described above.

The training cost of this method is not negligible. For these experiments I had to learn several surgical skills, the first of which was performing a laminectomy on an anesthetized mouse without injuring the spinal cord or the *dura mater*. Afterwards, I had to perform paravertebral muscular incisions, which must be deep enough to allow the fixation of the mouse with two pairs of clamps, but not so deep as to reach any internal organs. The fixation has to be stable enough to keep the sample unmoved during the impact injury and up to four hours after it. Acquiring these skills requires dexterity, perseverance, and – most importantly – close guidance from an experienced experimenter. With proper supervision, these skills can be acquired in approximately 6 months.

The ability to produce consistent results proved to be a major advantage of our method. As evidenced in the Results section, the disparity between two researchers with vastly different levels of experience was small. This has several reasons. First, the impactor device is controlled by a software program, which measures the force exerted by the impactor tip on the spinal cord tissue. This leaves hardly any room for error while performing the injury. Second, the grading method we introduced leaves little room for interpretation. Calcium dynamics are measured using the signal intensity, and the morphological changes fall into one of three categories (intact, swollen, or broken, as illustrated in the Materials and Methods section). These morphological characteristics are easily recognized when viewing the time lapse video of the acquired images. Third, a significant part of the post-processing steps was automated using a software program I wrote specifically to eliminate any risk of human error during this part of the process. All these aspects contribute to a method that repeatedly delivers consistent results.

4.5 Knowledge gaps and future perspectives

The results of my thesis show the existence of a window of opportunity for acute therapeutic intervention following a mild impact injury of the lumbar spinal cord. While there are still several unknowns regarding the specific approach of such an intervention, proving that such a therapeutic window exists and that the path of the injured axons does not necessarily lead to degeneration offers a strong impulse for pursuing this line of enquiry further.

The ion channel blockers I used during this project proved to make no difference in the fate of the injured axons. While these results should not discourage further experiments, they suggest broadening the research area and looking into different approaches. One such approach could involve compounds that can seal the mechanical defects in the cell membrane, thus limiting the rise of intracellular calcium. Experiments done by Shi, Borgens, and their collaborators have shown promising results using polyethylene glycol (Cho & Borgens, 2012; Luo, Borgens, & Shi, 2002; Shi & Borgens, 2000). This is a synthetic material produced by the polymerization of ethylene oxide. It has several advantages, including low toxicity and high biocompatibility, making it widely used in pharmaceutical and cosmetic industry products. Its mechanical properties and rate of biodegradation can be varied depending on its molecular weight (Temenoff, Athanasiou, Lebaron, & Mikos, 2002). There have been studies showing that polyethylene glycol can minimize adverse immune response, promote neuroprotective behaviour, and improve functional recovery after SCI (Amani, Kazerooni, Hassanpoor, Akbarzadeh, & Pazoki-Toroudi, 2019; Lampe, Bjugstad, & Mahoney, 2010). *Ex vivo* experiments have also shown the ability of this polymer to enhance axolemmal resealing after transection (Nehrt, Hamann, Ouyang, & Shi, 2010). Such studies have inspired experiments done in our laboratory, using the SCI injury model I describe in this thesis, which were unsuccessful (Williams et al., 2014). This suggests that the molecular characteristics of polyethylene glycol may need to be more finely tuned, exploring its use in both local and systemic administration for rapid resealing of breaches in the axonal membrane.

Another promising polymer is chitosan. These natural, biodegradable nanoparticles have been used for controlled drug delivery due to their non-toxicity and low immunogenicity (Cho & Borgens, 2012). Chitosan-based hydrogels have also been used as a scaffold at the site of SCI, promoting axon regeneration and cell migration in rat and canine models (Amr et al.,

2014; G. Li et al., 2016; K. Wang, Buschle-Diller, & Misra, 2015). These results warrant further exploration.

Axonal repair and regeneration strategies are an umbrella term covering a variety of approaches that require long-term studies and go beyond the scope of this thesis. Briefly, some of the more promising approaches focus on promoting axonal regeneration by enabling the assembly of a new axonal growth cone (Bradke et al., 2012) or supressing glial scar formation and promoting axonal regeneration by implanting cell sheets containing bone marrow stem cells (Okuda et al., 2017). The implantation of autologous mesenchymal stroma cells (Satti et al., 2016) and of mesenchymal stem cells from the umbilical cord (H. Cheng et al., 2014) have also been successful in aiding the functional recovery of patients with chronic SCI (Zipser et al., 2022). Still, most of these regenerative therapies with encouraging preclinical results are followed by weak and conflicting outcomes during clinical trials (Cofano et al., 2019).

Results from preclinical studies may be improved by deploying an interdisciplinary approach that involves several research teams and laboratories, combining acute molecular therapies and long-term behavioural interventions. Having standardized and reproducible injury models, such as the one I describe in this thesis, is a first step toward such collaborations. A further step may involve the implantation of a spinal imaging window, which will allow longitudinal imaging of the axons, going beyond the acute phase of injury (Figley et al., 2013; Haghayegh Jahromi et al., 2017). Once some of these interventions have proven successful, larger animal models may be required to also study their effect on higher impact SCI. Experiments done on large animals may then help bridge the gap of translation and refine the required surgical procedures prior to application on human patients (Kwon et al., 2015).

Spinal cord injury continues to escape breakthrough clinical interventions, despite the growing interest and progress in the field (Eli et al., 2021; Fouad, Popovich, Kopp, & Schwab, 2021; Karsy & Hawryluk, 2019). Nevertheless, further studies should seek to expand our understanding of this pathology. Even minor improvements in functional outcomes can make a significant difference in the lives of patients suffering from such a lifelong debilitating pathology like spinal cord injury.

5 References

Agrawal, S. K., & Fehlings, M. G. (1996). Mechanisms of secondary injury to spinal cord axons in vitro: role of Na+, Na(+)-K(+)-ATPase, the Na(+)-H+ exchanger, and the Na(+)-Ca2+ exchanger. *J Neurosci, 16*(2), 545-552. Retrieved from https://www.ncbi.nlm.nih.gov/pubmed/8551338

Ahuja, C. S., & Fehlings, M. (2016). Concise Review: Bridging the Gap: Novel Neuroregenerative and Neuroprotective Strategies in Spinal Cord Injury. *Stem Cells Transl Med, 5*(7), 914-924. doi:10.5966/sctm.2015-0381

Ahuja, C. S., Nori, S., Tetreault, L., Wilson, J., Kwon, B., Harrop, J., . . . Fehlings, M. G. (2017). Traumatic Spinal Cord Injury-Repair and Regeneration. *Neurosurgery, 80*(3s), S9-s22. doi:10.1093/neuros/nyw080

Ahuja, C. S., Wilson, J. R., Nori, S., Kotter, M. R. N., Druschel, C., Curt, A., & Fehlings, M. G. (2017). Traumatic spinal cord injury. *Nature Reviews Disease Primers, 3*(1), 17018. doi:10.1038/nrdp.2017.18

Alilain, W. J., Horn, K. P., Hu, H., Dick, T. E., & Silver, J. (2011). Functional regeneration of respiratory pathways after spinal cord injury. *Nature, 475*(7355), 196-200. doi:10.1038/nature10199

Alkabie, S., & Boileau, A. J. (2016). The Role of Therapeutic Hypothermia After Traumatic Spinal Cord Injury--A Systematic Review. *World Neurosurg, 86*, 432-449. doi:10.1016/j.wneu.2015.09.079

Allen, A. (1911). Surgery of experimental lesion of spinal cord equivalent to crush injury of fracture dislocation of spinal column: A preliminary report. *Journal of the American Medical Association, LVII*(11), 878-880. doi:10.1001/jama.1911.04260090100008

Amani, H., Kazerooni, H., Hassanpoor, H., Akbarzadeh, A., & Pazoki-Toroudi, H. (2019). Tailoring synthetic polymeric biomaterials towards nerve tissue engineering: a review. *Artificial Cells, Nanomedicine, and Biotechnology, 47*(1), 3524-3539. doi:10.1080/21691401.2019.1639723

Aminoff, M. J. D. R. B. (2014). *Encyclopedia of the neurological sciences*.

Amr, S. M., Gouda, A., Koptan, W. T., Galal, A. A., Abdel-Fattah, D. S., Rashed, L. A., . . . Abdel-Aziz, M. T. (2014). Bridging defects in chronic spinal cord injury using peripheral nerve grafts combined with a chitosan-laminin scaffold and enhancing regeneration through them by co-transplantation with bone-marrow-derived mesenchymal stem cells: case series of 14 patients. *J Spinal Cord Med, 37*(1), 54-71. doi:10.1179/2045772312y.0000000069

Anderson, M. A., Burda, J. E., Ren, Y., Ao, Y., O'Shea, T. M., Kawaguchi, R., . . . Sofroniew, M. V. (2016). Astrocyte scar formation aids central nervous system axon regeneration. *Nature, 532*(7598), 195-200. doi:10.1038/nature17623

Anderson, T. E., & Stokes, B. T. (1992). Experimental models for spinal cord injury research: physical and physiological considerations. *J Neurotrauma, 9 Suppl 1*, S135-142.

Anjum, A., Yazid, M. D., Fauzi Daud, M., Idris, J., Ng, A. M. H., Selvi Naicker, A., . . . Lokanathan, Y. (2020). Spinal Cord Injury: Pathophysiology, Multimolecular Interactions, and Underlying Recovery Mechanisms. *Int J Mol Sci, 21*(20). doi:10.3390/ijms21207533

Azbill, R. D., Mu, X., Bruce-Keller, A. J., Mattson, M. P., & Springer, J. E. (1997). Impaired mitochondrial function, oxidative stress and altered antioxidant enzyme activities following traumatic spinal cord injury. *Brain Res, 765*(2), 283-290.

Back, S. A., Craig, A., Kayton, R. J., Luo, N. L., Meshul, C. K., Allcock, N., & Fern, R. (2007). Hypoxia-ischemia preferentially triggers glutamate depletion from oligodendroglia and axons in perinatal cerebral white matter. *J Cereb Blood Flow Metab, 27*(2), 334-347. doi:10.1038/sj.jcbfm.9600344

Bakiri, Y., Hamilton, N. B., Karadottir, R., & Attwell, D. (2008). Testing NMDA receptor block as a therapeutic strategy for reducing ischaemic damage to CNS white matter. *Glia, 56*(2), 233-240. doi:10.1002/glia.20608

Barritt, A. W., Davies, M., Marchand, F., Hartley, R., Grist, J., Yip, P., . . . Bradbury, E. J. (2006). Chondroitinase ABC promotes sprouting of intact and injured spinal systems after spinal cord injury. *J Neurosci, 26*(42), 10856-10867. doi:10.1523/jneurosci.2980-06.2006

Bartus, R. T. (1997). The Calpain Hypothesis of Neurodegeneration: Evidence for a Common Cytotoxic Pathway. *The Neuroscientist, 3*(5), 314-327. doi:10.1177/107385849700300513

Bhatt, J. M., & Gordon, P. H. (2007). Current clinical trials in amyotrophic lateral sclerosis. *Expert Opin Investig Drugs, 16*(8), 1197-1207. doi:10.1517/13543784.16.8.1197

Biering-Sorensen, F., Bickenbach, J. E., El Masry, W. S., Officer, A., & von Groote, P. M. (2011). ISCoS-WHO collaboration. International Perspectives of Spinal Cord Injury (IPSCI) report. *Spinal Cord, 49*(6), 679-683. doi:10.1038/sc.2011.12

Biering-Sorensen, F., Biering-Sorensen, T., Liu, N., Malmqvist, L., Wecht, J. M., & Krassioukov, A. (2017). Alterations in cardiac autonomic control in spinal cord injury. *Auton Neurosci*. doi:10.1016/j.autneu.2017.02.004

Blight, A. R. (1983). Cellular morphology of chronic spinal cord injury in the cat: analysis of myelinated axons by line-sampling. *Neuroscience, 10*(2), 521-543.

Blight, A. R. (1991). Morphometric analysis of a model of spinal cord injury in guinea pigs, with behavioral evidence of delayed secondary pathology. *J Neurol Sci, 103*(2), 156-171.

Blight, A. R., Toombs, J. P., Bauer, M. S., & Widmer, W. R. (1991). The effects of 4-aminopyridine on neurological deficits in chronic cases of traumatic spinal cord injury in dogs: a phase I clinical trial. *J Neurotrauma, 8*(2), 103-119. doi:10.1089/neu.1991.8.103

Boldt, I., Eriks-Hoogland, I., Brinkhof, M. W., de Bie, R., Joggi, D., & von Elm, E. (2014). Non-pharmacological interventions for chronic pain in people with spinal cord injury. *Cochrane Database Syst Rev*(11), Cd009177. doi:10.1002/14651858.CD009177.pub2

Bracken, M. B. (2012). Steroids for acute spinal cord injury. *Cochrane Database Syst Rev, 1*, Cd001046. doi:10.1002/14651858.CD001046.pub2

Bradke, F., Fawcett, J. W., & Spira, M. E. (2012). Assembly of a new growth cone after axotomy: the precursor to axon regeneration. *Nature Reviews Neuroscience, 13*(3), 183-193. doi:10.1038/nrn3176

Breckwoldt, M. O., Pfister, F. M., Bradley, P. M., Marinkovic, P., Williams, P. R., Brill, M. S., . . . Misgeld, T. (2014). Multiparametric optical analysis of mitochondrial redox signals during neuronal physiology and pathology in vivo. *Nat Med, 20*(5), 555-560. doi:10.1038/nm.3520

Bros, H., Millward, J. M., Paul, F., Niesner, R., & Infante-Duarte, C. (2014). Oxidative damage to mitochondria at the nodes of Ranvier precedes axon degeneration in ex vivo transected axons. *Exp Neurol, 261*, 127-135. doi:10.1016/j.expneurol.2014.06.018

Buki, A., & Povlishock, J. T. (2006). All roads lead to disconnection?--Traumatic axonal injury revisited. *Acta Neurochir (Wien), 148*(2), 181-193; discussion 193-184. doi:10.1007/s00701-005-0674-4

Buki, A., Siman, R., Trojanowski, J. Q., & Povlishock, J. T. (1999). The role of calpain-mediated spectrin proteolysis in traumatically induced axonal injury. *J Neuropathol Exp Neurol, 58*(4), 365-375.

Bunge, M. B., Holets, V. R., Bates, M. L., Clarke, T. S., & Watson, B. D. (1994). Characterization of photochemically induced spinal cord injury in the rat by light and electron microscopy. *Exp Neurol, 127*(1), 76-93. doi:10.1006/exnr.1994.1082

Carter, L. M., McMahon, S. B., & Bradbury, E. J. (2011). Delayed treatment with chondroitinase ABC reverses chronic atrophy of rubrospinal neurons following spinal cord injury. *Exp Neurol, 228*(1), 149-156. doi:10.1016/j.expneurol.2010.12.023

Casha, S., Zygun, D., McGowan, M. D., Bains, I., Yong, V. W., & Hurlbert, R. J. (2012). Results of a phase II placebo-controlled randomized trial of minocycline in acute spinal cord injury. *Brain, 135*(Pt 4), 1224-1236. doi:10.1093/brain/aws072

Castaldo, P., Cataldi, M., Magi, S., Lariccia, V., Arcangeli, S., & Amoroso, S. (2009). Role of the mitochondrial sodium/calcium exchanger in neuronal physiology and in the pathogenesis of neurological diseases. *Prog Neurobiol, 87*(1), 58-79. doi:10.1016/j.pneurobio.2008.09.017

Chen, M. S., Huber, A. B., van der Haar, M. E., Frank, M., Schnell, L., Spillmann, A. A., . . . Schwab, M. E. (2000). Nogo-A is a myelin-associated neurite outgrowth inhibitor and an

antigen for monoclonal antibody IN-1. *Nature, 403*(6768), 434-439. Retrieved from http://dx.doi.org/10.1038/35000219

Cheng, G., Kong, R. H., Zhang, L. M., & Zhang, J. N. (2012). Mitochondria in traumatic brain injury and mitochondrial-targeted multipotential therapeutic strategies. *Br J Pharmacol, 167*(4), 699-719. doi:10.1111/j.1476-5381.2012.02025.x

Cheng, H., Liu, X., Hua, R., Dai, G., Wang, X., Gao, J., & An, Y. (2014). Clinical observation of umbilical cord mesenchymal stem cell transplantation in treatment for sequelae of thoracolumbar spinal cord injury. *J Transl Med, 12*, 253. doi:10.1186/s12967-014-0253-7

Cheriyan, T., Ryan, D. J., Weinreb, J. H., Cheriyan, J., Paul, J. C., Lafage, V., . . . Errico, T. J. (2014). Spinal cord injury models: a review. *Spinal Cord, 52*(8), 588-595. doi:10.1038/sc.2014.91

Cho, Y., & Borgens, R. B. (2012). Polymer and nano-technology applications for repair and reconstruction of the central nervous system. *Exp Neurol, 233*(1), 126-144. doi:10.1016/j.expneurol.2011.09.028

Choo, A. M., Liu, J., Liu, Z., Dvorak, M., Tetzlaff, W., & Oxland, T. R. (2009). Modeling spinal cord contusion, dislocation, and distraction: characterization of vertebral clamps, injury severities, and node of Ranvier deformations. *J Neurosci Methods, 181*(1), 6-17. doi:10.1016/j.jneumeth.2009.04.007

Chu, T. H., Cummins, K., & Stys, P. K. (2020). Traumatic Injury Reduces Amyloid Plaque Burden in the Transgenic 5xFAD Alzheimer's Mouse Spinal Cord. *J Alzheimers Dis, 77*(3), 1315-1330. doi:10.3233/jad-200387

Cofano, F., Boido, M., Monticelli, M., Zenga, F., Ducati, A., Vercelli, A., & Garbossa, D. (2019). Mesenchymal Stem Cells for Spinal Cord Injury: Current Options, Limitations, and Future of Cell Therapy. *Int J Mol Sci, 20*(11). doi:10.3390/ijms20112698

Early acute management in adults with spinal cord injury: a clinical practice guideline for health-care professionals, 31 C.F.R. (2008).

Coyle, J. T., & Puttfarcken, P. (1993). Oxidative stress, glutamate, and neurodegenerative disorders. *Science, 262*(5134), 689-695.

Davalos, D., Lee, J. K., Smith, W. B., Brinkman, B., Ellisman, M. H., Zheng, B., & Akassoglou, K. (2008). Stable in vivo imaging of densely populated glia, axons and blood vessels in the mouse spinal cord using two-photon microscopy. *J Neurosci Methods, 169*(1), 1-7. doi:10.1016/j.jneumeth.2007.11.011

Dawson, V. L., & Dawson, T. M. (1996). Free radicals and neuronal cell death. *Cell Death Differ, 3*(1), 71-78.

de Freria, C. M., Van Niekerk, E., Blesch, A., & Lu, P. (2021). Neural Stem Cells: Promoting Axonal Regeneration and Spinal Cord Connectivity. *Cells, 10*(12). doi:10.3390/cells10123296

Denk, W., Strickler, J. H., & Webb, W. W. (1990). Two-photon laser scanning fluorescence microscopy. *Science, 248*(4951), 73-76. doi:10.1126/science.2321027

Derakhshanrad, N., Saberi, H., Yekaninejad, M. S., Joghataei, M. T., & Sheikhrezaei, A. (2018). Granulocyte-colony stimulating factor administration for neurological improvement in patients with postrehabilitation chronic incomplete traumatic spinal cord injuries: a double-blind randomized controlled clinical trial. *J Neurosurg Spine, 29*(1), 97-107. doi:10.3171/2017.11.Spine17769

Ding, W., Hu, S., Wang, P., Kang, H., Peng, R., Dong, Y., & Li, F. (2022). Spinal Cord Injury: The Global Incidence, Prevalence, and Disability From the Global Burden of Disease Study 2019. *Spine (Phila Pa 1976), 47*(21), 1532-1540. doi:10.1097/brs.0000000000004417

Direnberger, S., Mues, M., Micale, V., Wotjak, C. T., Dietzel, S., Schubert, M., . . . Griesbeck, O. (2012). Biocompatibility of a genetically encoded calcium indicator in a transgenic mouse model. *Nature communications, 3*, 1031. doi:10.1038/ncomms2035 [doi]

Ditunno, J. F., Little, J. W., Tessler, A., & Burns, A. S. (2004). Spinal shock revisited: a four-phase model. *Spinal Cord, 42*(7), 383-395. Retrieved from http://dx.doi.org/10.1038/sj.sc.3101603

Dobkin, B. H., & Havton, L. A. (2004). Basic advances and new avenues in therapy of spinal cord injury. *Annu Rev Med, 55*, 255-282. doi:10.1146/annurev.med.55.091902.104338

Domercq, M., Etxebarria, E., Perez-Samartin, A., & Matute, C. (2005). Excitotoxic oligodendrocyte death and axonal damage induced by glutamate transporter inhibition. *Glia, 52*(1), 36-46. doi:10.1002/glia.20221

Dumont, R. J., Okonkwo, D. O., Verma, S., Hurlbert, R. J., Boulos, P. T., Ellegala, D. B., & Dumont, A. S. (2001). Acute spinal cord injury, part I: pathophysiologic mechanisms. *Clin Neuropharmacol, 24*(5), 254-264. doi:10.1097/00002826-200109000-00002

Eckert, M. J., & Martin, M. J. (2017). Trauma: Spinal Cord Injury. *Surg Clin North Am, 97*(5), 1031-1045. doi:10.1016/j.suc.2017.06.008

Eli, I., Lerner, D. P., & Ghogawala, Z. (2021). Acute Traumatic Spinal Cord Injury. *Neurol Clin, 39*(2), 471-488. doi:10.1016/j.ncl.2021.02.004

Evaniew, N., Noonan, V. K., Fallah, N., Kwon, B. K., Rivers, C. S., Ahn, H., . . . Dvorak, M. F. (2015). Methylprednisolone for the Treatment of Patients with Acute Spinal Cord Injuries: A Propensity Score-Matched Cohort Study from a Canadian Multi-Center Spinal Cord Injury Registry. *J Neurotrauma, 32*(21), 1674-1683. doi:10.1089/neu.2015.3963

Fakhoury, M. (2015). Spinal cord injury: overview of experimental approaches used to restore locomotor activity. *Rev Neurosci, 26*(4), 397-405. doi:10.1515/revneuro-2015-0001

Fan, B., Wei, Z., & Feng, S. (2022). Progression in translational research on spinal cord injury based on microenvironment imbalance. *Bone Research, 10*(1), 35. doi:10.1038/s41413-022-00199-9

Farkas, O., Lifshitz, J., & Povlishock, J. T. (2006). Mechanoporation induced by diffuse traumatic brain injury: an irreversible or reversible response to injury? *J Neurosci, 26*(12), 3130-3140. doi:10.1523/jneurosci.5119-05.2006

Fatima, G., Sharma, V. P., Das, S. K., & Mahdi, A. A. (2015). Oxidative stress and antioxidative parameters in patients with spinal cord injury: implications in the pathogenesis of disease. *Spinal Cord, 53*(1), 3-6. doi:10.1038/sc.2014.178

Fehlings, M. G., Badhiwala, J. H., Ahn, H., Farhadi, H. F., Shaffrey, C. I., Nassr, A., . . . Kopjar, B. (2021). Safety and efficacy of riluzole in patients undergoing decompressive surgery for degenerative cervical myelopathy (CSM-Protect): a multicentre, double-blind, placebo-controlled, randomised, phase 3 trial. *Lancet Neurol, 20*(2), 98-106. doi:10.1016/s1474-4422(20)30407-5

Fehlings, M. G., Theodore, N., Harrop, J., Maurais, G., Kuntz, C., Shaffrey, C. I., . . . McKerracher, L. (2011). A phase I/IIa clinical trial of a recombinant Rho protein antagonist in acute spinal cord injury. *J Neurotrauma, 28*(5), 787-796. doi:10.1089/neu.2011.1765

Fehlings, M. G., Wilson, J. R., Frankowski, R. F., Toups, E. G., Aarabi, B., Harrop, J. S., . . . Grossman, R. G. (2012). Riluzole for the treatment of acute traumatic spinal cord injury: rationale for and design of the NACTN Phase I clinical trial. *J Neurosurg Spine, 17*(1 Suppl), 151-156. doi:10.3171/2012.4.aospine1259

Fern, R., Ransom, B. R., & Waxman, S. G. (1995). Voltage-gated calcium channels in CNS white matter: role in anoxic injury. *J Neurophysiol, 74*(1), 369-377.

Figley, S. A., Chen, Y., Maeda, A., Conroy, L., McMullen, J. D., Silver, J. I., . . . DaCosta, R. S. (2013). A Spinal Cord Window Chamber Model for In Vivo Longitudinal Multimodal Optical and Acoustic Imaging in a Murine Model. *PLoS One, 8*(3), e58081. doi:10.1371/journal.pone.0058081

Fouad, K., Popovich, P. G., Kopp, M. A., & Schwab, J. M. (2021). The neuroanatomical-functional paradox in spinal cord injury. *Nat Rev Neurol, 17*(1), 53-62. doi:10.1038/s41582-020-00436-x

Franke, T., & Rhode, S. (2012). Two-Photon Microscopy for Deep Tissue Imaging of Living Specimens. *Microscopy Today, 20(4)*, 12-16. doi:10.1017/S1551929512000430

Garaschuk, O., Griesbeck, O., & Konnerth, A. (2007). Troponin C-based biosensors: a new family of genetically encoded indicators for in vivo calcium imaging in the nervous system. *Cell Calcium, 42*(4-5), 351-361. doi:10.1016/j.ceca.2007.02.011

Geiger, A., Russo, L., Gensch, T., Thestrup, T., Becker, S., Hopfner, K. P., . . . Griesbeck, O. (2012). Correlating calcium binding, Forster resonance energy transfer, and conformational change in the biosensor TN-XXL. *Biophys J, 102*(10), 2401-2410. doi:10.1016/j.bpj.2012.03.065

Griesbeck, O., Baird, G. S., Campbell, R. E., Zacharias, D. A., & Tsien, R. Y. (2001). Reducing the environmental sensitivity of yellow fluorescent protein. Mechanism and applications. *The Journal of biological chemistry, 276*(31), 29188-29194. doi:10.1074/jbc.M102815200 [doi]

Hagen, E. M., Lie, S. A., Rekand, T., Gilhus, N. E., & Gronning, M. (2010). Mortality after traumatic spinal cord injury: 50 years of follow-up. *Journal of Neurology, Neurosurgery & Psychiatry, 81*(4), 368-373. doi:10.1136/jnnp.2009.178798

Haghayegh Jahromi, N., Tardent, H., Enzmann, G., Deutsch, U., Kawakami, N., Bittner, S., . . . Engelhardt, B. (2017). A Novel Cervical Spinal Cord Window Preparation Allows for Two-Photon Imaging of T-Cell Interactions with the Cervical Spinal Cord Microvasculature during Experimental Autoimmune Encephalomyelitis. *Frontiers in Immunology, 8*. doi:10.3389/fimmu.2017.00406

Hall, E. D., & Braughler, J. M. (1989). Central nervous system trauma and stroke. II. Physiological and pharmacological evidence for involvement of oxygen radicals and lipid peroxidation. *Free Radic Biol Med, 6*(3), 303-313.

Harrison, M., O'Brien, A., Adams, L., Cowin, G., Ruitenberg, M. J., Sengul, G., & Watson, C. (2013). Vertebral landmarks for the identification of spinal cord segments in the mouse. *Neuroimage, 68*, 22-29. doi:10.1016/j.neuroimage.2012.11.048

Hernández, D. E., Salvadores, N. A., Moya-Alvarado, G., Catalán, R. J., Bronfman, F. C., & Court, F. A. (2018). Axonal degeneration induced by glutamate excitotoxicity is mediated by necroptosis. *J Cell Sci, 131*(22). doi:10.1242/jcs.214684

Hill, C. S., Coleman, M. P., & Menon, D. K. (2016). Traumatic Axonal Injury: Mechanisms and Translational Opportunities. *Trends Neurosci, 39*(5), 311-324. doi:10.1016/j.tins.2016.03.002

Imaizumi, T., Kocsis, J. D., & Waxman, S. G. (1999). The role of voltage-gated Ca2+ channels in anoxic injury of spinal cord white matter. *Brain Res, 817*(1-2), 84-92.

Instrumentation, P. S. (2012). IH Spinal Cord Impactor User's Manual. In *IH Spinal Cord Impactor User's Manual*: Precision Systems and Instrumentation, LLC.

Jacobi, A., & Bareyre, F. M. (2015). Regulation of axonal remodeling following spinal cord injury. *Neural regeneration research, 10*(10), 1555-1557. doi:10.4103/1673-5374.167748

Jamme, I., Petit, E., Divoux, D., Gerbi, A., Maixent, J. M., & Nouvelot, A. (1995). Modulation of mouse cerebral Na+,K(+)-ATPase activity by oxygen free radicals. *Neuroreport, 7*(1), 333-337.

Jerome, C., Hoch, B., & Carlson, C. S. (2018). 5 - Skeletal System. In P. M. Treuting, S. M. Dintzis, & K. S. Montine (Eds.), *Comparative Anatomy and Histology (Second Edition)* (pp. 67-88). San Diego: Academic Press.

Joshi, M., & Fehlings, M. G. (2002). Development and characterization of a novel, graded model of clip compressive spinal cord injury in the mouse: Part 1. Clip design, behavioral outcomes, and histopathology. *J Neurotrauma, 19*(2), 175-190. doi:10.1089/08977150252806947

Karsy, M., & Hawryluk, G. (2019). Modern Medical Management of Spinal Cord Injury. *Curr Neurol Neurosci Rep, 19*(9), 65. doi:10.1007/s11910-019-0984-1

Katoh, H., Yokota, K., & Fehlings, M. G. (2019). Regeneration of Spinal Cord Connectivity Through Stem Cell Transplantation and Biomaterial Scaffolds. *Front Cell Neurosci, 13*, 248. doi:10.3389/fncel.2019.00248

Kerschensteiner, M., Schwab, M. E., Lichtman, J. W., & Misgeld, T. (2005). In vivo imaging of axonal degeneration and regeneration in the injured spinal cord. *Nat Med, 11*(5), 572-577. doi:10.1038/nm1229

Khayrullina, G., Bermudez, S., & Byrnes, K. R. (2015). Inhibition of NOX2 reduces locomotor impairment, inflammation, and oxidative stress after spinal cord injury. *J Neuroinflammation, 12*, 172. doi:10.1186/s12974-015-0391-8

Khazaeipour, Z., Taheri-Otaghsara, S. M., & Naghdi, M. (2015). Depression Following Spinal Cord Injury: Its Relationship to Demographic and Socioeconomic Indicators. *Top Spinal Cord Inj Rehabil, 21*(2), 149-155. doi:10.1310/sci2102-149

Kilinc, D., Gallo, G., & Barbee, K. A. (2008). Mechanically-induced membrane poration causes axonal beading and localized cytoskeletal damage. *Exp Neurol, 212*(2), 422-430. doi:10.1016/j.expneurol.2008.04.025

Kilinc, D., Gallo, G., & Barbee, K. A. (2009). Mechanical membrane injury induces axonal beading through localized activation of calpain. *Exp Neurol, 219*(2), 553-561. doi:10.1016/j.expneurol.2009.07.014

Kirichok, Y., Krapivinsky, G., & Clapham, D. E. (2004). The mitochondrial calcium uniporter is a highly selective ion channel. *Nature, 427*(6972), 360-364. doi:10.1038/nature02246

Kjell, J., & Olson, L. (2016). Rat models of spinal cord injury: from pathology to potential therapies. *Disease Models & Mechanisms, 9*(10), 1125. Retrieved from http://dmm.biologists.org/content/9/10/1125.abstract

Koozekanani, S. H., Vise, W. M., Hashemi, R. M., & McGhee, R. B. (1976). Possible mechanisms for observed pathophysiological variability in experimental spinal cord injury by the method of Allen. *J Neurosurg, 44*(4), 429-434. doi:10.3171/jns.1976.44.4.0429

Kostyuk, P., & Verkhratsky, A. (1994). Calcium stores in neurons and glia. *Neuroscience, 63*(2), 381-404.

Krause, J. S., Sternberg, M., Lottes, S., & Maides, J. (1997). Mortality after spinal cord injury: an 11-year prospective study. *Arch Phys Med Rehabil, 78*(8), 815-821. doi:10.1016/s0003-9993(97)90193-3

Kucher, K., Johns, D., Maier, D., Abel, R., Badke, A., Baron, H., . . . Curt, A. (2018). First-in-Man Intrathecal Application of Neurite Growth-Promoting Anti-Nogo-A Antibodies in Acute Spinal Cord Injury. *Neurorehabilitation and Neural Repair, 32*(6-7), 578-589. doi:10.1177/1545968318776371

Kuner, T., & Augustine, G. J. (2000). A genetically encoded ratiometric indicator for chloride: capturing chloride transients in cultured hippocampal neurons. *Neuron, 27*(3), 447-459. doi:S0896-6273(00)00056-8 [pii]

Kwon, B. K., Streijger, F., Hill, C. E., Anderson, A. J., Bacon, M., Beattie, M. S., . . . Tetzlaff, W. (2015). Large animal and primate models of spinal cord injury for the testing of novel therapies. *Exp Neurol, 269*, 154-168. doi:10.1016/j.expneurol.2015.04.008

Lampe, K. J., Bjugstad, K. B., & Mahoney, M. J. (2010). Impact of degradable macromer content in a poly(ethylene glycol) hydrogel on neural cell metabolic activity, redox state, proliferation, and differentiation. *Tissue Eng Part A, 16*(6), 1857-1866. doi:10.1089/ten.TEA.2009.0509

Leppanen, L., & Stys, P. K. (1997). Ion transport and membrane potential in CNS myelinated axons. II. Effects of metabolic inhibition. *J Neurophysiol, 78*(4), 2095-2107.

Li, G., Che, M.-T., Zhang, K., Qin, L.-N., Zhang, Y.-T., Chen, R.-Q., . . . Zeng, Y.-S. (2016). Graft of the NT-3 persistent delivery gelatin sponge scaffold promotes axon regeneration, attenuates inflammation, and induces cell migration in rat and canine with spinal cord injury. *Biomaterials, 83*, 233-248. doi:https://doi.org/10.1016/j.biomaterials.2015.11.059

Li, S., & Stys, P. K. (2000). Mechanisms of ionotropic glutamate receptor-mediated excitotoxicity in isolated spinal cord white matter. *J Neurosci, 20*(3), 1190-1198. doi:10.1523/jneurosci.20-03-01190.2000

Lin, M. T., & Beal, M. F. (2006). Mitochondrial dysfunction and oxidative stress in neurodegenerative diseases. *Nature, 443*(7113), 787-795. doi:10.1038/nature05292

Lingor, P., Koch, J. C., Tönges, L., & Bähr, M. (2012). Axonal degeneration as a therapeutic target in the CNS. *Cell and Tissue Research, 349*(1), 289-311. doi:10.1007/s00441-012-1362-3

Liu, D., Shan, Y., Valluru, L., & Bao, F. (2013). Mn (III) tetrakis (4-benzoic acid) porphyrin scavenges reactive species, reduces oxidative stress, and improves functional recovery after experimental spinal cord injury in rats: comparison with methylprednisolone. *BMC Neurosci, 14*, 23. doi:10.1186/1471-2202-14-23

Liu, D., Xu, G. Y., Pan, E., & McAdoo, D. J. (1999). Neurotoxicity of glutamate at the concentration released upon spinal cord injury. *Neuroscience, 93*(4), 1383-1389. doi:10.1016/s0306-4522(99)00278-x

Liu, F. T., Xu, S. M., Xiang, Z. H., Li, X. N., Li, J., Yuan, H. B., & Sun, X. J. (2014). Molecular hydrogen suppresses reactive astrogliosis related to oxidative injury during spinal cord injury in rats. *CNS Neurosci Ther, 20*(8), 778-786. doi:10.1111/cns.12258

Luo, J., Borgens, R., & Shi, R. (2002). Polyethylene glycol immediately repairs neuronal membranes and inhibits free radical production after acute spinal cord injury. *J Neurochem, 83*(2), 471-480. doi:10.1046/j.1471-4159.2002.01160.x

Ma, M. (2013). Role of calpains in the injury-induced dysfunction and degeneration of the mammalian axon. *Neurobiol Dis, 60*, 61-79. doi:10.1016/j.nbd.2013.08.010

Mank, M., Santos, A. F., Direnberger, S., Mrsic-Flogel, T. D., Hofer, S. B., Stein, V., . . . Griesbeck, O. (2008). A genetically encoded calcium indicator for chronic in vivo two-photon imaging. *Nature methods, 5*(9), 805-811. doi:10.1038/nmeth.1243 [doi]

McAdoo, D. J., Xu, G. Y., Robak, G., & Hughes, M. G. (1999). Changes in amino acid concentrations over time and space around an impact injury and their diffusion through the rat spinal cord. *Exp Neurol, 159*(2), 538-544. doi:10.1006/exnr.1999.7166

Meininger, V., Pradat, P. F., Corse, A., Al-Sarraj, S., Rix Brooks, B., Caress, J. B., . . . Wurthner, J. (2014). Safety, pharmacokinetic, and functional effects of the nogo-a monoclonal antibody in amyotrophic lateral sclerosis: a randomized, first-in-human clinical trial. *PLoS One, 9*(5), e97803. doi:10.1371/journal.pone.0097803

Misgeld, T., & Kerschensteiner, M. (2006). In vivo imaging of the diseased nervous system. *Nat Rev Neurosci, 7*(6), 449-463. doi:10.1038/nrn1905

Misgeld, T., Nikic, I., & Kerschensteiner, M. (2007). In vivo imaging of single axons in the mouse spinal cord. *Nat Protoc, 2*(2), 263-268. doi:10.1038/nprot.2007.24

Mokalled, M. H., Patra, C., Dickson, A. L., Endo, T., Stainier, D. Y., & Poss, K. D. (2016). Injury-induced ctgfa directs glial bridging and spinal cord regeneration in zebrafish. *Science, 354*(6312), 630-634. doi:10.1126/science.aaf2679

Myers, J., Lee, M., & Kiratli, J. (2007). Cardiovascular disease in spinal cord injury: an overview of prevalence, risk, evaluation, and management. *Am J Phys Med Rehabil, 86*(2), 142-152. doi:10.1097/PHM.0b013e31802f0247

Nagoshi, N., Nakashima, H., & Fehlings, M. G. (2015). Riluzole as a neuroprotective drug for spinal cord injury: from bench to bedside. *Molecules, 20*(5), 7775-7789. doi:10.3390/molecules20057775

National Clinical Guideline, C. (2016). National Institute for Health and Care Excellence: Clinical Guidelines. In *Spinal Injury: Assessment and Initial Management*. London: National Institute for Health and Care Excellence (UK)

Copyright (c) National Clinical Guideline Centre, 2016.

NCT01828203. Minocycline in Acute Spinal Cord Injury (MASC).

Nehrt, A., Hamann, K., Ouyang, H., & Shi, R. (2010). Polyethylene glycol enhances axolemmal resealing following transection in cultured cells and in ex vivo spinal cord. *J Neurotrauma, 27*(1), 151-161. doi:10.1089/neu.2009.0993

Nehrt, A., Rodgers, R., Shapiro, S., Borgens, R., & Shi, R. (2007). The critical role of voltage-dependent calcium channel in axonal repair following mechanical trauma. *Neuroscience, 146*(4), 1504-1512. doi:10.1016/j.neuroscience.2007.02.015

Nikic, I., Merkler, D., Sorbara, C., Brinkoetter, M., Kreutzfeldt, M., Bareyre, F. M., . . . Kerschensteiner, M. (2011). A reversible form of axon damage in experimental autoimmune encephalomyelitis and multiple sclerosis. *Nat Med, 17*(4), 495-499. doi:10.1038/nm.2324

Nikolaeva, M. A., Mukherjee, B., & Stys, P. K. (2005). Na+-dependent sources of intra-axonal Ca2+ release in rat optic nerve during in vitro chemical ischemia. *J Neurosci, 25*(43), 9960-9967. doi:10.1523/jneurosci.2003-05.2005

Nishio, Y., Koda, M., Kamada, T., Someya, Y., Kadota, R., Mannoji, C., . . . Yamazaki, M. (2007). Granulocyte colony-stimulating factor attenuates neuronal death and promotes functional

recovery after spinal cord injury in mice. *J Neuropathol Exp Neurol, 66*(8), 724-731. doi:10.1097/nen.0b013e3181257176

Norberg, E., Gogvadze, V., Ott, M., Horn, M., Uhlen, P., Orrenius, S., & Zhivotovsky, B. (2008). An increase in intracellular Ca2+ is required for the activation of mitochondrial calpain to release AIF during cell death. *Cell Death Differ, 15*(12), 1857-1864. doi:10.1038/cdd.2008.123

Okuda, A., Horii-Hayashi, N., Sasagawa, T., Shimizu, T., Shigematsu, H., Iwata, E., . . . Tanaka, Y. (2017). Bone marrow stromal cell sheets may promote axonal regeneration and functional recovery with suppression of glial scar formation after spinal cord transection injury in rats. *J Neurosurg Spine, 26*(3), 388-395. doi:10.3171/2016.8.Spine16250

Onifer, S. M., Smith, G. M., & Fouad, K. (2011). Plasticity after spinal cord injury: relevance to recovery and approaches to facilitate it. *Neurotherapeutics : the journal of the American Society for Experimental NeuroTherapeutics, 8*(2), 283-293. doi:10.1007/s13311-011-0034-4

Orem, B. C., Pelisch, N., Williams, J., Nally, J. M., & Stirling, D. P. (2017). Intracellular calcium release through IP(3)R or RyR contributes to secondary axonal degeneration. *Neurobiol Dis, 106*, 235-243. doi:10.1016/j.nbd.2017.07.011

Orem, B. C., Rajaee, A., & Stirling, D. P. (2021). Inhibiting Calcium Release from Ryanodine Receptors Protects Axons after Spinal Cord Injury. *Journal of neurotrauma, 39*(3-4), 311-319. doi:10.1089/neu.2021.0350

Orr, M. B., & Gensel, J. C. (2018). Spinal Cord Injury Scarring and Inflammation: Therapies Targeting Glial and Inflammatory Responses. *Neurotherapeutics : the journal of the American Society for Experimental NeuroTherapeutics, 15*(3), 541-553. doi:10.1007/s13311-018-0631-6

Ouardouz, M., Coderre, E., Basak, A., Chen, A., Zamponi, G. W., Hameed, S., . . . Stys, P. K. (2009). Glutamate receptors on myelinated spinal cord axons: I. GluR6 kainate receptors. *Annals of Neurology, 65*(2), 151-159. doi:10.1002/ana.21533 [doi]

Ouardouz, M., Coderre, E., Zamponi, G. W., Hameed, S., Yin, X., Trapp, B. D., & Stys, P. K. (2009). Glutamate receptors on myelinated spinal cord axons: II. AMPA and GluR5 receptors. *Annals of Neurology, 65*(2), 160-166. doi:10.1002/ana.21539 [doi]

Ouardouz, M., Malek, S., Coderre, E., & Stys, P. K. (2006). Complex interplay between glutamate receptors and intracellular Ca2+ stores during ischaemia in rat spinal cord white matter. *J Physiol, 577*(Pt 1), 191-204. doi:10.1113/jphysiol.2006.116798

Ouardouz, M., Nikolaeva, M. A., Coderre, E., Zamponi, G. W., McRory, J. E., Trapp, B. D., . . . Stys, P. K. (2003). Depolarization-induced Ca2+ release in ischemic spinal cord white matter involves L-type Ca2+ channel activation of ryanodine receptors. *Neuron, 40*(1), 53-63. doi:S0896627303005403 [pii]

Ouardouz, M., Zamponi, G. W., Barr, W., Kiedrowski, L., & Stys, P. K. (2005). Protection of ischemic rat spinal cord white matter: Dual action of KB-R7943 on Na+/Ca2+ exchange and L-type Ca2+ channels. *Neuropharmacology, 48*(4), 566-575. doi:10.1016/j.neuropharm.2004.12.007

Oyinbo, C. A. (2011). Secondary injury mechanisms in traumatic spinal cord injury: a nugget of this multiply cascade. *Acta Neurobiol Exp (Wars), 71*(2), 281-299.

Park, E., Velumian, A. A., & Fehlings, M. G. (2004). The role of excitotoxicity in secondary mechanisms of spinal cord injury: a review with an emphasis on the implications for white matter degeneration. *J Neurotrauma, 21*(6), 754-774. doi:10.1089/0897715041269641

Pettus, E. H., Christman, C. W., Giebel, M. L., & Povlishock, J. T. (1994). Traumatically induced altered membrane permeability: its relationship to traumatically induced reactive axonal change. *J Neurotrauma, 11*(5), 507-522. doi:10.1089/neu.1994.11.507

Pettus, E. H., & Povlishock, J. T. (1996). Characterization of a distinct set of intra-axonal ultrastructural changes associated with traumatically induced alteration in axolemmal permeability. *Brain Res, 722*(1-2), 1-11.

Pitt, D., Gonzales, E., Cross, A. H., & Goldberg, M. P. (2010). Dysmyelinated axons in shiverer mice are highly vulnerable to alpha-amino-3-hydroxy-5-methylisoxazole-4-propionic acid

(AMPA) receptor-mediated toxicity. *Brain Res, 1309*, 146-154. doi:10.1016/j.brainres.2009.10.066

Povlishock, J. T., Becker, D. P., Cheng, C. L., & Vaughan, G. W. (1983). Axonal change in minor head injury. *J Neuropathol Exp Neurol, 42*(3), 225-242. doi:10.1097/00005072-198305000-00002

Rekand, T., Hagen, E. M., & Gronning, M. (2012). Chronic pain following spinal cord injury. *Tidsskr Nor Laegeforen, 132*(8), 974-979. doi:10.4045/tidsskr.11.0794

Rivlin, A. S., & Tator, C. H. (1978). Effect of duration of acute spinal cord compression in a new acute cord injury model in the rat. *Surg Neurol, 10*(1), 38-43.

Romanelli, E., Sorbara, C. D., Nikić, I., Dagkalis, A., Misgeld, T., & Kerschensteiner, M. (2013). Cellular, subcellular and functional in vivo labeling of the spinal cord using vital dyes. *Nat. Protocols, 8*(3), 481-490. Retrieved from http://dx.doi.org/10.1038/nprot.2013.022

Rubart, M. (2004). Two-photon microscopy of cells and tissue. *Circ Res, 95*(12), 1154-1166. doi:10.1161/01.Res.0000150593.30324.42

Ruzin, S., & Aaron, H. http://microscopy.berkeley.edu/courses/TLM/2P/index.html.

Saatman, K. E., Abai, B., Grosvenor, A., Vorwerk, C. K., Smith, D. H., & Meaney, D. F. (2003). Traumatic axonal injury results in biphasic calpain activation and retrograde transport impairment in mice. *J Cereb Blood Flow Metab, 23*(1), 34-42.

Sandler, A. N., & Tator, C. H. (1976). Review of the effect of spinal cord trama on the vessels and blood flow in the spinal cord. *J Neurosurg, 45*(6), 638-646. doi:10.3171/jns.1976.45.6.0638

Satti, H. S., Waheed, A., Ahmed, P., Ahmed, K., Akram, Z., Aziz, T., . . . Malik, S. A. (2016). Autologous mesenchymal stromal cell transplantation for spinal cord injury: A Phase I pilot study. *Cytotherapy, 18*(4), 518-522. doi:https://doi.org/10.1016/j.jcyt.2016.01.004

Scheff, S., & Roberts, K. N. (2009). Infinite Horizon Spinal Cord Contusion Model. In J. Chen, Z. C. Xu, X.-M. Xu, & J. H. Zhang (Eds.), *Animal Models of Acute Neurological Injuries* (pp. 423-432). Totowa, NJ: Humana Press.

Scheff, S. W., Rabchevsky, A. G., Fugaccia, I., Main, J. A., & Lumpp, J. E., Jr. (2003). Experimental modeling of spinal cord injury: characterization of a force-defined injury device. *Journal of neurotrauma, 20*(2), 179-193. doi:10.1089/08977150360547099 [doi]

Schindelin, J., Arganda-Carreras, I., Frise, E., Kaynig, V., Longair, M., Pietzsch, T., . . . Cardona, A. (2012). Fiji: an open-source platform for biological-image analysis. *Nat Methods, 9*(7), 676-682. doi:10.1038/nmeth.2019

Schumacher, P. A., Siman, R. G., & Fehlings, M. G. (2000). Pretreatment with calpain inhibitor CEP-4143 inhibits calpain I activation and cytoskeletal degradation, improves neurological function, and enhances axonal survival after traumatic spinal cord injury. *J Neurochem, 74*(4), 1646-1655.

Schwab, M. E. (2010). Functions of Nogo proteins and their receptors in the nervous system. *Nat Rev Neurosci, 11*(12), 799-811. Retrieved from http://dx.doi.org/10.1038/nrn2936

Seifert, J. L., Bell, J. E., Elmer, B. B., Sucato, D. J., & Romero, M. I. (2011). Characterization of a novel bidirectional distraction spinal cord injury animal model. *J Neurosci Methods, 197*(1), 97-103. doi:10.1016/j.jneumeth.2011.02.003

Sharif-Alhoseini, M., Khormali, M., Rezaei, M., Safdarian, M., Hajighadery, A., Khalatbari, M. M., . . . Rahimi-Movaghar, V. (2017). Animal models of spinal cord injury: a systematic review. *Spinal Cord, 55*(8), 714-721. doi:10.1038/sc.2016.187

Shi, R., & Borgens, R. B. (2000). Anatomical repair of nerve membranes in crushed mammalian spinal cord with polyethylene glycol. *J Neurocytol, 29*(9), 633-643. doi:10.1023/a:1010879219775

Silberstein, M., & McLean, K. (1994). Non-contiguous spinal injury: clinical and imaging features, and postulated mechanism. *Paraplegia, 32*(12), 817-823. doi:10.1038/sc.1994.129

Silva, N. A., Sousa, N., Reis, R. L., & Salgado, A. J. (2014). From basics to clinical: a comprehensive review on spinal cord injury. *Prog Neurobiol, 114*, 25-57. doi:10.1016/j.pneurobio.2013.11.002

Simons, M., Misgeld, T., & Kerschensteiner, M. (2014). A unified cell biological perspective on axon–myelin injury. *The Journal of Cell Biology, 206*(3), 335-345. doi:10.1083/jcb.201404154

Singh, A., Tetreault, L., Kalsi-Ryan, S., Nouri, A., & Fehlings, M. G. (2014). Global prevalence and incidence of traumatic spinal cord injury. (1179-1349 (Linking)). doi:D - NLM: PMC4179833 OTO - NOTNLM

Smith, K. J., Kapoor, R., Hall, S. M., & Davies, M. (2001). Electrically active axons degenerate when exposed to nitric oxide. *Ann Neurol, 49*(4), 470-476.

So, P. T. C. (2001). Two-photon Fluorescence Light Microscopy. In *eLS*: John Wiley & Sons, Ltd.

Sokolowski, J. D., Gamage, K. K., Heffron, D. S., Leblanc, A. C., Deppmann, C. D., & Mandell, J. W. (2014). Caspase-mediated cleavage of actin and tubulin is a common feature and sensitive marker of axonal degeneration in neural development and injury. *Acta Neuropathol Commun, 2*, 16. doi:10.1186/2051-5960-2-16

Sorbara, C., Misgeld, T., & Kerschensteiner, M. (2012). In vivo imaging of the diseased nervous system: an update. *Curr Pharm Des, 18*(29), 4465-4470.

Spinal cord injury facts and figures at a glance. (2012). *J Spinal Cord Med, 35*(4), 197-198. doi:10.1179/1079026812z.00000000063

Steward, O., Zheng, B., & Tessier-Lavigne, M. (2003). False resurrections: distinguishing regenerated from spared axons in the injured central nervous system. *J Comp Neurol, 459*(1), 1-8. doi:10.1002/cne.10593

Stirling, D. P., Cummins, K., Wayne Chen, S. R., & Stys, P. (2014). Axoplasmic reticulum Ca(2+) release causes secondary degeneration of spinal axons. *Annals of Neurology, 75*(2), 220-229. doi:10.1002/ana.24099

Stirling, D. P., & Stys, P. K. (2010). Mechanisms of axonal injury: internodal nanocomplexes and calcium deregulation. *Trends Mol Med, 16*(4), 160-170. doi:10.1016/j.molmed.2010.02.002

Stone, J. R., Okonkwo, D. O., Singleton, R. H., Mutlu, L. K., Helm, G. A., & Povlishock, J. T. (2002). Caspase-3-mediated cleavage of amyloid precursor protein and formation of amyloid Beta peptide in traumatic axonal injury. *J Neurotrauma, 19*(5), 601-614. doi:10.1089/089771502753754073

Stys, P. K. (1998). Anoxic and ischemic injury of myelinated axons in CNS white matter: from mechanistic concepts to therapeutics. *J Cereb Blood Flow Metab, 18*(1), 2-25. doi:10.1097/00004647-199801000-00002

Stys, P. K. (2004). White matter injury mechanisms. *Curr Mol Med, 4*(2), 113-130. doi:10.2174/1566524043479220

Stys, P. K. (2005). General mechanisms of axonal damage and its prevention. *J Neurol Sci, 233*(1-2), 3-13. doi:10.1016/j.jns.2005.03.031

Stys, P. K., Lehning, E., Saubermann, A. J., & LoPachin, R. M., Jr. (1997). Intracellular concentrations of major ions in rat myelinated axons and glia: calculations based on electron probe X-ray microanalyses. *J Neurochem, 68*(5), 1920-1928.

Stys, P. K., & Lopachin, R. M. (1998). Mechanisms of calcium and sodium fluxes in anoxic myelinated central nervous system axons. *Neuroscience, 82*(1), 21-32.

Stys, P. K., Waxman, S. G., & Ransom, B. R. (1992). Ionic mechanisms of anoxic injury in mammalian CNS white matter: role of Na+ channels and Na(+)-Ca2+ exchanger. *The Journal of neuroscience : the official journal of the Society for Neuroscience, 12*(2), 430-439. Retrieved from http://www.jneurosci.org/content/12/2/430.full.pdf

Temenoff, J. S., Athanasiou, K. A., Lebaron, R. G., & Mikos, A. G. (2002). Effect of poly (ethylene glycol) molecular weight on tensile and swelling properties of oligo (poly (ethylene glycol) fumarate) hydrogels for cartilage tissue engineering. *Journal of Biomedical Materials Research: An Official Journal of The Society for Biomaterials, The Japanese Society for Biomaterials, and The Australian Society for Biomaterials and the Korean Society for Biomaterials, 59*(3), 429-437.

Toborek, M., Malecki, A., Garrido, R., Mattson, M. P., Hennig, B., & Young, B. (1999). Arachidonic acid-induced oxidative injury to cultured spinal cord neurons. *J Neurochem, 73*(2), 684-692.

Tsutsui, S., & Stys, P. K. (2013). Metabolic injury to axons and myelin. *Exp Neurol, 246*, 26-34. doi:10.1016/j.expneurol.2012.04.016

Turney, S. G., & Lichtman, J. W. (2012). Reversing the outcome of synapse elimination at developing neuromuscular junctions in vivo: evidence for synaptic competition and its mechanism. *PLoS Biol, 10*(6), e1001352. doi:10.1371/journal.pbio.1001352

van Den Hauwe, L., Sundgren, P. C., & Flanders, A. E. (2020). Spinal Trauma and Spinal Cord Injury (SCI). In J. Hodler, R. A. Kubik-Huch, & G. K. von Schulthess (Eds.), *Diseases of the Brain, Head and Neck, Spine 2020–2023: Diagnostic Imaging* (pp. 231-240). Cham (CH): Springer

Vergo, S., Craner, M. J., Etzensperger, R., Attfield, K., Friese, M. A., Newcombe, J., . . . Fugger, L. (2011). Acid-sensing ion channel 1 is involved in both axonal injury and demyelination in multiple sclerosis and its animal model. *Brain, 134*(Pt 2), 571-584. doi:10.1093/brain/awq337

Vismara, I., Papa, S., Rossi, F., Forloni, G., & Veglianese, P. (2017). Current Options for Cell Therapy in Spinal Cord Injury. *Trends Mol Med, 23*(9), 831-849. doi:10.1016/j.molmed.2017.07.005

Walker, S. E., & Echeverri, K. (2022). Spinal cord regeneration - the origins of progenitor cells for functional rebuilding. *Curr Opin Genet Dev, 75*, 101917. doi:10.1016/j.gde.2022.101917

Wang, J., & Pearse, D. D. (2015). Therapeutic Hypothermia in Spinal Cord Injury: The Status of Its Use and Open Questions. *Int J Mol Sci, 16*(8), 16848-16879. doi:10.3390/ijms160816848

Wang, K., Buschle-Diller, G., & Misra, R. D. K. (2015). Chitosan-based injectable hydrogels for biomedical applications. *Materials Technology, 30*(sup8), B198-B205. doi:10.1179/17535557B15Y.000000008

West, C. R., Alyahya, A., Laher, I., & Krassioukov, A. (2013). Peripheral vascular function in spinal cord injury: a systematic review. *Spinal Cord, 51*(1), 10-19. doi:10.1038/sc.2012.136

Williams, P. R., & He, Z. (2016). Building bridges to regenerate axons. *Science, 354*(6312), 544-545. doi:10.1126/science.aal2112

Williams, P. R., Marincu, B. N., Sorbara, C. D., Mahler, C. F., Schumacher, A. M., Griesbeck, O., . . . Misgeld, T. (2014). A recoverable state of axon injury persists for hours after spinal cord contusion in vivo. *Nature communications, 5*, 5683. doi:10.1038/ncomms6683 [doi]

Witiw, C. D., & Fehlings, M. G. (2015). Acute Spinal Cord Injury. *J Spinal Disord Tech, 28*(6), 202-210. doi:10.1097/bsd.0000000000000287

Witte, M. E., Schumacher, A. M., Mahler, C. F., Bewersdorf, J. P., Lehmitz, J., Scheiter, A., . . . Kerschensteiner, M. (2019). Calcium Influx through Plasma-Membrane Nanoruptures Drives Axon Degeneration in a Model of Multiple Sclerosis. *Neuron, 101*(4), 615-624.e615. doi:10.1016/j.neuron.2018.12.023

Wrathall, J. R., Choiniere, D., & Teng, Y. D. (1994). Dose-dependent reduction of tissue loss and functional impairment after spinal cord trauma with the AMPA/kainate antagonist NBQX. *J Neurosci, 14*(11 Pt 1), 6598-6607.

Wu, H., Che, X., Zheng, Q., Wu, A., Pan, K., Shao, A., . . . Hong, Y. (2014). Caspases: a molecular switch node in the crosstalk between autophagy and apoptosis. *Int J Biol Sci, 10*(9), 1072-1083. doi:10.7150/ijbs.9719

Yang, J., Wu, Z., Renier, N., Simon, D. J., Uryu, K., Park, D. S., . . . Tessier-Lavigne, M. (2015). Pathological axonal death through a MAPK cascade that triggers a local energy deficit. *Cell, 160*(1-2), 161-176. doi:10.1016/j.cell.2014.11.053

Yeo, J. D., Walsh, J., Rutkowski, S., Soden, R., Craven, M., & Middleton, J. (1998). Mortality following spinal cord injury. *Spinal Cord, 36*(5), 329-336.

Zatz, M., & Starling, A. (2005). Calpains and disease. *N Engl J Med, 352*(23), 2413-2423. doi:10.1056/NEJMra043361

Zerangue, N., & Kavanaugh, M. P. (1996). Flux coupling in a neuronal glutamate transporter. *Nature, 383*(6601), 634-637. doi:10.1038/383634a0

Zhang, N., Fang, M., Chen, H., Gou, F., & Ding, M. (2014). Evaluation of spinal cord injury animal models. *Neural regeneration research, 9*(22), 2008-2012. doi:10.4103/1673-5374.143436

Zhang, Y., Al Mamun, A., Yuan, Y., Lu, Q., Xiong, J., Yang, S., . . . Wang, J. (2021). Acute spinal cord injury: Pathophysiology and pharmacological intervention (Review). *Mol Med Rep, 23*(6). doi:10.3892/mmr.2021.12056

Zhang, Z., Nguyen, K. T., Barrett, E. F., & David, G. (2010). Vesicular ATPase inserted into the plasma membrane of motor terminals by exocytosis alkalinizes cytosolic pH and facilitates endocytosis. *Neuron, 68*(6), 1097-1108. doi:10.1016/j.neuron.2010.11.035 [doi]

Zheng, Y. H., Fang, Z., Cao, P., Zheng, T., Sun, C. H., Lu, J., & Shi, R. Y. (2012). [A model of acute compression spinal cord injury by a mini-invasive expandable balloon in goats]. *Zhonghua Yi Xue Za Zhi, 92*(23), 1591-1595.

Zhou, T., Zheng, Y., Sun, L., Badea, S. R., Jin, Y., Liu, Y., . . . Ren, Y. (2019). Microvascular endothelial cells engulf myelin debris and promote macrophage recruitment and fibrosis after neural injury. *Nature neuroscience, 22*(3), 421-435. doi:10.1038/s41593-018-0324-9

Zhou, Y., & Danbolt, N. C. (2014). Glutamate as a neurotransmitter in the healthy brain. *J Neural Transm (Vienna), 121*(8), 799-817. doi:10.1007/s00702-014-1180-8

Zipser, C. M., Cragg, J. J., Guest, J. D., Fehlings, M. G., Jutzeler, C. R., Anderson, A. J., & Curt, A. (2022). Cell-based and stem-cell-based treatments for spinal cord injury: evidence from clinical trials. *Lancet Neurol, 21*(7), 659-670. doi:10.1016/s1474-4422(21)00464-6

Ziskin, J. L., Nishiyama, A., Rubio, M., Fukaya, M., & Bergles, D. E. (2007). Vesicular release of glutamate from unmyelinated axons in white matter. *Nature neuroscience, 10*(3), 321-330. doi:10.1038/nn1854